2012

The mixed glass former effect in 0.35Na2O + 0.65[xB2O3 + (1-x)P2O5] glasses

Randilynn Beth Christensen
Iowa State University

The mixed glass former effect in 0.35Na2O + 0.65[xB2O3 + (1-x)P2O5] glasses

by

Randilynn Beth Christensen

A dissertation submitted to the graduate faculty

in partial fulfillment of the requirements for the degree of

DOCTOR OF PHILOSOPY

Major: Materials Science and Engineering

Program of Study Committee:
Steve W. Martin, Major Professor
Ralph Napolitano
James Cochran
Jöerg Schmalian
Nicola Bowler

Iowa State University

Ames, Iowa

2012

Table of Contents

Chapter 1. Introduction

1.1 Thesis Introduction

Energy storage is a growing concern in an ever increasingly battery driven society. Batteries power everything from cell phones to computers to medical devices. Development of safer, smaller, and longer lasting batteries is in demand. Ion conducting glasses are an important type of solid electrolytes that could be used to answer this need. Unfortunately, many known ion conducting glasses, such as binary lithium oxide doped glasses with conductivities in the $10^{-7} – 10^{-8}$ S/cm range, are not conductive enough for practical use [1]. In order for ion conducting glasses to be used as a commercial solid electrolyte, a method of increasing the glasses' ionic conductivity must be found. According to V.K. Deshpande [2], there are four methods of increasing the ionic conductivity; increased modifier content, rapid quenching, addition of salts, and the use of mixed glass formers. While alkali mixed glass former glasses such as Bi_2O_3+B_2O_3+LiO_2 and Li_2S+SiS_2+GeS_2 have shown increases in the alkali ion conductivity up to two orders of magnitude, the cause of this increase is unclear [3, 4]. This phenomenon has become known as the Mixed Glass Former Effect (MGFE) and is defined by a non-linear, non-additive change in ionic conductivity. Although the MGFE has been reported in the literature, it has not been found to be universal as it has not been observed in all mixed glass former (MGF) glasses and has also been seen as both a negative and positive effect [5-8]. However, the effect of decreased conductivity with increasing modifier has been observed when the amount of modifier is varied. In order to

engineer glasses with higher ionic conductivities by the MGFE, the cause of the MGFE must be investigated and determined. Therefore, a comprehensive study of the physical properties, structure, and the effect of composition on MGF glasses over multiple glass systems has been undertaken. This study will attempt to determine the cause of the MGFE, if that cause is universal, and the ion conduction method of the MGF glasses.

To achieve a more complete understanding of the MGFE, an extensive study of several MGFE glasses will need to be undertaken. For this purpose, a Materials World Network (MWN) was established between Iowa State University, Cornell University, Central Michigan University, University of Münster, Ilmenau University, University of Onsbrück, and Chalmers University. Each glass has been thoroughly examined to determine their physical properties, short and medium range structures, and ionic conductivities. By combining this data with data from simulations and modeling, a cause for the MGFE can be found.

1.2 Thesis Organization

This thesis consists of six chapters. The first chapter gives a literature review and background of the mixed glass former effect (MGFE), ionic conduction in glass, experimental processes, and proposed work.

The second chapter is a paper that examines and reports the physical properties density and molar volume of $0.35Na_2O + 0.65[xB_2O_3 + (1-x)P_2O_5]$ glasses with changing composition [9]. The density and molar volume were observed to have a non-linear and

non-additive trends, similar to the MGFE. In order to understand the structural origin of these physical changes a model was created to determine the molar volume of the short range order structural units. The molar volume and free-volume were found to have negative trends, which was unexpected given the positive MGFE.

The third chapter is a paper that examines and reports on the glass transition temperature, T_g, of $0.35Na_2O + 0.65[xB_2O_3 + (1-x)P_2O_5]$ glasses [10]. The Tg was found to have a positive MGF type trend with changing composition. The changes in T_g were found to be related to the increasing number of bridging oxygens (BOs) in the glass structures. Increasing BOs have been observed to have a strong correlation to the number of tetrahedral boron short range order (SRO) structural units present in the glasses.

The fourth chapter is a paper that examines and reports on the structure of $0.35Na_2O + 0.65[xB_2O_3 + (1-x)P_2O_5]$ glasses using Raman and ^{11}B and ^{31}P Magic Angle Spinning – Nuclear Magnetic Resonance (MAS-NMR) spectroscopy. By close examination of the Raman and MAS-NMR spectra if the glasses, an atomic fraction SRO model was created to quantify the numbers and types of SRO structural units present in the glasses. The glass formers were found to be over-modified, possessing more Na_2O than equal sharing between the P_2O_5 and B_2O_3 glass formers would suggest, when they were the minority glass former. Large shifts in frequencies of peaks in both the Raman and the NMR spectra indicated that P-O-B bonding must play a major role in the intermediate range structures of these glasses. A first-order thermodynamic analysis

based on the Gibbs Free Energy of Formation of the various SRO units in the glasses was developed and used to support the preferential formation of tetrahedral boron groups.

The fifth chapter is a paper that examines and reports on the ionic conductivity of $0.35Na_2O + 0.65[xB_2O_3 + (1-x)P_2O_5]$ glasses. These glasses exhibit a strong and positive MGFE trend in the ionic conduction with a corresponding negative non-additive and non-linear trend in the activation energy with changing glass former content. The changing activation energy was evaluated in terms of the Anderson-Stuart model [11] The minimum in the conductivity activation energy was found to correlate well with a minimum in the columbic energy required for separating the positive cations in the glasses, Na^+, from the anionic sites in the glasses, such as the non-bridging oxygens (NBOs) and the negatively charged BO_4^- units. The composition dependence of the strain energy for cation conduction arising from the volume requirement for cation movement from one site to the next was found to be a small fraction of the overall conductivity activation energy and was shown to be smoothly changing function of the composition of the glasses and therefore is not a likely cause of the minimum in activation energy. The primary cause of the changing columbic energy was the changing dielectric permittivity, which was explained in terms of B-O-P intermediate range order bonding.

The final chapter is a general conclusion of this thesis and is used to suggest future work that could be done to expand upon this research.

1.3 Background

1.3.1 Mixed Glass Former Effect

In 1980, T. Tsuchiya and T. Moriya [12] published a paper in the Journal of Non-Crystalline Solids entitled "Anomalous Behavior of Physical and Electrical Properties in Borophosphate Glasses Containing R_2O (R=Na or Li) and V_2O_5". This paper reported maxima in the density, Vickers hardness, T_g, and conductivity of $30R_2O + xB_2O_3 + (70-x)P_2O_5$ and $40R_2O + xB_2O_3 + (60-x)P_2O_5$ glasses. The ionic conductivity in the mixed glass former glasses (MGF) were two orders of magnitude higher than either of the binary glasses. Tsuchiya proposed that the maxima were related to the formation of a mixed network between the boron and the phosphorus [12]. The work of Anantha and Hariharan supported the cross-linking and interpenetrating nature of the glassy network in $50Na_2O + 50[xB_2O_3 + (1-x)P_2O_5]$ glasses based on T_g, density, and infrared (IR) absorption spectroscopy data [13]. By studying the ionic conductivity as a function of composition, temperature, DC polarization, AC conductivity, and permittivity, Anantha and Hariharan were able to confirm that the charge transport was mainly due to ionic Na^+ ions that traveled by the ionic hopping mechanism. The relationship between structure and physical properties was further well studied in the MGF system $Na_2O + P_2O_5 + B_2O_3$ by Zielniok for $0.4Na_2O + 0.6[xB_2O_3 + (1-x)P_2O_5]$ glasses with Raman and NMR studies [5]. They concluded that the compositional trend of the physical properties could be explained by the average network connectivity concept.

When two maxima occurred in silver borophosphate glasses, Magistris proposed an idea based on the weak electrolyte theory and the assumption of hindered phase

separation [14]. Pradel showed the MGFE in the chalcogenide glasses $0.3Li_2S + 0.7[(1-x)SiS_2 + xGeS_2]$ [8]. By studying the physical properties and the structure with Raman spectroscopy and small angle x-ray scattering (SAXS), Pradel proposed an alternate theory. They argued that the MGFE was caused by phase separation with one phase containing almost all the modifier, Li^+, cations. Maia studied the electrical conductivity of glasses from the $0.4Li_2O + 0.6[xB_2O_3 + (1-x)Si_2O_4]$ system in 2004 [7]. However, they observed a decrease in conductivity. In 2004, Despande reported that the enhancement in conductivity is more pronounced for lower lithium content MGF glasses than for those with higher lithium contents [2]. Surprisingly, the conductivity $0.4Li_2O + 0.6[xB_2O_3 + (1-x)2SiO_2]$ glasses was investigated by Kluvanek et al. and no MGFE was found [6].

Gedam and Deshpande investigated the $27.5Li_2O + (72.5-x)B_2O_3 + xAl_2O_3$ glasses and reported a maximum in conductivity and a minimum in T_g [15]. They explained the extrema with the Anderson and Stuart model [11]. They argued that as one network former is substituted for another, the average interionic bond distance would change. Larger ions would increase the interionic bond length, leading to a more open structure. However, the continued addition of Al_2O_3 eliminates nNBOs, creating BOs, thereby making the structure more rigid and leading to a decrease in the ionic conductivity. Kim et al. studied $0.5Li_2S + 0.5[xGeS_2 + (1-x)GeO_2]$ glasses [16]. The MGFE was observed and was explained through the Anderson Stuart Model.

1.3.2 Ionic Conductivity

1.3.2.1 Direct Current Ionic Conductivity

The conductivity of glasses containing monovalent ions is controlled by the diffusion of these monovalent ions under the influence of an external field. Since the charge carriers are monovalent ions instead of electrons, the glasses are ionic conductors. The diffusion of the ion can be thought of as the ion jumping from one charge compensating site to another energetically favorable and comparable site. The conductivity of a glass depends on the type of ions available for conduction, concentration of mobile ions, and the mobility of the ion. The total conductivity of a glass is given by the sum of the contributions of all of charge carriers, Equation 1-1, where σ_{dc} is the total ionic conductivity, t_i is the transport number and σ_i is the conductivity of the i^{th} charge carrying species. Each charge carrying species contributes to the total ionic conduction. In a MGF glass, there would only be one ionic charge carrier the alkali ion $t_i = 1$, and Equation 1-2 is used to describe the conductivity, where n is the concentration of the charge carrier, Ze is the charge of the charge carrier, and μ is the mobility of the $i = 1$ charge carrier. The Nernst-Einstein equation relates the diffusion of a single ionic species and its ionic conductivity Equation 1-3. Diffusion is a thermally activated process, which can be expressed as Equation 1-4, where, in three dimensions, r is the jumping distance between energetically favorable sites, v_o is the frequency of attempted jumps, ΔE_a is the height of the potential energy barrier between the two cation sites. By combining Equation 1-3 and Equation 1-4 and multiply by Avogadro's constant

we get Equation 1-5, where the pre-exponential factor is $\sigma_0 = \frac{nr^2(Ze)^2v_0}{6R}$. However, it has been found in the literature that a better fit to experimental data is obtained if the ionic conductivity is written as Equation 1-6 [17, 18].

$$\sigma_{dc} = \sum t_i \sigma_i \qquad \textit{Equation 1-1}$$

$$\sigma_{dc}(i = 1) = n|Ze|\mu \qquad \textit{Equation 1-2}$$

$$\sigma_{dc} = \frac{n(Ze)^2 D}{k_b T} \qquad \textit{Equation 1-3}$$

$$D = \frac{1}{6} r^2 v_0 exp\left(\frac{-\Delta E_a}{k_b T}\right) \qquad \textit{Equation 1-4}$$

$$\sigma_{dc} = \frac{\sigma_0}{T} exp\left(-\frac{\Delta E_a}{RT}\right) \qquad \textit{Equation 1-5}$$

$$\sigma_{dc} = \sigma_0 exp\left(-\frac{\Delta E_a}{RT}\right) \qquad \textit{Equation 1-6}$$

1.3.2.2 Alternating Current Conductivity

In order to avoid electrode polarization effects, the d.c. conductivity is often measured by performing a a.c. conductivity measurements over a range of frequencies.

In an a.c. circuit, Ohm's law is modified to Equation 1-7, where Z^* is the complex impedance, V^* is the complex voltage, I^* is the complex current, and θ is the phase between the current and the voltage, and Z' and $Z^{"}$ are the real and imaginary impedance, respectively. When $\theta = 0$, the impedance has only the real component and Equation 1-7 can be written as Equation 1-8, where $V'$is the real voltage, I' is the real current, and R is the resistance. This allows us to calculate the d.c. conductivity by Equation 1-9, where d is the sample thickness and A is the sample area.

$$Z^* = \frac{V^*}{I^*} = |Z|e^{i\theta} = Z' + Z^{"} \qquad \textit{Equation 1-7}$$

$$Z^* = \frac{V'}{I'} = R \qquad \textit{Equation 1-8}$$

$$\sigma_{dc} = \frac{1}{R}\frac{d}{A} \qquad \textit{Equation 1-9}$$

1.3.2.3 Anderson-Stuart Model

Anderson and Stuart proposed a model of the mechanism of ion diffusion in 1954 [11]. Their model is based on the idea that in order for an ion to diffuse from one charge compensating site to a second charge compensating site, the ion must overcome the bonding energies of its immediate surroundings, before passing through adjacent interstices. The energy required to overcome its local energy was called the electrostatic binding energy, ΔE_b. The energy to pass through the "doorway" between adjacent

interstices was called the strain energy, ΔE_s. Therefore, the activation energy can be written as the sum of these two activation energies in Equation 1-10. Anderson and Stuart further suggested that the binding energy could be approximated as in Equation 1-11, where ΔE_c is the columbic energy, β is the finite displacement factor, γ is the covalency parameter and is equal to the dielectric constant, r is the radius of the cation, r_o is the radius of the anion, z and z_o are the valence of the cation and anion respectively. Likewise, the strain energy was approximated as in Equation 1-12, where G is the shear modulus, r_D is the doorway radius, and r is the radius of the cation. Since 1954, many modifications and variations have been proposed to improve the Anderson-Stuart model. However, the concept of activation energy consisting of a binding and strain energies has remained constant.

$$\Delta E_a = \Delta E_b + \Delta E_s \qquad \textit{Equation 1-10}$$

$$\Delta E_b = \Delta E_c \sim \frac{\beta z z_o e^2}{\gamma(r + r_o)} \qquad \textit{Equation 1-11}$$

$$\Delta E_s = 4\pi G r_D (r - r_D)^2 \qquad \textit{Equation 1-12}$$

1.4 Proposed Work

1.4.1 Glass Systems To Be Studied

To better understand the effect of composition on ionic conductivity, we must consider the effect of all ions in the glass and choose them to maximize our research. We

will use P and B as cations and O as an anion. The cations P and B were chosen because they have isotopes that are well suited to NMR spectroscopy. Oxygen is an ideal anion as P_2O_5 and B_2O_3 are strong glass formers that do not oxidize in air. We will use Na as a modifier as it has radioactive isotopes that can be used for our collaborators tracer diffusion measurements and is also has a nuclei that is well suited to NMR spectroscopy. In addition, B_2O_3 and P_2O_5 glasses and their binary counterparts, $Na_2O + B_2O_3$ and $Na_2O + P_2O_5$, have been well studied. While not as well studied as their single and binary counterparts, the ternary glass $Na_2O + B_2O_3 + P_2O_5$ has also been studied, Figure 1-2.

1.4.2 Experiments

1.4.2.1 Sample Preparation

The glasses have been made according to the formula, y(glass modifier) + (1-y)[x(glass former) + (1-x)(glass former)]. The modifier, y, will be held constant while the amount of glass former, x, is varied in each series. The sodium borophosphate glasses $0.35Na_2O + 0.65[xP_2O_5 + (1-x)B_2O_3]$, $0 \leq x \leq 1$ were studied.

Sodium borophosphate glasses were prepared as follows. Starting materials were sodium carbonate (Na_2CO_3, Fisher Scientific), ammonium dihydrogen phosphate ($(NH_4)H_2PO_4$, Fisher Scientific), and boric acid (H_3BO_3, Fisher Scientific). Enriched samples used in neutron diffraction studies used enriched boric acid ($H_3{}^{11}BO_3$, Ceradyne). All glasses were melted in platinum crucibles. After weighing and mixing, the starting materials were calcined at 900-1100^{o}C for ½ an hour in an electric furnace to

remove CO_2, H_2O, and NH_3 from the starting materials to produce appropriate amounts of Na_2O, P_2O_5 and B_2O_3. The decomposed materials were then cooled to room temperature, weighed, and transferred to a nitrogen atmosphere glove box. The decomposed materials were then remelted in an electric furnace at 1000°C-1100°C for 10 minutes. Depending on the glass forming ability of the melts, they were quenched to room temperature in one of two ways. To create bulk samples, the melt was quenched in preheated brass molds at temperatures 40°C below the T_g of the glass. These bulk samples were round discs ~ 20 mm in diameter and ~2 mm thick. The samples were annealed 40°C below the T_g for ½ an hour, then cooled to room temperature at a rate of 2°C/minute. Due to their hygroscopic character, all samples were kept inside the N_2 glovebox. All samples were checked for crystallization with XRD, Figure 1-3. Samples were checked for weight loss and found to be within 1.5 wt% of their target weights. Sodium, oxygen, and phosphorous concentrations were checked by Electron Dispersion Spectroscopy (EDS) and found to be within ± 2 atom% of the target compositions, Figure 1-4.

1.4.2.2 Glass Transition Temperature

The T_g and glass density (ρ) of all of the glasses were measured. T_gs for the sodium borophosphate glasses were determined from Differential Scanning Calorimetry (DSC) using a Perkin Elmer Pyris Diamond DSC. T_gs were determined by the onset method. Samples were heated and cooled at a rate of 20°C/min. Each sample was scanned in the DSC from room temperature to 10°C above the T_g and back to room

temperature to give all samples a common thermal history. The samples were then run from room temperature to approximately 500°C to determine T_g.

1.4.2.3 Density

Density was determined using the Archimedes method with paraffin oil (Fisher Scientific, $\rho = 0.848 g/cm^3$) as the submersion liquid for bulk sodium borophosphate glasses.

1.4.2.4 Infrared Spectroscopy

Infrared spectra were collected using a Bruker IFS 66v/S Infrared Spectrometer on pressed pellets made of a mixture of glass powders and cesium iodide. Sodium borophosphate glasses were mixed at a ratio of 2:10. Mid-infrared and far-infrared absorption spectra were recorded in the range of 4000 to 400 cm^{-1} and 750 to 150 cm^{-1}, respectively, using 32 scans at 4 cm^{-1} resolution. All experiments were run in vacuum at room temperature.

1.4.2.5 Raman Spectroscopy

Raman spectra were collected using a Renishaw InVia Raman Spectrometer Microscope. An Argon laser at 488 nm with 20 mW of power was used for excitation. All experiments were run on bulk samples in air at room temperature.

1.4.2.6 Ionic Conductivity

Ionic conductivity data was collected on a Novocontrol Dielectric Analyzer. Samples were bulk disks or pressed pellets sputtered with gold electrodes. Disks were

analyzed using brass electrode discs in a N_2 purging environment. The samples were tested from 0.1Hz to 10 MHz from 303 K to 573 K in 20 K increments.

1.5 References

[1] C.H. Lee, K.H. Joo, J.H. Kim, S.G. Woo, H.J. Sohn, T. Kang, Y. Park, J.Y. Oh, Solid State Ionics, 149 (2002) 59-65.
[2] V.K. Deshpande, Ionics, 10 (2004) 20-26.
[3] A. Pradel, N. Kuwata, M. Ribes, J. Phys. Condens. Matter, 15 (2003) S1561-S1571.
[4] A. Agarwal, V.P. Seth, P.S. Gahlot, S. Khasa, M. Arora, S.K. Gupta, J. Alloys Compd., 377 (2004) 225-231.
[5] D. Zielniok, C. Cramer, H. Eckert, Chem. Mater., 19 (2007) 3162-3170.
[6] P. Kluvanek, R. Klement, M. Karacon, J. Non-Cryst. Solids, 353 (2007) 2004-2007.
[7] L.F. Maia, A.C.M. Rodrigues, Solid State Ionics, 168 (2004) 87-92.
[8] A. Pradel, C. Rau, D. Bittencourt, P. Armand, E. Philippot, M. Ribes, Chem. Mater., 10 (1998) 2162-2166.
[9] R. Christensen, J. Byer, G. Olson, S.W. Martin, J. Non-Cryst. Solids, 358 (2012) 583-589.
[10] R. Christensen, J. Byer, G. Olson, S.W. Martin, J. Non-Cryst. Solids, 358 (2012) 826-831.
[11] O.L. Anderson, D.A. Stuart, J. Am. Ceram. Soc., 37 (1954) 573-580.
[12] T. Tsuchiya, T. Moriya, J. Non-Cryst. Solids, 38-39 (1980) 323-328.
[13] P.S. Anantha, K. Hariharan, Mater. Chem. Phys., 89 (2005) 428-437.
[14] A. Magistris, G. Chiodelli, M. Duclot, Solid State Ionics, 9-10 (1983) 611-615.
[15] R.S. Gedam, V.K. Deshpande, Solid State Ionics, 177 (2006) 2589-2592.
[16] Y. Kim, J. Saienga, W. Martin Steve, J Phys Chem B, 110 (2006) 16318-16325.
[17] J.E. Shelby, Introduction to Glass Science and Technology, The Royal Society of Chemistry, Cambridge, 2005.
[18] K.J. Rao, Structural Chemistry of Glasses, Elsevier, Oxford, 2002.

1.6 Figures

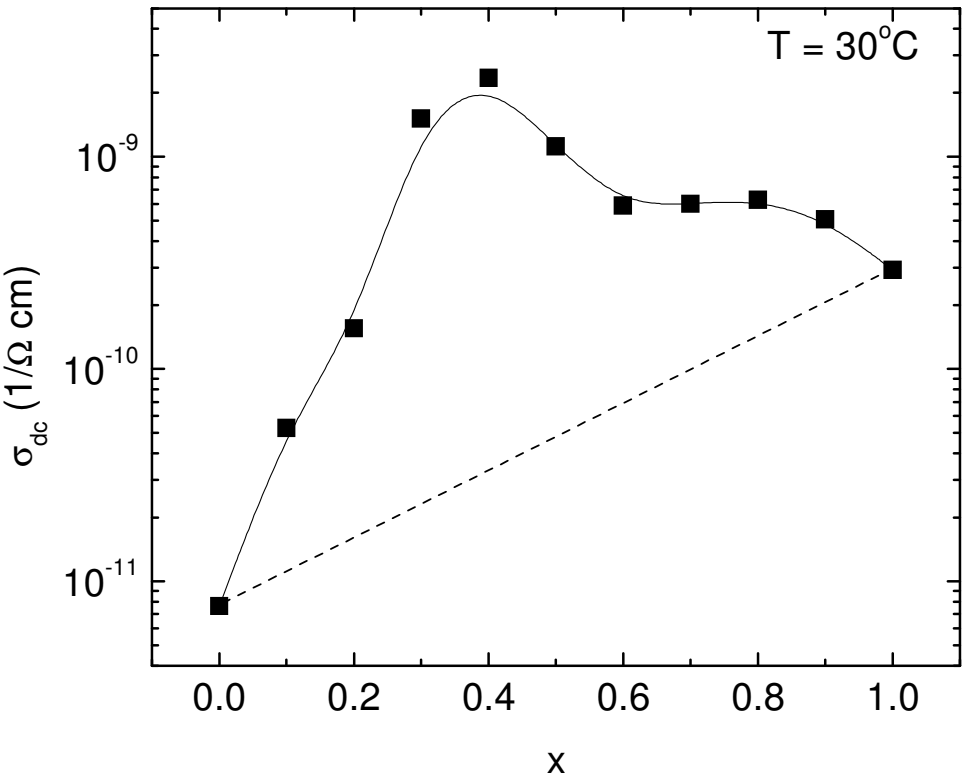

Figure 1-1

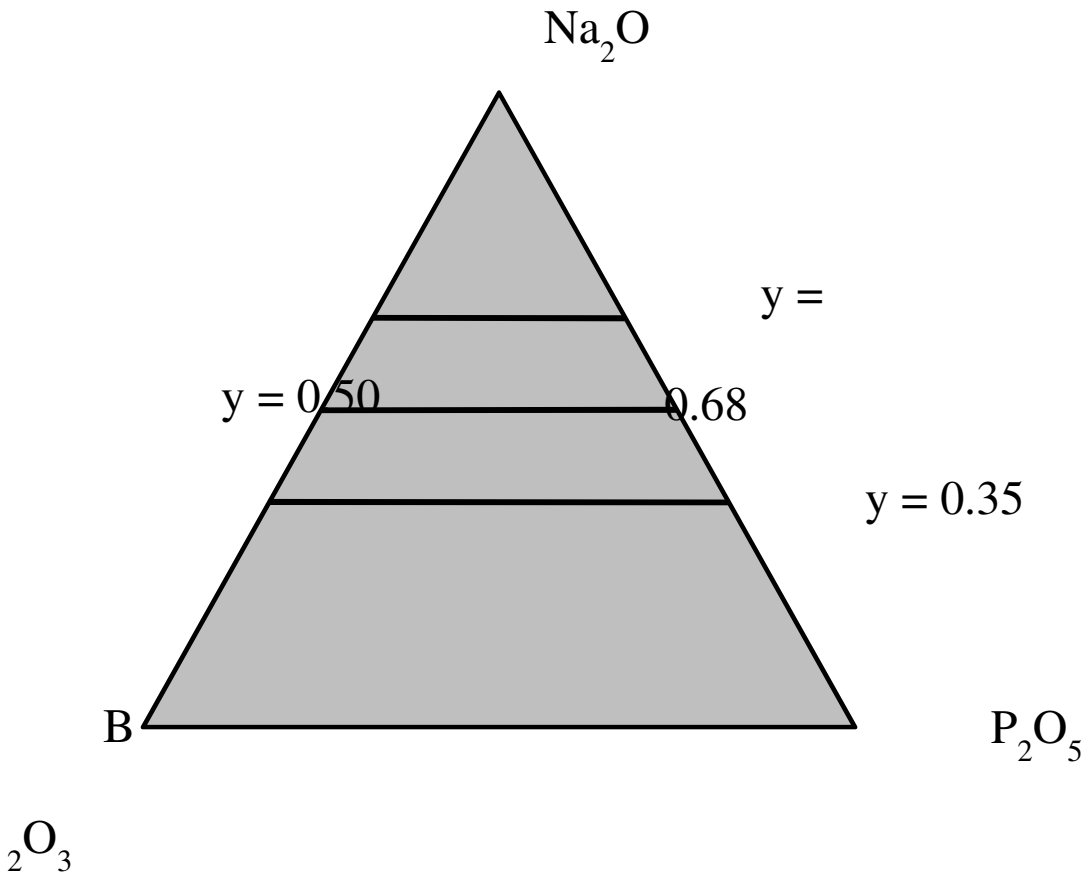

Figure 1-2

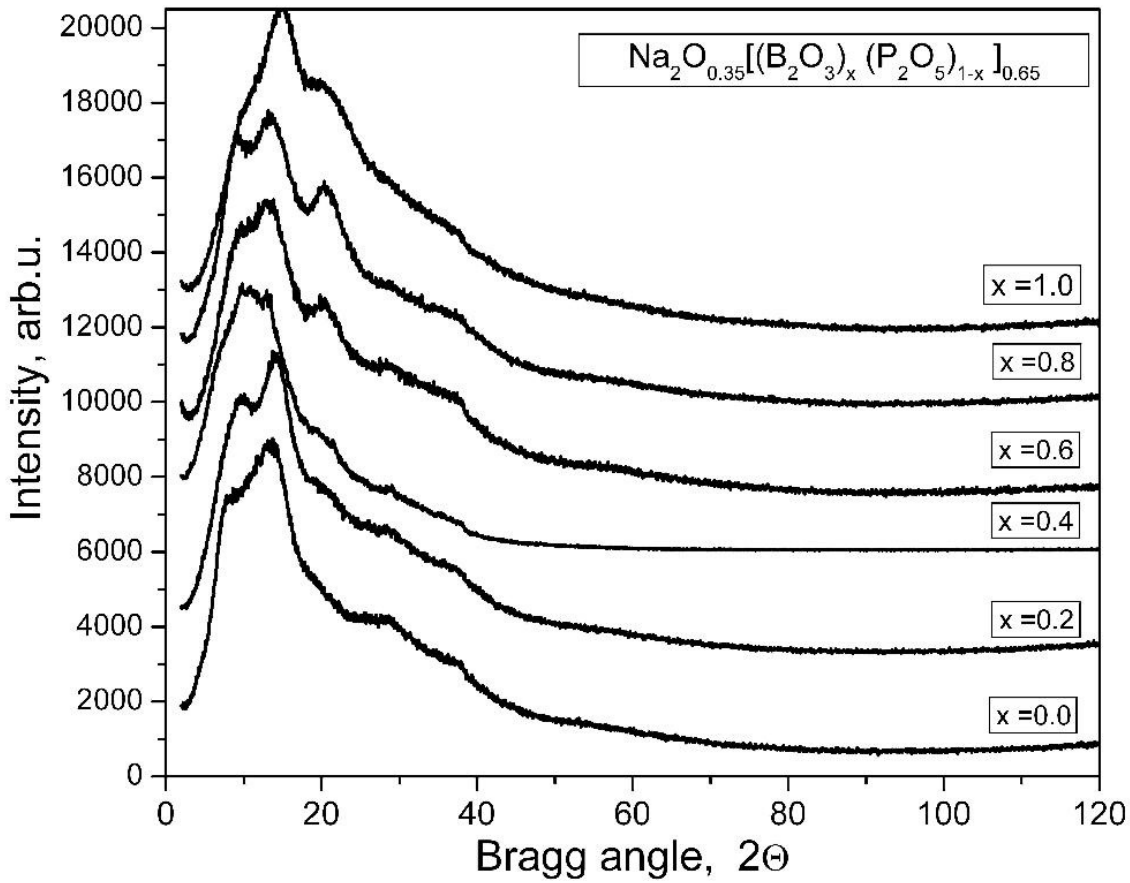
Na2O0.35[(B2O3)x (P2O5)1-x]0.65
x =1.0
x =0.8
x =0.6
x =0.4
x =0.2
x =0.0
Intensity, arb.u.
Bragg angle, 2Θ
0
2000
4000
6000
8000
10000
12000
14000
16000
18000
20000
0
20
40
60
80
100
120

Figure 1-3

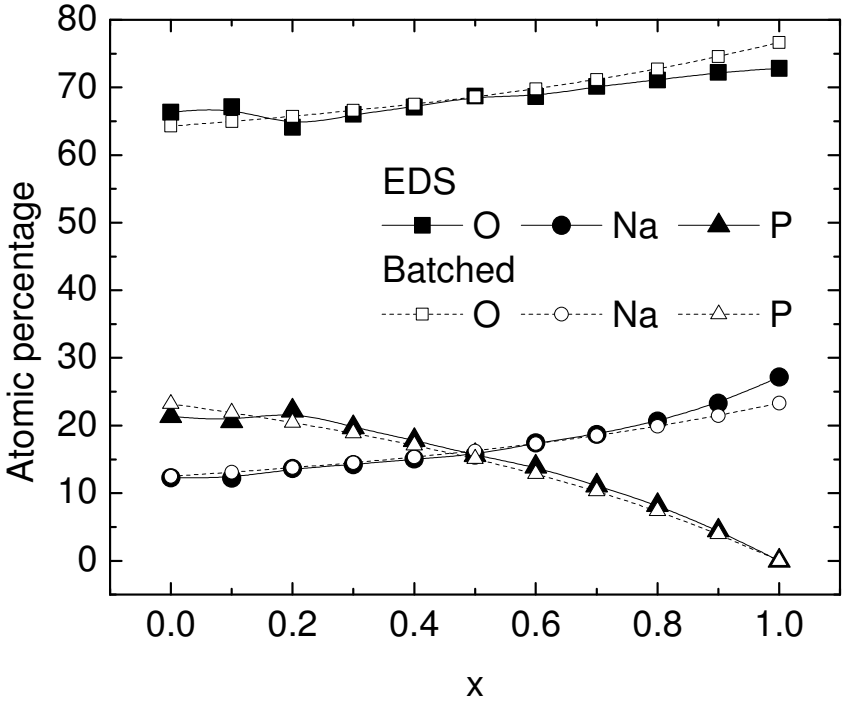
Atomic percentage
x
EDS
O
Na
P
Batched
O
Na
P
0
10
20
30
40
50
60
70
80
0.0
0.2
0.4
0.6
0.8
1.0

Figure 1-4

Chapter 2. The Densities of Mixed Glass Former 0.35 Na_2O + 0.65 [xB_2O_3 + (1-x)P_2O_5] Glasses Related to the Atomic Fractions and Volumes of Short Range Structures

A paper published in the *Journal of Non-Crystalline Solids*[1]

Randilynn Christensen[1], Jennifer Byer[2], Garrett Olson[2], Steve W. Martin[3]

2.1 Abstract

The mixed glass former effect (MGFE) is defined as a non-linear and non-additive change in the ionic conductivity with changing glass former fraction at constant modifier composition between two binary glass forming compositions. In this study, mixed glass former (MGF) sodium borophosphate glasses, 0.35 Na_2O + 0.65 [xB_2O_3 + (1-x)P_2O_5], $0 \leq x \leq 1$, which have been shown to have a strong positive MGFE, have been prepared and their physical properties, density and molar volume, have been examined as predictors of structural change. The density exhibits a strong positive non-linear and non-additive change in the density with x and a corresponding negative non-

---

[1] Primary researcher and author.

[2] Undergraduate research assistant

[3] Author for correspondence and principle investigator. 2220 Hoover Hall, Iowa State University, Ames, IA 50011

linear and non-additive change in the molar volume. In order to understand the structural origins of these changes, a model of the molar volume was created and best-fit to the experimentally determined molar volumes in order to determine the volumes of the short range order (SRO) structural units in these glasses, how these volume change from the molar volumes of the binary glasses, and how these volumes change across the range of x in the ternary glasses. The best-fit model was defined as the model that required the smallest changes in the volumes of the ternary phosphate and borate SRO structural groups from their values determined by the densities of the binary sodium phosphate and sodium borate glasses. In this best-fit molar volume model, it was found that the volumes of the various phosphate and borate SRO structural groups decreased by values ranging from a minimum value of ~1% for x = 0.1 and 0.9 to a maximum value of ~6% for the phosphate and ~9% for the borate SRO groups at the minimum in molar volume at x = 0.4. The free volume was found to have a negative deviation from linear which is unexpected given the positive deviation in ionic conductivity.

2.2 Introduction

Energy storage is a growing concern in an ever increasingly portable energy society. Batteries power everything from cell phones to computers to medical devices to automobiles. The development of safer, smaller, and more energy dense batteries is in demand. Ion conducting glasses are an important type of solid electrolyte that may be used to answer this need. A currently unexplained change in the ionic conductivity known as the mixed glass former effect (MGFE) has been seen in many mixed glass

former (MGF) glasses [2-9] such as $Li_2S + GeS_2 + GeO_2$ glasses [10] and $Li_2S + SiS_2 + GeS_2$ glasses [4]. This change in the ionic conductivity is non-linear and non-additive and can be observed as either a decrease or an increase with changing glass former fraction at constant modifier composition between two binary glass forming systems. A positive MGFE with a maximum deviation from linearity at x = 0.4 in the ionic conductivity has been observed in the $0.35\ Na_2O + 0.65\ [xB_2O_3 + (1-x)P_2O_5]$ glass system and is shown in Figure 2-1. While this phenomena has not been fully explained [3, 4, 8, 11], increases in the ionic conductivity of up to two orders of magnitude have been observed in other MGF glasses reported in the literature [2, 3]. Understanding the cause of the MGFE is crucial to the effort of engineering glasses with higher ionic conductivities and other improved physical properties.

It is our hypothesis that structural changes at the SRO level, the first coordination sphere, caused by the mixing of the two glass formers is the underlying cause of the MGFE. In order to confirm this, the link between the physical properties, structure, and composition of MGF glasses is being explored. To better understand the effect of composition on physical properties and structure, all components of the glasses in the present study were carefully chosen. Oxygen was selected as the anion with Na, P, and B as the cations. Boron and phosphorous were chosen because of their nuclear magnetic resonance spectroscopy (NMR) accessible isotopes. Oxygen was chosen as the anion because of the strong glass forming nature of B_2O_3 and P_2O_5. In addition, B_2O_3 [12-15] and P_2O_5 [16-18] glasses and their binary glassy counter parts, $Na_2O + B_2O_3$ and $Na_2O + P_2O_5$, have been well studied in the literature [13, 19-21]. The binary glasses have been

used to verify the x = 0 and x = 1 experimental data and provide starting points for the analysis of the ternary glass forming system. Sodium was chosen as the glass modifier and ionic charge carrier because its radioactive isotope is useful for tracer diffusion measurements and ^{23}Na is useful in NMR studies.

2.3 Experimental methods

2.3.1 Sample preparation

Starting materials were sodium carbonate (Na_2CO_3, 99.5% Fisher Scientific), ammonium di-hydrogen phosphate dibasic ($(NH_4)_2H_2PO_4$, 98.8% Fisher Scientific), and boric acid (H_3BO_3, 99.5% Fisher Scientific). After weighing and mixing the appropriate amounts, the starting materials were calcined in platinum crucibles between 900^{o}C and 1100^{o}C for 0.5 hour to 1 hour in an electric furnace in a fume hood. After the melt was bubble free, the crucible was removed from the furnace and allowed to cool to room temperature. Once cool, the sample was weighed to determine the weight lost from NH_3, H_2O, and CO_2. The slightly hygroscopic samples were then transferred to a high quality nitrogen atmosphere glove box (< 5ppm O_2 and H_2O) and remelted in an electric furnace at 1000^{o}C-1100^{o}C for 10 minutes. To create bulk samples, the melt was quenched in preheated brass molds at temperatures 40^{o}C below the glass transition temperature, (T_g). Bulk samples were round discs approximately 20 mm in diameter and 2 mm thick. The bulk samples were annealed 40^{o}C below the T_g for 0.5 hour, then cooled to room temperature at a rate of 2^{o}C/minute. Due to their hygroscopic character, all samples were

stored in the N_2 atmosphere glove box. All of the glasses were checked for crystallization with x-ray diffraction (XRD) and found to be x-ray amorphous. Samples were checked for weight loss and found to be within 1.5 wt% of their target weight. Sodium, oxygen, and phosphorous concentrations were checked by energy dispersive spectroscopy (EDS) and found to be within ± 4 at.% of the target compositions. Infrared spectroscopy was used to ensure that all of the glasses did not contain residual NH_3, CO_2, and H_2O.

2.3.2 Density

Densities of the 0.35 Na_2O + 0.65 [xB_2O_3 + $(1-x)P_2O_5$] glasses were determined using the Archimedes method on bulk glass samples using paraffin oil (Fisher Scientific) as the suspension liquid ($\rho = 0.848 \pm 0.005$ g/cm^3) inside the N_2 glove box.

2.3.3 Glass structure notations

The SRO glass structures will be identified as $J^n_{mK,}$ where J is the glass former connected to n number of bridging oxygens (BO), m number of the BO bonded to glass former K and n-m BO bonded to glass former J. For example, P^n_{mB} indicates a phosphorous atom with n number of BO that are bonded to m number of boron atoms and (n-m) number of phosphorous atoms. If no mK is denoted, then it is unknown to what glass former is being bridged to by oxygen. The SRO structures present in binary Na_2O

+ P_2O_5 and $Na_2O + B_2O_3$ glasses [22-24] and their compositional ranges are shown in Figure 2-2 and Figure 2-3.

2.4 Results

2.4.1 Density

Figure 2-4 shows the composition dependence of the density of the $0.35Na_2O + 0.65[xB_2O_3 + (1\text{-}x)P_2O_5]$ glasses and the data are given in Table (1). The density increases from 2.34g/cm^3 at x = 0 to a maximum of 2.54g/cm^3 at x = 0.4 and then decreases to 2.37g/cm^3 at x= 1. All densities are believed to be accurate to ±0.01g/cm^3. The changes in the density are non-linear and non-additive and are in agreement with the values found in the literature for comparable glasses of the binary and ternary systems [13, 15, 20, 21, 25-27]. The maximum deviation from linearity occurs at x = 0.4. The molar volumes, Figure 2-5, were calculated from the density using Equation 2-1 to allow the MGFE trend to be seen with the compositional atomic mass effects removed.

$$\bar{V}(x) = \frac{\overline{M_\iota}(x)}{\rho(x)} = \frac{\sum f_i(x)\,\overline{M_\iota}}{\rho(x)} \qquad \textit{Equation 2-1}$$

$\bar{V}$ is the molar volume, $\rho(x)$ is the experimental density, $\overline{M_\iota}(x)$ is the molar mass at composition x, $f_i(x)$ is the mole fraction of the various ith SRO structural units shown in Figure 2-2 and Figure 2-3, $\overline{M_\iota}$ is the molar mass of the various SRO structural groups and is calculated using the atomic masses and the number of the constituent elements. The values of $f_i(x)$ have been determined experimentally by combining Raman and ^{31}P

and ^{11}B MAS-NMR spectroscopies with a requirement of charge neutrality and are shown in Figure 2-6. The data shown in Figure 2-6 will be reported separately in a forthcoming paper [28].

2.5 Discussion

2.5.1 Density and Molar Volume

Like the ionic conductivity, the density shows a non-linear and non-additive increase. The molar volume shows a corresponding non-linear and non-additive decrease. However, the density, molar volume, and ionic conductivity all reach a maximum deviation from linearity at x = 0.4. This correlation suggests that the underlying structural and compositional cause of the MGFE may also be affecting the density and molar volume. As shown in Equation 2-1, the non-linear and non-additive changes in the density, in turn, is attributed to the changing masses and volumes of the various short range structures. The molar volume does not depend on the compositional mass, but still shows a non-linear and non-additive decrease with changing composition. Therefore, changes in the molar volume are the most likely cause of the MGFE seen in the density.

2.5.2 Molar Volume Model

In order to explore the changes in density with composition, the cause of the changes in the molar volume were examined. The total molar volume can be calculated by Equation 2-2.

$$\overline{V_{Total}}(x) = f_{P3}(x)\overline{V_{P3}}(x) + f_{P2}(x)\overline{V_{P2}}(x) + f_{P1}(x)\overline{V_{P1}}(x) + f_{B4}(x)\overline{V_{B4}}(x) + f_{B3}(x)\overline{V_{B3}}(x) + f_{B2}(x)\overline{V_{B2}}(x) \qquad \textit{Equation 2-2}$$

It is known from Raman and NMR spectroscopy that $f_i(x)$ changes with composition, Figure 2-6. However, it is unknown how $\overline{V_i}(x)$ changes with composition. Therefore, the first question that was investigated was: Are the changes in the molar volume dependent only on the changing numbers of SRO structural units, where $\overline{V_i}(x) = \overline{V_i}$, or are the volumes of the individual SRO structural units also changing with composition, $\overline{V_i}(x) \neq \overline{V_i}$? This can be tested by determining the volumes of the SRO structural units present in the binary glasses, assuming the volumes remain constant over the range $0 \leq x \leq 1$, and then comparing the calculated molar volume to the experimental molar volume.

The volumes of the SRO structural units in the binary sodium phosphate glass, Table 2-1, $yNa_2O + (1\text{-}y)P_2O_5$, were calculated setting Equation 2-1 equal to Equation 2-2 and solving for $\overline{V_i}(x)$. Because it was found that three phosphorous structural groups, P^3, P^2, and P^1, are present in the ternary glasses, to determine the molar volumes for these structural groups in the binary sodium phosphate glasses, the binary glasses had to be examined over sufficiently wide compositional ranges such that these three structural

groups would be present. This required the use of density data and calculated values for the atomic fractions of the groups from this and other studies in the literature, Table 2-2. Using the data in Table 2-2 as input for Equation 2-1 and Equation 2-2, the volumes of the three phosphate structural groups, $\overline{V_{P3}}$, $\overline{V_{P2}}$, and $\overline{V_{P1}}$ were calculated and are reported in Table 2-3.

The calculation of the volumes of the SRO structural units present in sodium borate glasses, $yNa_2O + (1\text{-}y)B_2O_3$ is not as straightforward as in the phosphate glasses as more than two SRO units are present at any one composition. Fortunately, the volumes of the SRO structural units in sodium borate glasses have already been determined by Feil *et al.*[12] who related all the volumes of the sodium borate structural groups to the volume of the B^3 group in pure B_2O_3 glass. This allowed us to use the ratios of the molar volumes of the borate SRO structural units, for example $\overline{V_{B3}}$: $\overline{V_{B4}}$, from Feil's study and apply them to the slightly different molar volumes found in the binary glasses in this study. Using these ratios, the volumes of the ternary borate structural groups were related to the volume of B^3 in binary $0.35Na_2O + 0.65B_2O_3$ glass, as seen in Eqs. (3a-c). In order to get the correct structural volumes for our glasses, the value of $\overline{V_{B3}}(1)$ was adjusted until the calculated molar volumes equaled the experimental molar volumes and these values are given in Table 2-3.

$$\overline{V_{B4}}(1) = 1.32\overline{V_{B3}}(1) \qquad \textit{Equation 2-3}$$

$$\overline{V_{B3}}(1) = 1\overline{V_{B3}}(1) \qquad \textit{Equation 2-4}$$

$\overline{V_{B2}}(1) = 1.71\overline{V_{B3}}(1)$ *Equation 2-5*

The densities of the ternary glasses were then calculated using Equation 2-2 according to Model 0 which assumes that the SRO structural volumes of all units at all x were equal to their binary glass counterparts volumes, $\overline{V_P}(x) = \overline{V_P}(0)$ and $\overline{V_B}(x) = \overline{V_B}(1)$. As seen in Figure 2-7, the calculated molar volume is in good agreement with the experimental molar volume for the binary glasses, but is in very poor agreement with the experimental molar volumes of the ternary glasses. This indicates that the volumes of the individual structural units must be changing with composition x, ie. $\overline{V_i}(x) \neq \overline{V_i}$ and furthermore that the SRO volumes of the ternary glasses must be less than the SRO volumes of the binary glasses. Therefore, the change (decrease) in the molar volumes of the various borate and phosphate SRO structural units is the mostly likely cause of the MGFE seen in the density.

These results lead to the question: How do the volumes of the individual structural units change across the range of $0 \leq x \leq 1$ in order to account for the total volume changes as required in Figure 2-7? As seen in Equation 2-2 and discussed above, the system of equations is underdetermined and therefore the volumes cannot be solved for uniquely. By assuming that the boron volume ratios of Equation 2-3, Equation 2-4, and Equation 2-5 hold for the ternary glasses and assuming that the volumes of the SRO structural groups of sodium phosphate glasses behave in the same manner, Equation 2-6, Equation 2-7, and Equation 2-8, Equation 2-2 was simplified to Equation 2-9. In this

way, the system of equations is still underdetermined, but there are now only two unknowns, $\overline{V_{P3}}$ and $\overline{V_{B3}}$.

$$\overline{V_{P3}}(x) = \overline{V_{P3}}(x) \qquad \textit{Equation 2-6}$$

$$\overline{V_{P2}}(x) = 1.1966\overline{V_{P3}}(x) \qquad \textit{Equation 2-7}$$

$$\overline{V_{P1}}(x) = 1.8645\overline{V_{P3}}(x) \qquad \textit{Equation 2-8}$$

$$\begin{aligned} V_{Total}(x) &= V(x) \\ &= \overline{V_{P3}}(x)[1 * f_{P3}(x) + 1.1966 * f_{P2}(x) + 1.8645 \\ &* f_{P1}(x)] + \overline{V_{B3}}(x)[1.32 * f_{B4}(x) + 1 * f_{B3}(x) + 1.71 \\ &* f_{B2}(x)] = \overline{V_P}(x) + \overline{V_B}(x) \end{aligned} \qquad \textit{Equation 2-9}$$

Because the experimental total molar volumes and the calculated total molar volumes of Model 0 are known, the difference between the calculated (Model 0) and experimental volumes (Figure 2-7) equals the total change in volume, $\Delta\bar{V}(x)$, that the structural units must undergo from their respective binary volumes in order to fit the experimental volumes of the ternary glasses, Equation 2-10. Since the volumes can't be solved for uniquely, it is assumed that some part of the total volume change is attributed to the collective volumes of the phosphorous SRO structural units and the remainder is attributed to the collective volumes of the boron SRO structural units, Equation 2-11 and Equation 2-12. The factor determining the ratio of the volume change due to the

phosphorous SRO structural volume changes and the boron SRO structural volume changes, A, allows the various SRO structural unit volumes for phosphorous and boron groups to be calculated, Equation 2-13 and Equation 2-14.

$$\Delta\bar{V}(x) = \overline{V_{experimental}}(x) - \overline{V_{Model\,0}}(x) = \Delta\overline{V_P}(x) + \Delta\overline{V_B}(x) \qquad \textit{Equation 2-10}$$

$$\Delta\overline{V_P}(x) = A * \Delta\bar{V}(x) \qquad \textit{Equation 2-11}$$

$$\Delta\overline{V_B}(x) = (1 - A) * \Delta\bar{V}(x) \qquad \textit{Equation 2-12}$$

$$\overline{V_P}(x) = \Delta\overline{V_P}(x) + \overline{V_P}(0) \qquad \textit{Equation 2-13}$$

$$\overline{V_B}(x) = \Delta\overline{V_B}(x) + \overline{V_B}(1) \qquad \textit{Equation 2-14}$$

where in Equation 2-13 and Equation 2-14 the 0 and 1 refer to binary sodium phosphate and sodium borate glass volumes, respectively.

Since this system of equations is still underdetermined, the agreement with the experimental density does not indicate a unique solution. Therefore, the criteria for "best-fit" that is used here is that the calculated volumes of both the boron and phosphorous SRO structural groups have a minimum deviation from their original volumes for the binary glasses, Equation 2-15 and Equation 2-16, and a minimum change with x, Equation 2-17 and Equation 2-18.

$$V_p(0) - V_p(x \neq 0) = minimum \qquad \textit{Equation 2-15}$$

$$V_B(1) - V_B(x \neq 1) = minimum \qquad \textit{Equation 2-16}$$

$$V_P(x) - V_P(x + 0.1) = minimum \qquad \textit{Equation 2-17}$$

$$V_B(x) - V_B(x - 0.1) = minimum \qquad \textit{Equation 2-18}$$

To determine the volumes that are required to fit the experimental molar volume data, five different models for A were examined. The relationships for each model are given in Table 2-5. Model 1 assumes that only the phosphorous SRO structural volumes change with x, $A = 1$. Model 2 assumes that only the boron SRO structural volumes change with x, $A = 0$. Model 3 assumes that half of the structural SRO volume change is from each glass former, $A = 0.5$. Model 4 assumes that the relative volumes of the binary SRO structures influences how the volumes changed. Finally, Model 5 assumes the volume change arising from the various phosphate and borate SRO groups present in the glasses depends upon the fraction of glass former in the glass, $A = 1 - x$.

As discussed above, all of the models can be made to achieve a perfect agreement with the experimental density data. However, Table 2-5 shows that Models 1-4 give unphysically large changes (decreases) in the volumes of the SRO structural groups in the ternary glasses compared to the volumes of the same structural groups in the binary glasses. For example, Model 2 requires a 50% change in the volumes of the borate

groups to achieve a fit to the data. Model 5 gives the "best-fit" in that it provides a perfect fit to the molar volumes of the glasses with the smallest of the required volume changes from the binary SRO structural volumes of 5.6% for the phosphorous groups and 8.7% for the boron groups with an average compositional change of 1.2% for phosphorous and 1.5% for boron. The individual volumes and the changes in volume for each composition calculated from Model 5 are shown in Table 2-6 and Table 2-7 and Figure 2-8 and Figure 2-9, respectively. The volumes of all the SRO structural units of phosphorous and boron decrease from their values for the binary glasses and go through a shallow minimum over the compositional range. The maximum deviation from linearity occurs at x = 0.3 for all phosphorous SRO structural units and at x = 0.4 for all borate SRO structural units. This is the same compositional region where the conductivity [29] and the glass transition temperature (T_g) [30] go through maximum values and indicates that the maximum in the conductivity and the T_g may be associated with the same factor that caused the density maximum, the decreasing volumes of the various structural groups.

2.5.3 Free Volume and Ionic Conductivity

To investigate this hypothesis, the free volume of the glasses was determined. It's a significant finding that the conductivity maximizes in the region, x = 0.4, of the composition where the total molar volume and the molar volume of all the SRO structural groups is a minimum because it is a well known association that glasses often have

higher ionic conductivities than their corresponding crystalline materials due to their larger "free" volumes. Free volume is often correlated to the molar volume of a system. In order to see if this correlation holds true in the $0.35Na_2O + 0.65[xB_2O_3 + (1\text{-}x)P_2O_5]$ glass system, the free volume was calculated using Equation 2-19, Equation 2-20, and Equation 2-21 from the atomic radi determined by Shannon [31], $r_P = 0.31$Å, $r_{B\ trigonal} = 0.15$Å, $r_{B\ tetrahedral} = 0.25$Å, $r_O = 1.21$Å, and $r_{Na} = 1.16$Å .

$$V_i = \sum (\frac{4}{3}\pi r_j^3)\, N_j \qquad \textit{Equation 2-19}$$

$$V_{ionic}(x) = \sum f_i * V_i \qquad \textit{Equation 2-20}$$

$$V_{free}(x) = V_{experimental}(x) - V_{ionic}(x) \qquad \textit{Equation 2-21}$$

where V_i is the calculated ionic volume of SRO structural unit i, r_j is the atomic radius of atom j, N_j is the number of atoms j in the SRO structural unit. The free volume was found to have a strong, but perhaps negative correlation, to the molar volume, with a minima at x = 0.4.

That the conductivity of the MGF glasses maximizes when the free volume is a minimum, Figure 2-10 and the density is at a maximum suggests that the second factor affecting the ionic conductivity, the collective and many-body long range columbic forces acting between the moblie cations, Na^+, and the anions, NBO in the P^2, P^1, and B^2 groups, and the BO of the B^4 groups in the glasses must be a more important factor. We

will explore this hypothesis further in future reports on the behavior of the ionic conductivity in theses glasses [29].

2.6 Conclusions

A positive MGFE trend was observed in the density of $0.35Na_2O + 0.65[xB_2O_3 + (1-x)P_2O_5]$ glasses. The correlation in the maximum deviation from linear behavior between the density, molar volume, and conductivity suggested that the cause of changing density is related to the causes of the MGFE. It was determined that although the changing numbers of different structural units effects the molar volume, it is the changing volumes of these SRO units that are the cause of the MGFE trend in the density. In order to explain why the changing SRO units molar volume effects the conductivity, we analyzed several different molar volume models. We found that the most physically plausible was Model 5, where the fraction of the volume change required in the phosphorous and boron structural groups to fit the molar volumes of the ternary glasses was proportional to the amount of the glass former, P_2O_5 and B_2O_3 present, respectively. These findings support the hypothesis that the MGFE is caused by SRO structural change. In addition, the minimum in molar volume corresponds to a minima in free volume, which is anti-correlated to the ionic conductivity. This suggests that the ionic conductivity of the glasses is dominated by the collective columbic forces, rather than the free volume effects.

2.7 Acknowledgements

This research was supported by the National Science Foundation under grant number DMR-0710564 and this research support is gratefully acknowledged.

2.8 References

[1] A. Agarwal, V.P. Seth, P.S. Gahlot, S. Khasa, M. Arora, S.K. Gupta, J. Alloys Compd., 377 (2004) 225-231.
[2] A. Pradel, N. Kuwata, M. Ribes, J. Phys. Condens. Matter, 15 (2003) S1561-S1571.
[3] A. Pradel, C. Rau, D. Bittencourt, P. Armand, E. Philippot, M. Ribes, Chem. Mater., 10 (1998) 2162-2166.
[4] P.S.S. Prasad, A.N.D. Rani, S. Radhakrishna, Solid State Commun., 77 (1991) 967-971.
[5] P.S.S. Prasad, A.N.D. Rani, S. Radhakrishna, Mater. Chem. Phys., 25 (1990) 487-499.
[6] R.V. Salodkar, V.K. Deshpande, K. Singh, J. Power Sources, 25 (1989) 257-263.
[7] M. Jamal, G. Venugopal, M. Shareefuddin, M. Narasimha Chary, Mater. Lett., 39 (1999) 28-32.
[8] D. Zielniok, C. Cramer, H. Eckert, Chem. Mater., 19 (2007) 3162-3170.
[9] Y. Kim, J. Saienga, W. Martin Steve, J Phys Chem B, 110 (2006) 16318-16325.
[10] R.S. Gedam, V.K. Deshpande, Solid State Ionics, 177 (2006) 2589-2592.
[11] D. Feil, S. Feller, J. Non-Cryst. Solids, 119 (1990) 103-111.
[12] J.H. Strimple, E.A. Giess, J. Am. Ceram. Soc., 41 (1958) 231-237.
[13] J.E. Shelby, J. Appl. Phys., 45 (1974) 5272-5277.
[14] J.E. Shelby, L.K. Downie, Phys. Chem. Glasses, 30 (1989) 151-154.
[15] J.J. Hudgens, S.W. Martin, J. Am. Ceram. Soc., 76 (1993) 1691-1696.
[16] U. Hoppe, E.E.-d. Metwalli, R.K. Brow, J. Neuefeind, J. Non-Cryst. Solids, 297 (2002) 263-274.
[17] K. Meyer, Phys. Chem. Glasses, 39 (1998) 108-117.
[18] A. Shaim, M. Et-Tabirou, Phys. Chem. Glasses, 42 (2001) 381-384.
[19] V.N. Naraev, A.A. Pronkin, Glass Physics and Chemistry, 24 (1998) 361-365.
[20] A.A. Pronkin, V.N. Naraev, S.Y. Eliseev, Fiz. Khim. Stekla, 14 (1988) 926-928.
[21] J.R. Van Wazer, Phosphorus and its compounds, Interscience Publishers, New York,, 1958.
[22] E.I. Kamitsos, M.A. Karakassides, Phys. Chem. Glasses, 30 (1989) 19-26.
[23] G.E. Jellison, P.J. Bray, J. Non-Cryst. Solids, 29 (1978) 187-206.
[24] H. Doweidar, G.M. El-Damrawi, Y.M. Moustafa, R.M. Ramadan, Physica B-Condensed Matter, 362 (2005) 123-132.
[25] J.M. Fernandez Navarro, J.L. Oteo Mazo, Bol. Soc. Espan. Ceram., 10 (1971) 37-70.
[26] J.F. Ducel, J.J. Videau, Mater. Lett., 13 (1992) 271-274.
[27] R. Christensen, J. Byer, G. Olson, S.W. Martin, To Be Published, (2011).
[28] R. Christensen, J. Byer, G. Olson, S.W. Martin, To Be Published, (2011).
[29] R. Christensen, J. Byer, G. Olson, W. Martin Steve, Journal of Non-Crystalline Solids, (2012).
[30] R.D. Shannon, Acta Crystallogr., Sect. A, A32 (1976) 751-767.
[31] R. Christensen, J. Byer, G. Olson, S.W. Martin, To Be Published, (2011).
[32] R. Christensen, J. Byer, G. Olson, S.W. Martin, (2011).

2.9 Figures

2.10 Tables

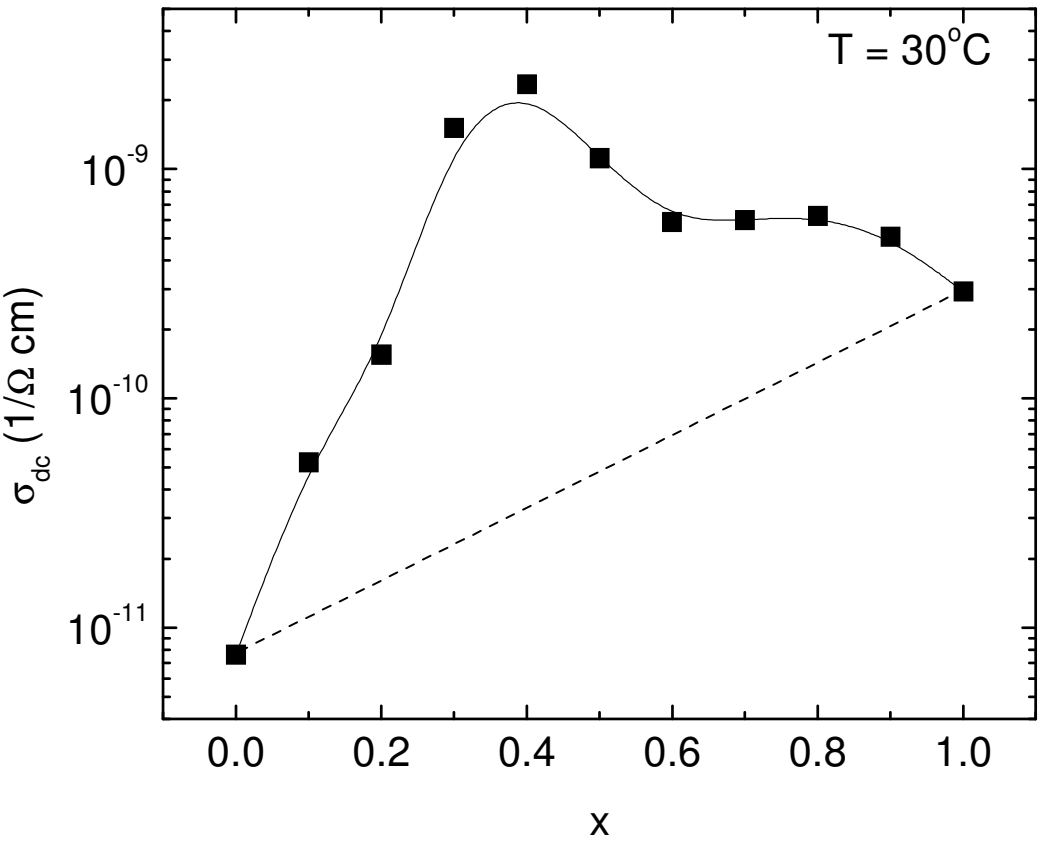

Figure 2-1

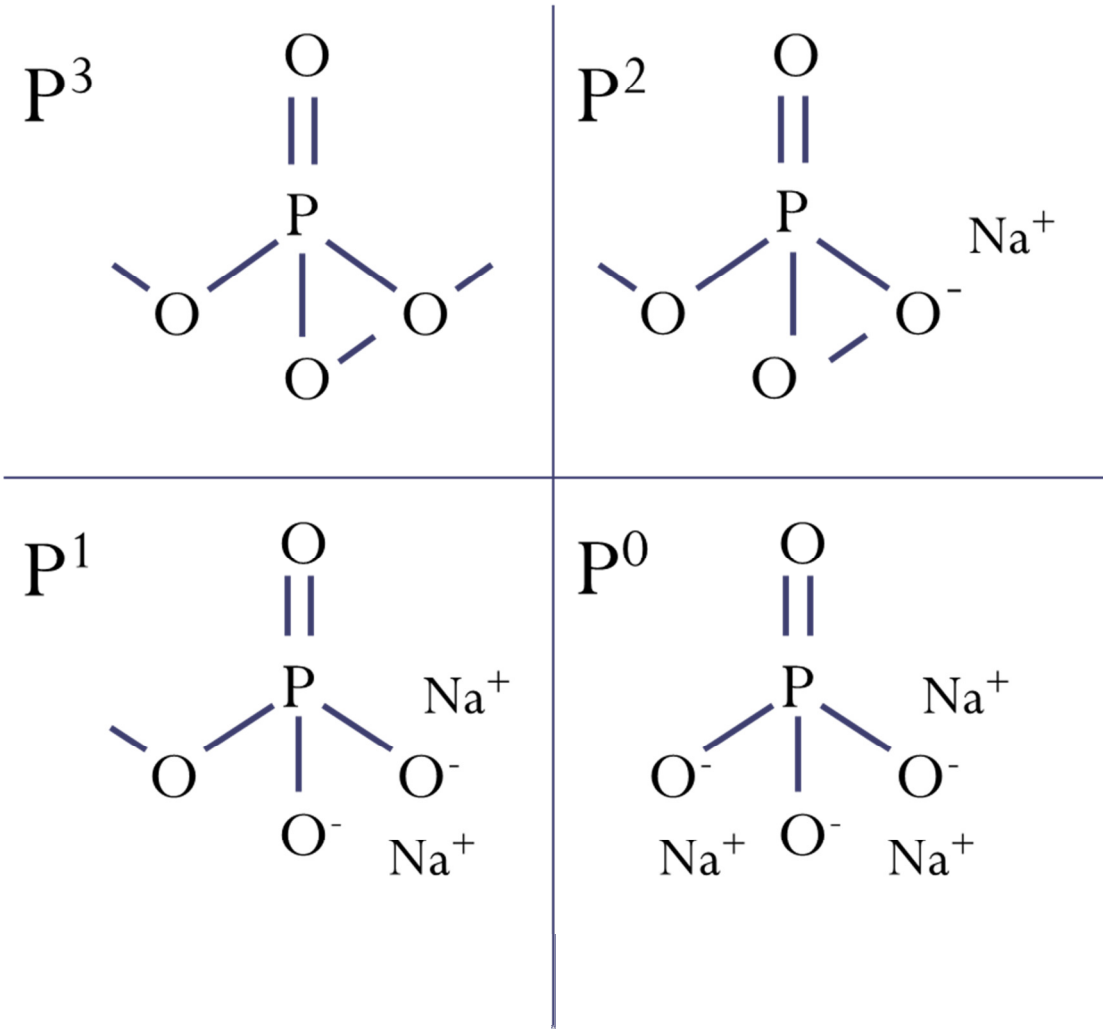

Figure 2-2

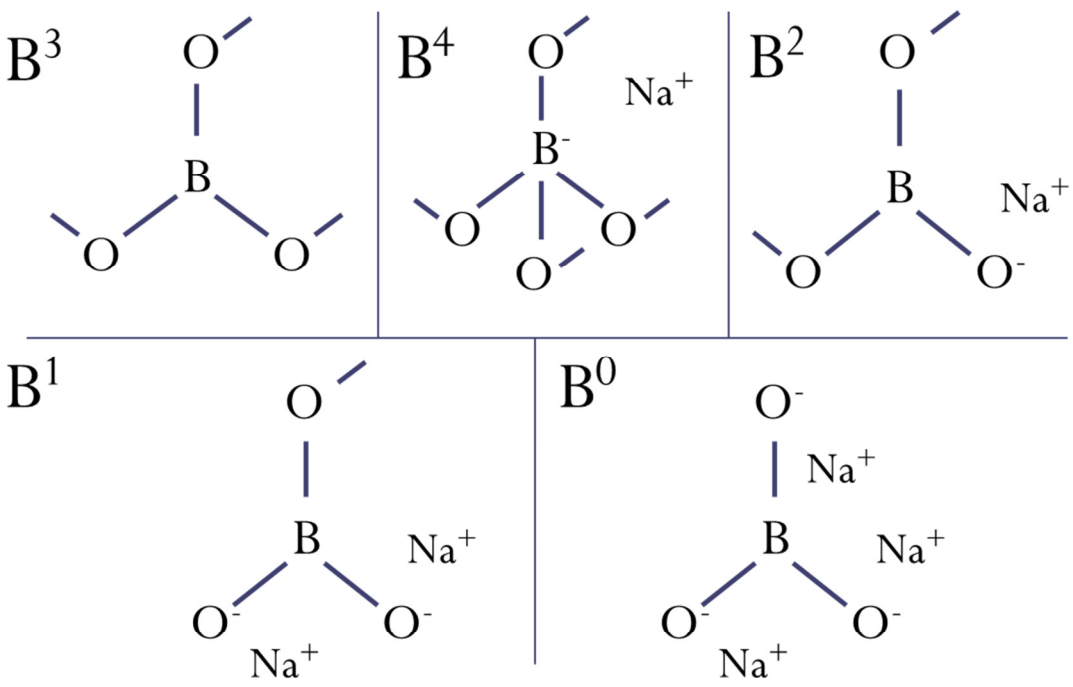

Figure 2-3

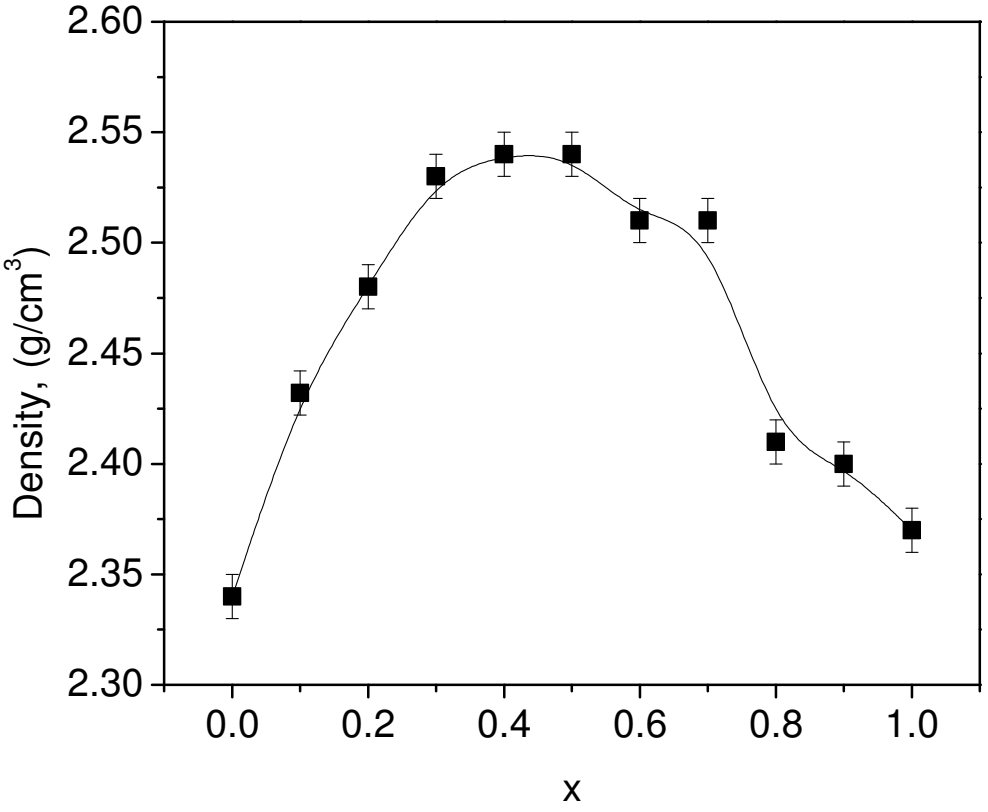

Figure 2-4

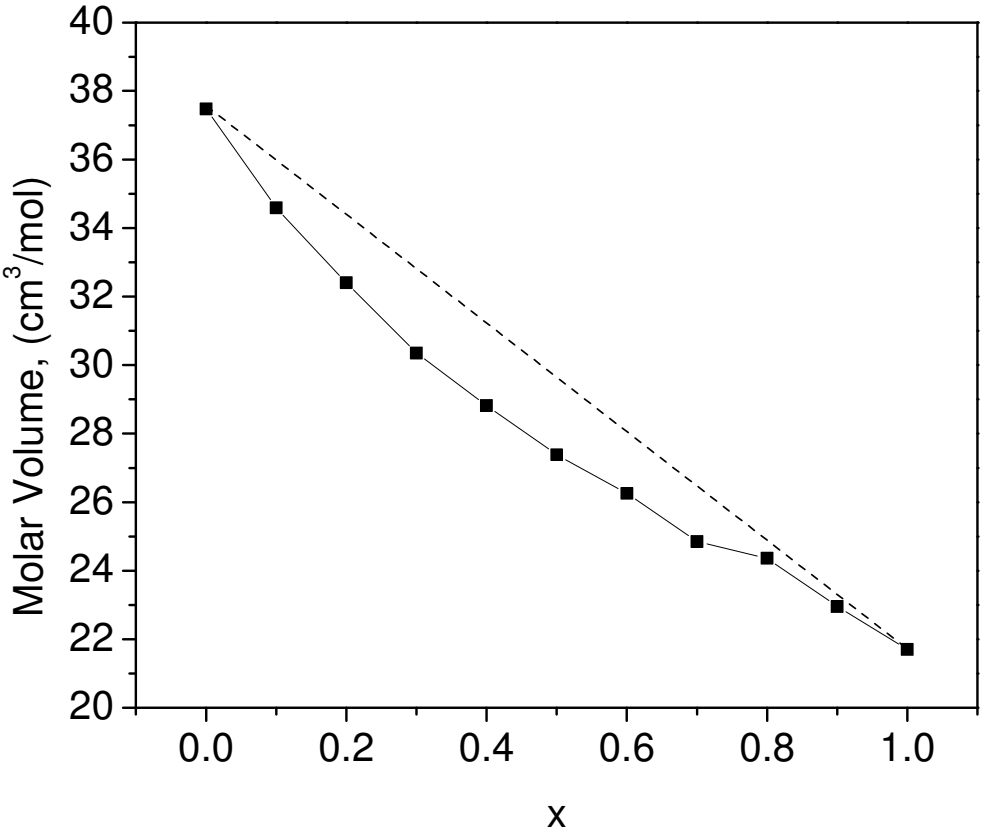
Molar Volume, (cm3/mol)
40
38
36
34
32
30
28
26
24
22
20
0.0
0.2
0.4
0.6
0.8
1.0
x

Figure 2-5

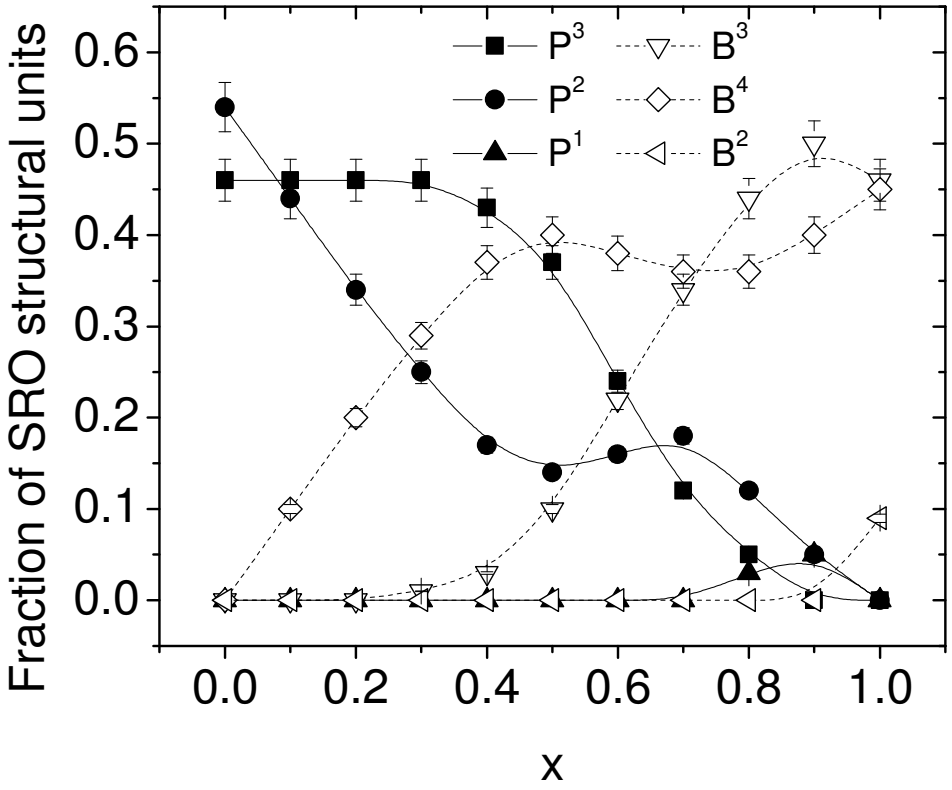
Fraction of SRO structural units
0.0
0.1
0.2
0.3
0.4
0.5
0.6
0.0
0.2
0.4
0.6
0.8
1.0
x
P3
P2
P1
B3
B4
B2

Figure 2-6

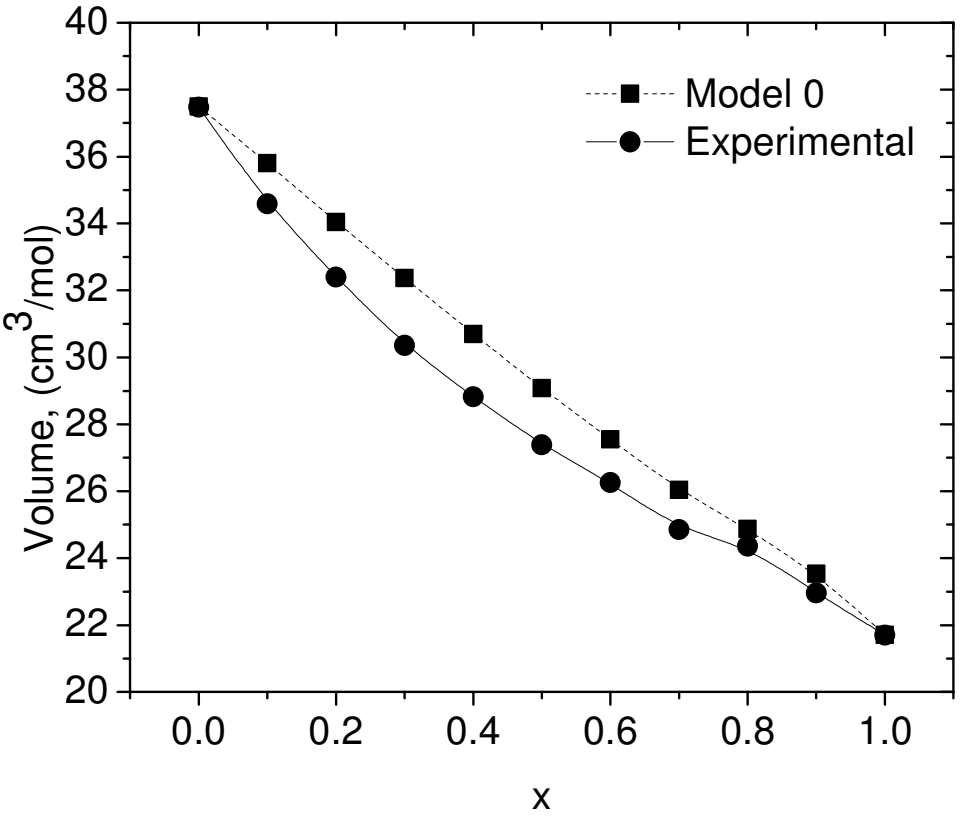
Model 0
Experimental
Volume, (cm3/mol)
x
40
38
36
34
32
30
28
26
24
22
20
0.0
0.2
0.4
0.6
0.8
1.0

Figure 2-7

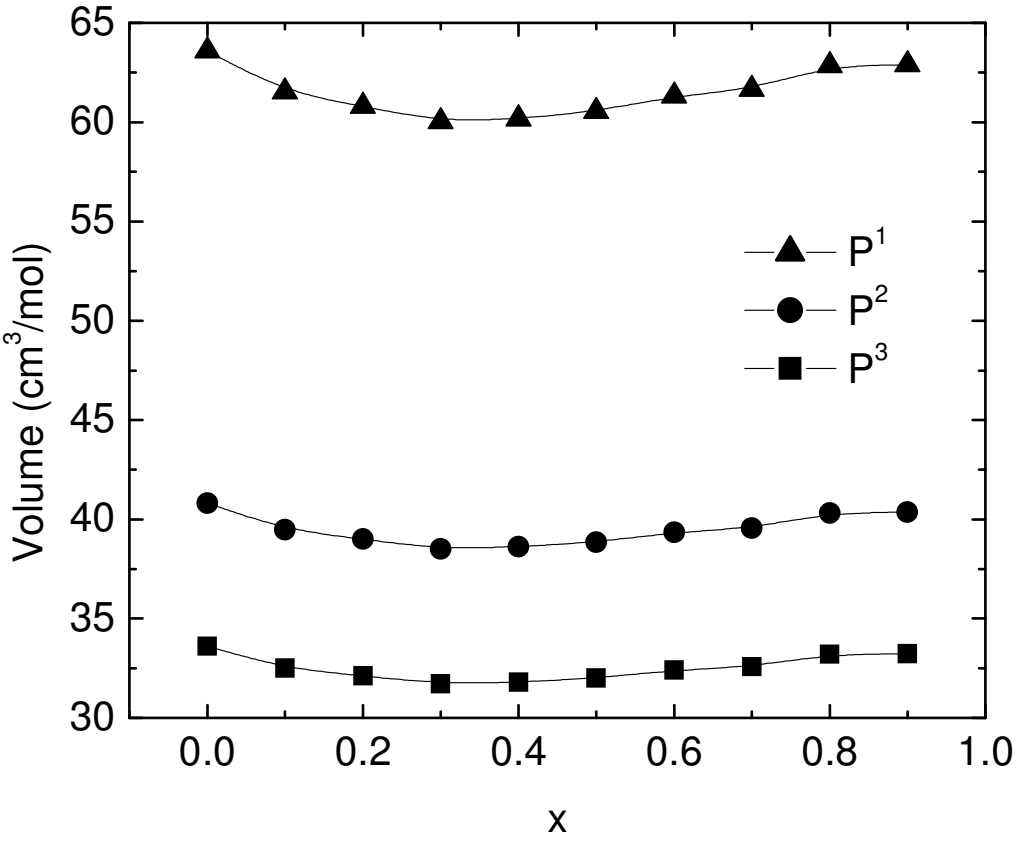

Figure 2-8

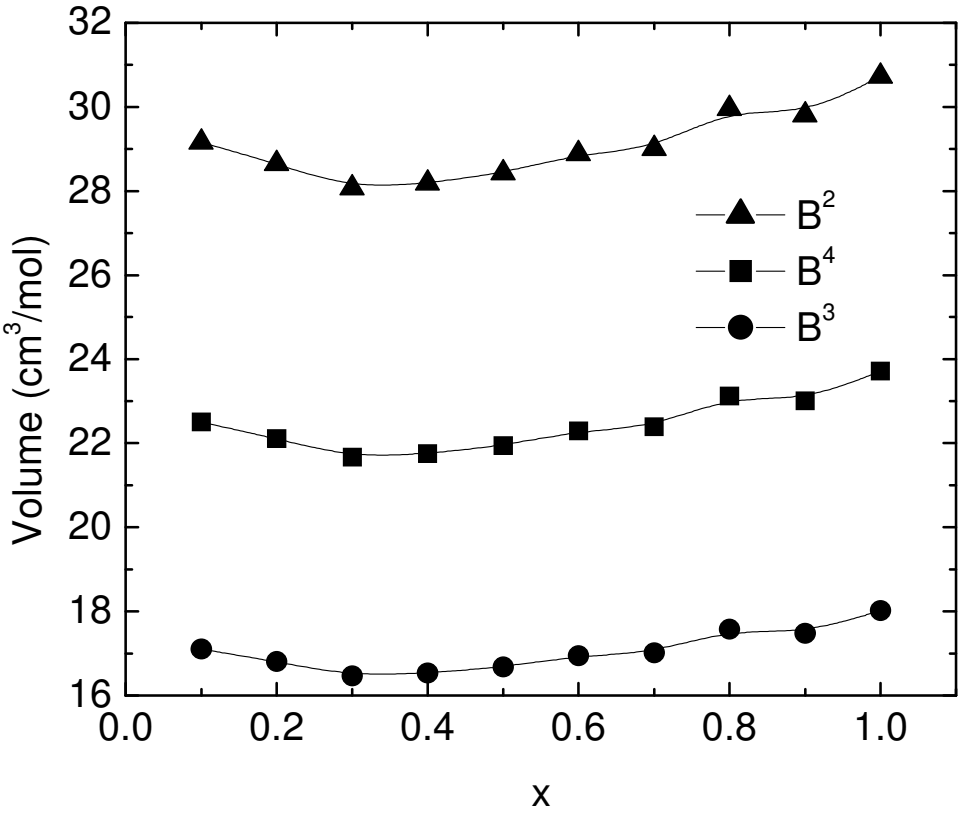

Figure 2-9

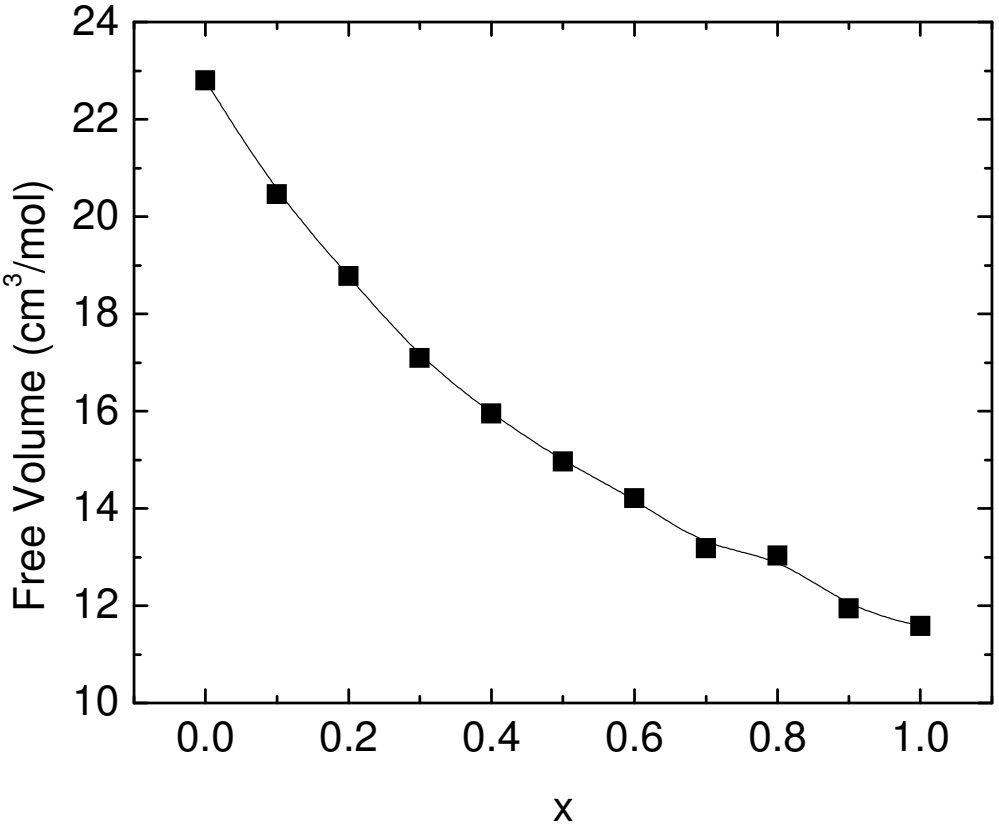

Figure 2-10

Table 2-1

x	Density	Molar Volume
	g/cm^3 ±0.01	cm^3/mol
0	2.34	37.50
0.1	2.43	34.59
0.2	2.48	32.43
0.3	2.53	30.33
0.4	2.54	28.78
0.5	2.54	27.39
0.6	2.51	26.24
0.7	2.51	24.86
0.8	2.41	24.35
0.9	2.40	22.93
1.0	2.37	21.68

Table 2-2

Glass	Density (ρ)	Density Reference	P^3	P^2	P^1	P^0	Atomic Fraction Reference
	g/cm^3		%	%	%	%	
$0.35Na_2O + 0.65P_2O_5$	2.34	This work	46	54	0	0	[28]
$0.50Na_2O + 0.50P_2O_5$	2.50	[32]	0	100	0	0	[33]
$0.60Na_2O + 0.40P_2O_5$	2.25	[19]	0	50	50	0	[22]

Table 2-3

$Na_2O + P_2O_5$	volume	$Na_2O + B_2O_3$	volume
	cm^3/mol		cm^3/mol
V_{P3}	33.61	V_{B3}	18.02
V_{P2}	40.81	V_{B4}	23.71
V_{P1}	63.60	V_{B2}	30.72

Table 2-4

Model	A	$\Delta V_P(x)$	$\Delta V_B(x)$
1	1	$\Delta V_{Total}(x)$	0
2	0	0	$\Delta V_{Total}(x)$
3	0.5	$0.5*\Delta V_{Total}(x)$	$0.5*\Delta V_{Total}(x)$
4	$\Delta V_P(0)/[\Delta V_P(0)+\Delta V_B(1)]$	$(\Delta V_P(0)/[\Delta V_P(0)+\Delta V_B(1)])*\Delta V_{Total}(x)$	$(\Delta V_B(1)/[\Delta V_P(0)+\Delta V_B(1)])*\Delta V_{Total}(x)$
5	1-x	$(1-x)*\Delta V_{Total}(x)$	$x*\Delta V_{Total}(x)$

Table 2-5

Maximum	$\left\|\frac{V_p(0) - V_p(x \neq 0)}{V_P(0)}\right\|$	$\left\|\frac{V_P(x) - V_P(x + 0.1)}{V_P(x)}\right\|$	$\left\|\frac{V_B(1) - V_B(x \neq 1)}{V_B(1)}\right\|$	$\left\|\frac{V_B(x) - V_B(x - 0.1)}{V_B(x)}\right\|$
Model 1	0.119	0.061	0.000	0.000
Model 2	0.000	0.000	0.509	0.255
Model 3	0.061	0.031	0.252	0.098
Model 4	0.076	0.039	0.184	0.068
Model 5	0.056	0.033	0.087	0.032

Table 2-6

x	P^3	P^2	P^1	B^4	B^3	B^2
	cm^3/mol	cm^3/mol	cm^3/mol	cm^3/mol	cm^3/mol	cm^3/mol
0	33.61	40.81	63.59	--	--	--
0.1	32.51	39.47	61.52	22.50	17.10	29.16
0.2	32.13	39.01	60.80	22.11	16.80	28.64
0.3	31.72	38.51	60.02	21.66	16.46	28.06
0.4	31.80	38.61	60.17	21.75	16.53	28.18
0.5	32.00	38.85	60.55	21.94	16.67	28.42
0.6	32.40	39.34	61.31	22.29	16.94	28.88
0.7	32.58	39.56	61.65	22.39	17.01	29.00
0.8	33.21	40.32	62.84	23.12	17.57	29.96
0.9	33.24	40.36	62.90	23.00	17.48	29.80
1	--	--	--	23.71	18.02	30.72

Table 2-7

x	$\frac{V_p(0) - V_p(x \neq 0)}{V_P(0)}$	$\frac{V_P(x) - V_P(x + 0.1)}{V_P(x)}$	$\frac{V_B(1) - V_B(x \neq 1)}{V_B(1)}$	$\frac{V_B(x) - V_B(x - 0.1)}{V_B(x)}$
0	0.000	0.033		
0.1	0.033	0.012	0.051	
0.2	0.044	0.013	0.068	-0.018
0.3	0.056	-0.003	0.087	-0.021
0.4	0.054	-0.006	0.083	0.004
0.5	0.048	-0.013	0.075	0.008
0.6	0.036	-0.006	0.060	0.016
0.7	0.031	-0.019	0.056	0.004
0.8	0.012	-0.001	0.025	0.032
0.9	0.011		0.030	-0.005
1			0.000	0.030
Max.	0.056	0.033	0.087	0.032
Average of absolute values		0.012		0.015

Chapter 3. The Glass Transition Temperatures of Mixed Glass Former $0.35Na_2O + 0.65[xB_2O_3 + (1-x)P_2O_5]$ Glasses

A paper published in the *Journal of Non-Crystalline Solids*[1]

Randilynn Christensen[1], Jennifer Byer[2], Garrett Olson[2], Steve W. Martin[3]

3.1 Abstract

The mixed glass former effect (MGFE) is defined as the non-linear and non-additive change in the ionic conductivity with changing glass former fraction at constant modifier composition between two binary glass former compositions. In this study, sodium borophosphate glasses, $0.35Na_2O + 0.65[xB_2O_3 + (1-x)P_2O_5]$ with $0 \leq x \leq 1$, have been prepared and their glass transition temperatures (T_g) have been examined as an alternative indicator of the MGFE and as an indicator of changes in the short range order (SRO) structural network units that could cause or contribute to the MGFE. The changes in T_g shows a positive non-additive and non-linear trend over changing glass former fraction, x. The increase in T_g is related to the increasing number of bridging oxygens (BO) in the glass samples, which is caused by the increase in the number of tetrahedral boron, B^4, units in the SRO structure.

3.2 Introduction

Energy storage is a growing concern in an ever increasingly battery driven society. Batteries power everything from cell phones to computers to medical devices to automobiles. The development of safer, smaller, and more energy dense batteries is in demand. Ion conducting glasses are an important type of solid electrolyte that can be used to answer this need. A currently unexplained change in the ionic conductivity known as the mixed glass former effect (MGFE) has been seen in many mixed glass former (MGF) glasses [2-9] such as $Li_2S + GeS_2 + GeO_2$ glasses [10] and $Li_2S + SiS_2 + GeS_2$ glasses [4]. This change in the ionic conductivity is non-linear and non-additive, and can be observed as either a decrease or an increase with changing glass former fraction at constant modifier composition between two binary systems. Figure 3-1shows an example of the MGF $Na_2O+B_2O_3+P_2O_5$ system under study in this report. A positive MGFE with a maximum deviation from linearity at x = 0.4 in the ionic conductivity has been observed in this system, as shown in Figure 3-2. While this phenomena has not been fully explained [3, 4, 8, 11], increases in the ionic conductivity of up to two orders of magnitude have been observed in other MGF glasses reported in the literature [2, 3]. Understanding the cause of the MGFE is crucial to the effort of engineering glasses with higher ionic conductivities and other improved physical properties.

It is our hypothesis, that structural changes at the short range order (SRO) level, the first coordination sphere, caused by the mixing of the two glass formers, is the underlying cause of the MGFE. In order to confirm this, the link between the physical

properties, structure, and composition of MGF glasses has been explored. To better understand the effect of composition on physical properties and structure, all components of the glasses in the present study were carefully chosen. Oxygen was selected as the anion with Na, P, and B as cations. Boron and phosphorous were chosen because of their Nuclear Magnetic Resonance spectroscopy (NMR) accessible isotopes. Oxygen was chosen as the anion because of the strong glass forming ability of B_2O_3 and P_2O_5. In addition, B_2O_3 and P_2O_5 glasses and their binary glassy counter parts, $Na_2O + B_2O_3$ and $Na_2O + P_2O_5$, have been well studied in the literature [12-17]. The binary glasses can be used to verify the x = 0 and x = 1 experimental data and provide starting points for the analysis of the ternary system. Sodium was chosen as the glass modifier and ionic charge carrier because its radioactive isotopes are useful for tracer diffusion measurements and ^{23}Na is useful in NMR studies.

3.3 Experimental methods

3.3.1 Sample Preparation

Starting materials were sodium carbonate (Na_2CO_3, 99.5% Fisher Scientific), ammonium di-hydrogen phosphate dibasic ($(NH_4)_2H_2PO_4$, 98.8% Fisher Scientific), and boric acid (H_3BO_3, 99.5% Fisher Scientific). After weighing and mixing the appropriate amounts, the starting materials were calcined in platinum crucibles between 900^oC and 1100^oC for 0.5 hour to 1 hour in an electric furnace in a fume hood. After the melt was bubble free, the crucible was removed from the furnace and allowed to cool to room

temperature. Once cool, the sample was weighed to determine the weight lost from NH_3, H_2O, and CO_2. The slightly hygroscopic samples were then transferred to a high quality nitrogen atmosphere glove box (< 5ppm O_2 and H_2O) and remelted in an electric furnace at 1000°C-1100°C for 10 minutes. To create bulk samples, the melt was quenched in preheated brass molds at temperatures 40°C below the glass transition temperature, (T_g). Bulk samples were round discs approximately 20 mm in diameter and 2 mm thick. The bulk samples were annealed 40°C below the T_g for ½ an hour, then cooled to room temperature at a rate of 2°C/minute. Due to their hygroscopic character, all samples were stored in the N_2 atmosphere glove box. All of the glasses were checked for crystallization with x-ray diffraction (XRD) and found to be x-ray amorphous. Samples were checked for weight loss and found to be within 1.5 wt.% of their target weight. Sodium, oxygen, and phosphorous levels were checked by energy dispersion spectroscopy (EDS) and found to be within ± 4 at.% of the target compositions. Infrared spectroscopy was used to ensure that all of the glasses did not contain residual NH_3, CO_2, and H_2O.

3.3.2 Glass Transition Temperatures

Glass transition temperatures (T_gs) were determined by Differential Scanning Calorimetry (DSC) using a Perkin Elmer Pyris Diamond DSC. T_gs were determined by the onset method, as shown in Figure 3-3. Powdered samples were heated and cooled at a rate of 20°C/min. Each sample was run from room temperature to ~20°C above the T_g

and back to room temperature to give all samples a common thermal history. The samples were then rerun from room temperature to 500°C to determine T_g.

3.3.3 Glass structures notation

The SRO glass structures will be identified as J^n_{mK} where J is the glass former connected to n number of bridging oxygens (BO), m is the number of the BOs bonding to glass former K and n-m if the number of BOs bonding to glass former J. For example, P^n_{mB} identifies a phosphorous atom with n number of BOs that are bonded to m number of boron atoms and (n-m) number phosphorous atoms. If no mK is denoted, then it is unknown what glass former is being bridged to by oxygen. The short range structures present in binary $Na_2O + P_2O_5$ and $Na_2O + B_2O_3$ glasses [18-20] and their compositional ranges are shown in Figure 3-4 and Figure 3-5.

3.4 Results

3.4.1 Glass Transition Temperatures

Figure 3-6 shows the experimental T_g values of $0.35Na_2O + 0.65[xB_2O_3 + (1-x)P_2O_5]$ glasses. T_g increases from 261°C at x = 0 to a maximum of 468°C at x = 0.5 and then decreases to 444°C before increasing once more to 470°C at x = 1. A maximum deviation from linear behavior is observed at x = 0.4. These results agree with values found in the literature for this glass-forming system [12, 13, 15, 21].

3.5 Discussion

3.5.1 Composition Dependence of T_g

Figure (6) shows that the T_gs of $0.35Na_2O + 0.65[xB_2O_3 + (1\text{-}x)P_2O_5]$ glasses exhibit a non-linear and non-additive trend. Both the T_g and the ionic conductivity reach a maximum deviation from linearity at x = 0.4. The non-linear and non-additive trend and the matching maximum deviations indicate that the cause of the MGFE in both the conductivity and T_g may have the same underlying structural and compositional origin. Although the T_g is dependent on thermal history, heating rate, and glass structure, all samples in this study were given the same thermal history and heating rate. Therefore, the cause of the trend in T_g can be attributed to changes in the glass structure. It is our hypothesis that the changes in glass structure are brought about by the change in the ratio of the modifier to the borate and phosphate glass formers in this system.

Increases in T_g are thought to arise from an increase in the connectivity between the SRO structures in the glass, an overall increase in the bond strengths between the various network forming atoms in the structure, or both. By examining the relationships between T_g and the number of BOs in the binary $Na_2O + P_2O_5$ and $Na_2O + B_2O_3$ glasses, we can gain insight into the T_g and BO relationships of the ternary glasses. A simple calculation of the number of BOs and NBOs for the $yNa_2O + (1\text{-}y)P_2O_5$ and $yNa_2O + (1\text{-}y)B_2O_3$ shows how the number of BOs from each glass former is affected by Na_2O modification. Bray et al. and many others, have experimentally determined the number of four coordinated boron, B^4, in the alkali borate glasses using NMR spectroscopy [22]. This resulted in an estimate of the B^4 fraction as $N_{B^4} = \frac{y}{(1-y)}$ for $y < 0.33$, Equation 3-1

to Equation 3-4. Only B^3 and B^4 units were shown to be present in the $y < 0.33$ range [23]. For compositions of $0.33 < y < 0.7$ Gupta et al. [24] estimated the fraction of B^4 units as $N_{B^4} = \left(3 - \frac{y}{(1-y)}\right) * 5$, Equation 3-5 to Equation 3-7. In this compositional range, there are B^4, B^2, B^1, and B^0 units present in these glasses [23]. However, it is not necessary to know the fractions of each trigonal group as it is assumed that each NBO on a trigonal structure corresponds to one Na^+. So, the number of Na^+ that are not bonded to B^4 groups, must be bonded to B^3 groups and are therefore equivalent to the number of NBOs from all boron trigonal structures. For $y > 0.75$ the samples are non-glass forming and are composed entirely of NBOs [23], Equation 3-8 and Equation 3-9. The results of these calculations are shown in Figure 3-7.

Hence, for a sodium borate glass, $yNa_2O + (1\text{-}y)B_2O_3$,

$$y = 0 \text{ to } y = 0.33 \qquad N_{B^4}(y) = \frac{y}{(1-y)} \qquad \textit{Equation 3-1}$$

$$N_{B^3}(y) = 1 - N_{B^4}(y) \qquad \textit{Equation 3-2}$$

$$BO(y) = M_B * N_{B^4} * 4 + M_B * N_{B^3} * 3 \qquad \textit{Equation 3-3}$$

$$NBO(y) = 0 \qquad \textit{Equation 3-4}$$

$$y = 0.33 \text{ to } y = 0.75 \quad N_{B^4}(y) = \left(3 - \frac{y}{(1-y)}\right) * 5 \qquad \textit{Equation 3-5}$$

$$NBO(y) = M_{Na} \qquad \textit{Equation 3-6}$$

$$BO(y) = M_B * N_{B^4}(y) * 4 + \left(M_B - M_B * N_{B^4}(y)\right) * 3 - N_{Na}(y) \qquad \textit{Equation 3-7}$$

$$y = 0.75 \text{ to } y = 1 \qquad NBO(y) = M_B * 3 \qquad \textit{Equation 3-8}$$

$$BO(y) = 0 \qquad \textit{Equation 3-9}$$

where M_B and M_{Na} are the total number of moles of boron and sodium, respectively, and N_j is the fraction of the SRO structural unit j present in the glass.

The fractions of all structural units for sodium phosphate glasses, $yNa_2O + (1-y)P_2O_5$, were calculated according to Van Wazer's fully ionic modifying model [20], Equation 3-10 to Equation 3-12. As all structural units are tetrahedral with 3, 2, 1, and 0 BO out of a possible 3, the number of BO and NBO can be calculated using Equation 3-13 and Equation 3-14. The results of these calculations are shown in Figure 3-8.

Hence, for a sodium phosphate glass, $yNa_2O + (1-y)P_2O_5$,

$$y = 0 \text{ to } y = 0.33 \qquad N_{P^2}(y) = \frac{y}{(1-y)} \qquad N_{P^3}(y) = 1 - N_{P^2} \qquad \textit{Equation 3-10}$$

$y = 0.33 \text{ to } y = 0.5 \quad N_{P^1}(y) = \frac{y}{(1-y)} \qquad N_{P^2}(y) = 1 - N_{P^1}$ *Equation 3-11*

$y = 0.5 \text{ to } y = 0.66 \quad N_{P^0}(y) = \frac{y}{(1-y)} \qquad N_{P^1}(y) = 1 - N_{P^0}$ *Equation 3-12*

$$BO(y) = N_{P^3}(y) * M_P * 3 + N_{P^2}(y) * M_P * 2 + N_{P^1}(y) * M_P$$ *Equation 3-13*

$$NBO(y) = N_{P^2}(y) * M_P + N_{P^1}(y) * M_P * 2 + N_{P^0}(y) * M_P * 3$$ *Equation 3-14*

where M_P is the total number of moles of phosphorous. Over the range of interest, $0 \leq y \leq 0.35$, the number of BOs in sodium phosphate glass decreases with increasing modification, y, while the number of BOs in sodium borate glass increases with y.

The results of these calculations can then be compared to the composition, y, dependence of the T_gs as reported by the literature [15-17, 25-28], and these are shown in Figure 3-9 and Figure 3-10. While there is not a direct correlation between the T_gs and the number of BO in sodium phosphate glasses, there is a good correlation in sodium borate glasses, where increasing or decreasing numbers of BO results in increasing or decreasing T_gs, respectively, although at differing rates of change. This suggests that if a correlation is found between the T_g and the number of BOs in the ternary glasses, it may come from the boron SRO structures in the glass.

In order to determine the composition dependence of the BO and to determine if the SRO structures in the ternary glasses were becoming more connected, Raman and ^{31}P and ^{11}B MAS-NMR spectroscopies were used to identify the short range order structures present in these glasses. These findings have been summarized in Figure 3-11 and will be published in a future paper [29]. From the fractions of SRO structural units in each glass, the number of BOs per glass former in each glass can be calculated from Equation 3-15.

$$\frac{Number\ of\ bridging\ oxygens}{glass\ former} = \frac{\sum f_i(x) BO_i(x)}{2} \qquad \textit{Equation 3-15}$$

and the number of NBO per glass former can be calculated from Equation 3-16

$$\frac{Number\ of\ non-bridging\ oxygens}{glass\ former} = \sum f_i(x) NBO_i\,(x) \qquad \textit{Equation 3-16}$$

where f_i is the fraction of structural unit i, BO_i is the number of BOs per structural unit i, and NBO_i is the number of NBOs per structural unit i. These are plotted in Figure 3-12 which shows that the number of BOs reaches a maximum deviation from linearity at x = 0.4, while the number of NBOs reaches a corresponding minimum at the same composition. This confirms the hypothesis that higher T_gs are related to the increased connectivity of the SRO structures in the ternary $0.35Na_2O + 0.65[xB_2O_3 + (1-x)P_2O_5]$ glasses caused by the creation of BOs through the addition of boron to the glasses. This can be seen more clearly by comparing the trends in the numbers of BOs per glass former and T_g in Figure 3-13.

An underlying question that needs to be addressed is why there is a change in the number of BOs and NBOs despite the fact that the amount of modifier Na_2O remains constant? While the total modifier to total glass former ratio, $N_{Na\ total}: N_{B+P}$ = 0.35:0.65 = 0.538:1, remains constant across this series of glasses, the amount of Na_2O modifying the borate, $N_{Na\ on\ B}: N_B$, and phosphate, $N_{Na\ on\ P}: N_P$, networks must not be in the ratio of 0.35:0.65 across the full range of x for boron and phosphorous. The changing sodium to boron ratio, $N_{Na\ on\ B}: N_B$ can be quantitatively seen through the changing ratio of B^4 to B^3 units across the composition of x. The change in the sodium to phosphorous, $N_{Na\ on\ P}: N_P$, ratio can be seen through the changing ratio of P^3, P^2, and P^1 units across the range of x, Figure 3-11. If the ratios were constant with x, the ratio of the various B and P SRO groups would not change with x. Since the fraction of SRO structural units is known from Raman and NMR spectroscopies, the $N_{Na\ on\ B}: N_B$ and $N_{Na\ on\ P}: N_P$ ratios present in the binary and ternary glasses can be calculated using Equation 3-17 to Equation 3-20.

$$N_P(x) = \left(f_{P^3}(x) + f_{P^2}(x) + f_{p^1}\right)(x) * 0.65 \qquad \textit{Equation 3-17}$$

$$N_B(x) = (f_{B^3}(x) + f_{B^4}(x) + f_{B^2}(x)) * 0.65 \qquad \textit{Equation 3-18}$$

$$N_{Na\ on\ P}(x) = \left(f_{P^2}(x) + 2 * f_{p^1}(x)\right) * 0.65 \qquad \textit{Equation 3-19}$$

$$N_{Na\ on\ B}(x) = (f_{B^4}(x) + f_{B^2}(x)) * 0.65 \qquad \textit{Equation 3-20}$$

where $N_P(x)$, $N_B(x)$, $N_{Na\ on\ P}(x)$, and $N_{Na\ on\ B}(x)$ represent the number of moles of P, B, and the Na charge compensating the phosphorous structural units, and the Na charge compensating the boron structural units, respectively, and $f_i(x)$ is the fraction of SRO structural units i as determined by NMR. As seen in Table 3-1 and Figure 3-14 when $0.1 \leq x \leq 0.6$, the borate anions are bonded to more Na per mole of B than P with the ratio $N_{Na\ on\ B}: N_B$ ranging from 1:1 to 0.63:1 and with the corresponding $N_{Na\ on\ P}: N_P$ ratios of 0.49:1 to 0.39:1. Recall, the expected ratio for both $N_{Na\ on\ P}: N_P$ and $N_{Na\ on\ B}: N_B$ in the case of equal sharing of the Na is expected to be 0.538:1. Similarly, when phosphorous is the minority glass former, $0.7 \leq x \leq 0.9$, P is bonded to more Na per mole of P than B with $N_{Na\ on\ P}: N_P$ ratios of 0.60:1 to 1.45:1 and with corresponding $N_{Na\ on\ B}: N_B$ ratios of 0.51:1 to 0.44:1. Hence, in both cases, the minority glass former is over modified compared to its state in its binary glass. Likewise, the majority glass former is under modified compared to its binary glass.

To examine this further, we now consider the question: As the fraction of glass former changes, x, how does the location of the Na change the glass former modification? From x = 0 to x = 0.6, the number of P^2 units lost with every change in x is equal to the number of B^4 units gained, , as seen in Equation 3-23 and Equation 3-24 and Table 3-2. So every Na^+ that was on a P^2 unit is moved to a B^4 unit as x goes to x + 0.1 in the $0 \leq x \leq 0.6$ range. This means that one NBO is eliminated on each P^2 unit to form one neutral P^3 unit and one additional BO is formed on each new B^4 units for every added B to the glass. In the range $0 \leq x \leq 0.6$ P^3 units are replaced by B^3 units. However, they possess

the same number of BO and NBO, so the overall change in the number of BOs and NBOs is zero in this compositional region namely:

$$\Delta P^i(x) = P^i(x) - P^i(x + 0.1) \qquad \textit{Equation 3-21}$$

$$\Delta B^i(x) = B^i(x) - B^i(x + 0.1) \qquad \textit{Equation 3-22}$$

$$\Delta P^3(x) = -\Delta B^3(x) \qquad \textit{Equation 3-23}$$

$$\Delta P^2(x) = -\Delta B^4(x) \qquad \textit{Equation 3-24}$$

where $\Delta Q^i(x)$ is the change in fraction of the structural group related to the next composition, x + 0.1.

At x = 0.7 and x = 0.8, the Na^+ that are charge compensating phosphorous units are not traded on a one-for-one basis with boron charge compensating units with increasing x, as it is observed in the x ≤ 0.6 glasses. At x = 0.7, for example, B^3 units are created, but the sodium that was charge compensating the P^2 units is now transferred to P^1 units, Equation 3-25. While there are now fewer modified structures, those remaining are more heavily modified, so the number of NBO remains unchanged. At x = 0.8, the sodium charge compensating the P^2 units are transferred to create P^1 and B^4 units, Equation 3-26. While the P^1 units create one NBO and eliminate one BO, the B^4 units create two additional BO and eliminate one NBO. At x = 0.9, all P units have been replaced by boron, Equation 3-27. Some B^3 units have been converted into B^4 and B^2

units. So, as the majority glass former goes from phosphorous to boron, the number of B^4 units increases. As the B^4 unit has the highest number of BO, it must be responsible for the increasing number of BO. This correlation can be seen more clearly in Figure 3-15.

$$\Delta P^2 + \Delta P^3 = -(\Delta P^1 + \Delta B^4) \qquad \textit{Equation 3-25}$$

$$\Delta P^2 + \Delta P^3 = -(\Delta P^1 + \Delta B^4 + \Delta B^3) \qquad \textit{Equation 3-26}$$

$$\Delta B^3 + \Delta P^2 + \Delta P^1 = -(\Delta B^4 + \Delta B^2) \qquad \textit{Equation 3-27}$$

3.6 Summary and Conclusions

A non-additive and non-linear trend with a maximum deviation from linear at x = 0.4 is seen in the T_g of $0.35Na_2O + 0.65[xB_2O_3 + (1\text{-}x)P_2O_5]$ glasses. Therefore, T_g can be used as a structural probe of the MGFE. The cause of these non-linear and non-additive changes in T_g is the changing numbers of BO on the glass forming SRO structural units which reaches a maximum deviation from linearity at x = 0.4. SRO structural studies have shown that the glass modifier to glass former ratios are not constant. Although the number of BO associated with phosphorous decreases with increasing x, the number of BOs associated with boron reaches a maximum value, ~0.4 at x = 0.8. This results in an overall change in the number of BOs that creates a positive, non-linear, non-additive trend in the T_g of these glasses. This change in the number of BO is directly caused by the changing number of B4 units as a function of x.

3.7 Acknowledgements

This research was supported by the National Science Foundation under grant number DMR-0710564 and this research support is gratefully acknowledged.

3.8 References

[1] T. Tsuchiya, T. Moriya, J. Non-Cryst. Solids, 38-39 (1980) 323-328.
[2] P.S. Anantha, K. Hariharan, Mater. Chem. Phys., 89 (2005) 428-437.
[3] D. Zielniok, C. Cramer, H. Eckert, Chem. Mater., 19 (2007) 3162-3170.
[4] A. Magistris, G. Chiodelli, M. Duclot, Solid State Ionics, 9-10 (1983) 611-615.
[5] A. Pradel, C. Rau, D. Bittencourt, P. Armand, E. Philippot, M. Ribes, Chem. Mater., 10 (1998) 2162-2166.
[6] L.F. Maia, A.C.M. Rodrigues, Solid State Ionics, 168 (2004) 87-92.
[7] V.K. Deshpande, Ionics, 10 (2004) 20-26.
[8] P. Kluvanek, R. Klement, M. Karacon, J. Non-Cryst. Solids, 353 (2007) 2004-2007.
[9] R.S. Gedam, V.K. Deshpande, Solid State Ionics, 177 (2006) 2589-2592.
[10] Y. Kim, J. Saienga, W. Martin Steve, J Phys Chem B, 110 (2006) 16318-16325.
[11] A. Agarwal, V.P. Seth, P.S. Gahlot, S. Khasa, M. Arora, S.K. Gupta, J. Alloys Compd., 377 (2004) 225-231.
[12] A. Pradel, N. Kuwata, M. Ribes, J. Phys. Condens. Matter, 15 (2003) S1561-S1571.
[13] P.S.S. Prasad, A.N.D. Rani, S. Radhakrishna, Solid State Commun., 77 (1991) 967-971.
[14] P.S.S. Prasad, A.N.D. Rani, S. Radhakrishna, Mater. Chem. Phys., 25 (1990) 487-499.
[15] R.V. Salodkar, V.K. Deshpande, K. Singh, J. Power Sources, 25 (1989) 257-263.
[16] M. Jamal, G. Venugopal, M. Shareefuddin, M. Narasimha Chary, Mater. Lett., 39 (1999) 28-32.
[17] D. Feil, S. Feller, J. Non-Cryst. Solids, 119 (1990) 103-111.
[18] J.H. Strimple, E.A. Giess, J. Am. Ceram. Soc., 41 (1958) 231-237.
[19] J.E. Shelby, J. Appl. Phys., 45 (1974) 5272-5277.
[20] J.E. Shelby, L.K. Downie, Phys. Chem. Glasses, 30 (1989) 151-154.
[21] J.J. Hudgens, S.W. Martin, J. Am. Ceram. Soc., 76 (1993) 1691-1696.
[22] U. Hoppe, E.E.-d. Metwalli, R.K. Brow, J. Neuefeind, J. Non-Cryst. Solids, 297 (2002) 263-274.
[23] K. Meyer, Phys. Chem. Glasses, 39 (1998) 108-117.
[24] A. Shaim, M. Et-Tabirou, Phys. Chem. Glasses, 42 (2001) 381-384.
[25] V.N. Naraev, A.A. Pronkin, Glass Physics and Chemistry, 24 (1998) 361-365.
[26] A.A. Pronkin, V.N. Naraev, S.Y. Eliseev, Fiz. Khim. Stekla, 14 (1988) 926-928.
[27] J.R. Van Wazer, Phosphorus and its compounds, Interscience Publishers, New York,, 1958.
[28] E.I. Kamitsos, M.A. Karakassides, Phys. Chem. Glasses, 30 (1989) 19-26.
[29] G.E. Jellison, P.J. Bray, J. Non-Cryst. Solids, 29 (1978) 187-206.
[30] H. Doweidar, G.M. El-Damrawi, Y.M. Moustafa, R.M. Ramadan, Physica B-Condensed Matter, 362 (2005) 123-132.
[31] J.M. Fernandez Navarro, J.L. Oteo Mazo, Bol. Soc. Espan. Ceram., 10 (1971) 37-70.
[32] J.F. Ducel, J.J. Videau, Mater. Lett., 13 (1992) 271-274.
[33] R. Christensen, J. Byer, G. Olson, S.W. Martin, To Be Published, (2011).
[34] R. Christensen, J. Byer, G. Olson, S.W. Martin, To Be Published, (2011).

[35] R. Christensen, J. Byer, G. Olson, W. Martin Steve, Journal of Non-Crystalline Solids, (2012).
[36] R.D. Shannon, Acta Crystallogr., Sect. A, A32 (1976) 751-767.
[37] R. Christensen, J. Byer, G. Olson, S.W. Martin, To Be Published, (2011).
[38] R. Christensen, J. Byer, G. Olson, S.W. Martin, (2011).
[39] M. Janssen, H. Eckert, Solid State Ionics, 136 (2000) 1007-1014.
[40] S.W. Martin, E.I. Cooper, C.A. Angell, J. Am. Ceram. Soc., 66 (1983) C153-C154.
[41] A.A. Ahmed, A.F. Abbas, S.M. Salman, Phys. Chem. Glasses, 26 (1985) 17-23.
[42] R.K. Brow, C.A. Click, T.M. Alam, J. Non-Cryst. Solids, 274 (2000) 9-16.
[43] P.J. Bray, J.G. O'Keefe, Phys. Chem. Glasses, 4 (1963) 37-46.
[44] C.M. Kuppinger, J.E. Shelby, J. Am. Ceram. Soc., 68 (1985) 463-467.
[45] P.K. Gupta, Collect. Pap. - Int. Congr. Glass, 14th, 1 (1986) 1-10.
[46] S. Suzuki, Y. Abe, J. Non-Cryst. Solids, 43 (1981) 141-143.
[47] A.A. Ahmed, A.F. Abbas, J. Non-Cryst. Solids, 80 (1986) 371-378.
[48] J.J. Hudgens, R.K. Brow, D.R. Tallant, S.W. Martin, J. Non-Cryst. Solids, 223 (1998) 21-31.
[49] Eisenberg.A, T. Sasada, Journal of Polymer Science Part C-Polymer Symposium, (1968) 3473-&.
[50] R. Christensen, To Be Published, (2011).

3.9 Figures

3.10 Tables

Table 3-1. The ratio of the number of moles of sodium charge compensating phosphorous SRO structural units to the number of moles of phosphorous present in the glass and the number of moles of sodium charge compensating boron SRO structural units to the number of moles of boron present in the glass.

Table 3-2. The fraction of structural units P^3, P^2, B^3, and B^4 as determined by ^{31}P and ^{11}B MAS-NMR. Change in fraction with changing x, $\Delta P = P(x)-P(x+0.1)$ and $\Delta B = B(x)-B(x+0.1)$.

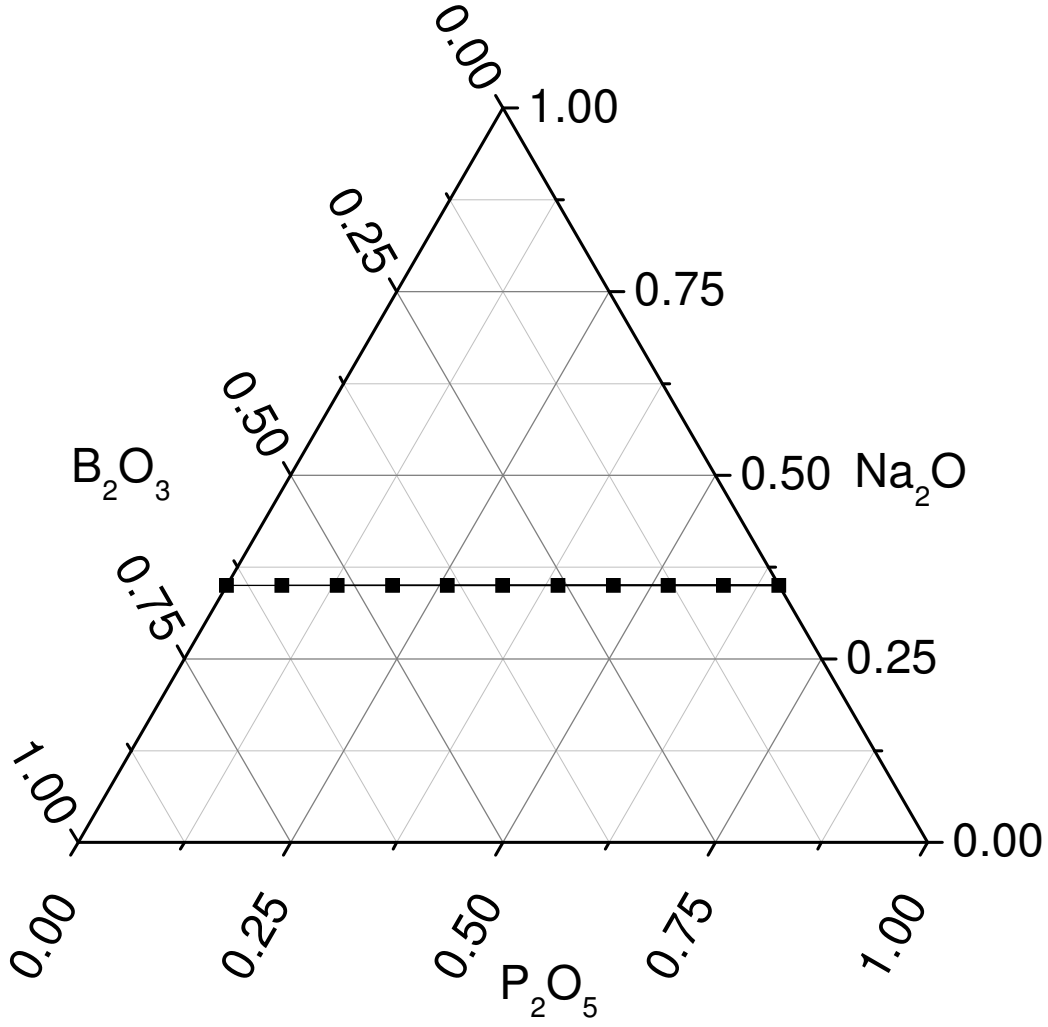
0.00
1.00
0.25
0.75
0.50
0.50
Na_2O
B_2O_3
0.75
0.25
1.00
0.00
0.00
0.25
0.50
0.75
1.00
P_2O_5

Figure 3-1

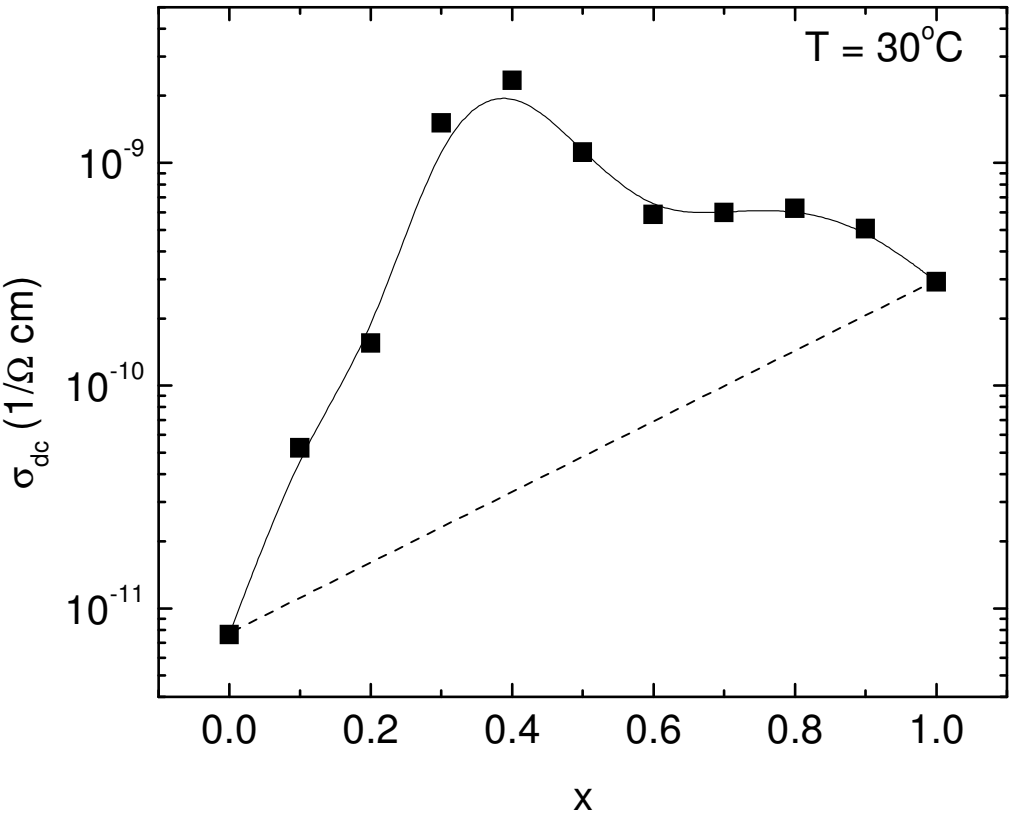

Figure 3-2

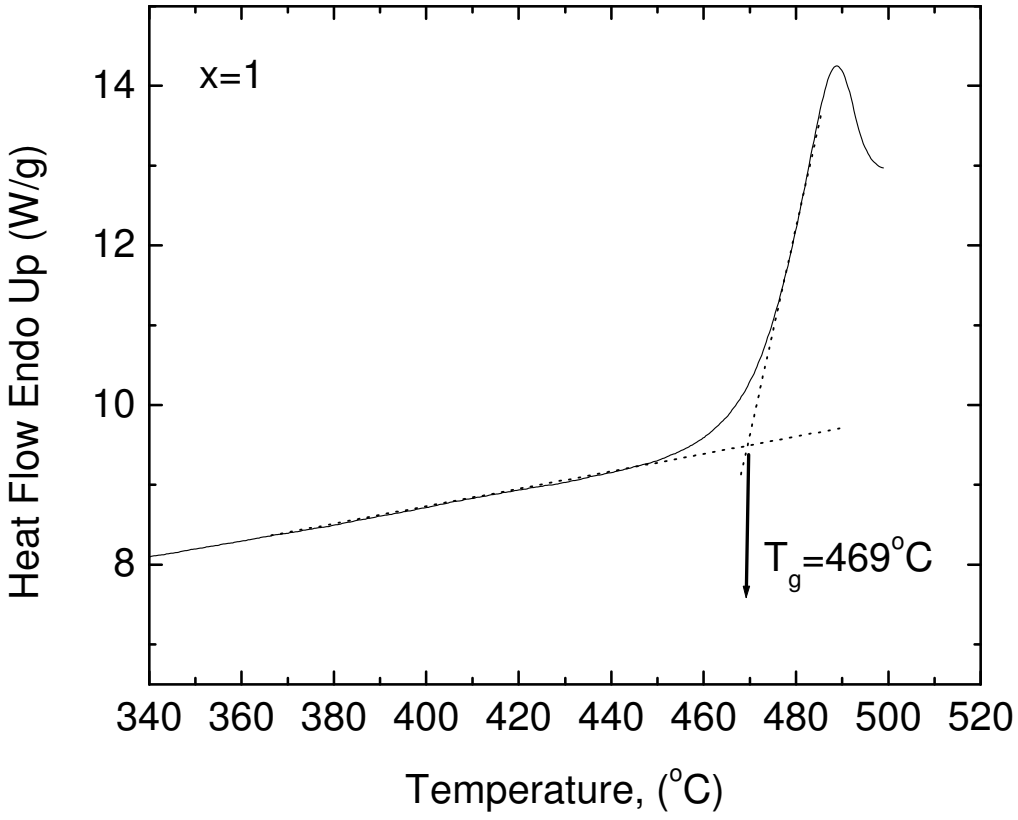
x=1
Heat Flow Endo Up (W/g)
14
12
10
8
340
360
380
400
420
440
460
480
500
520
Temperature, (°C)
T_g=469°C

Figure 3-3

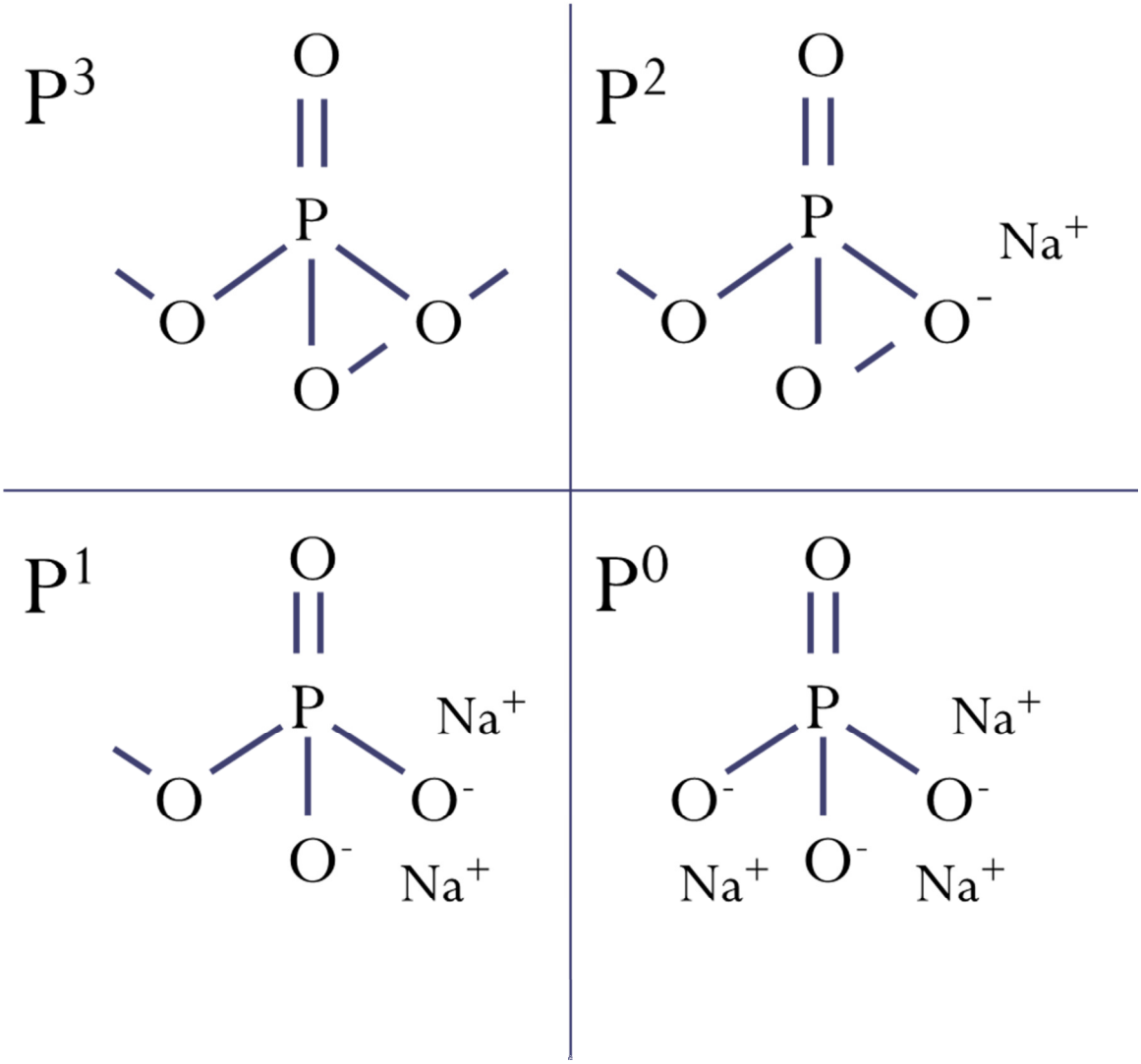

Figure 3-4

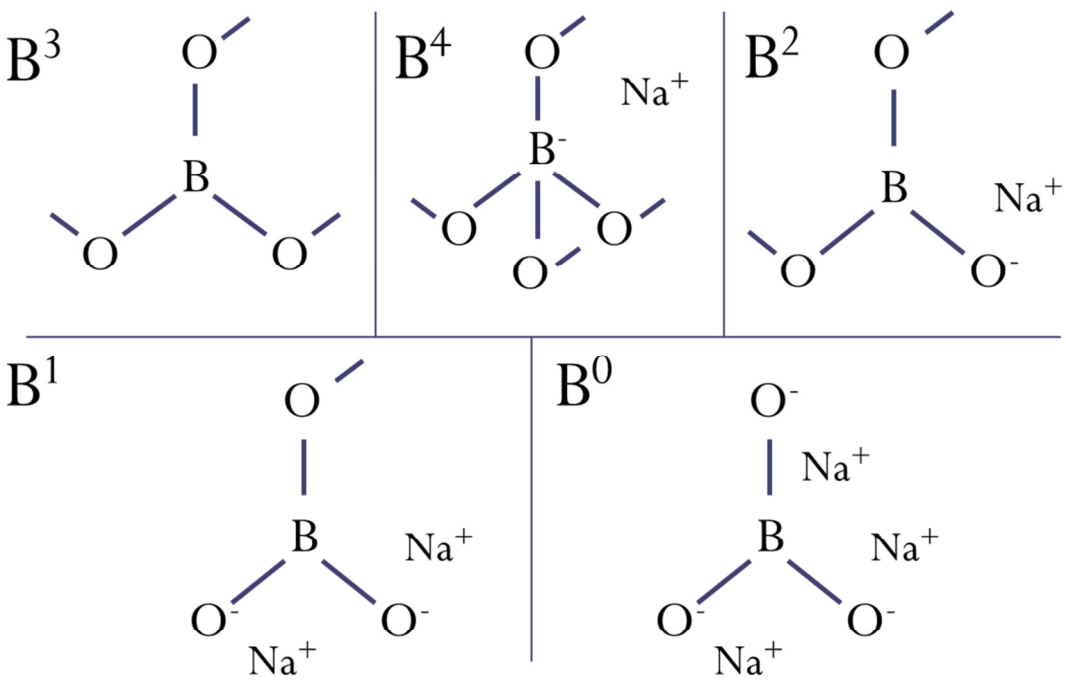

Figure 3-5

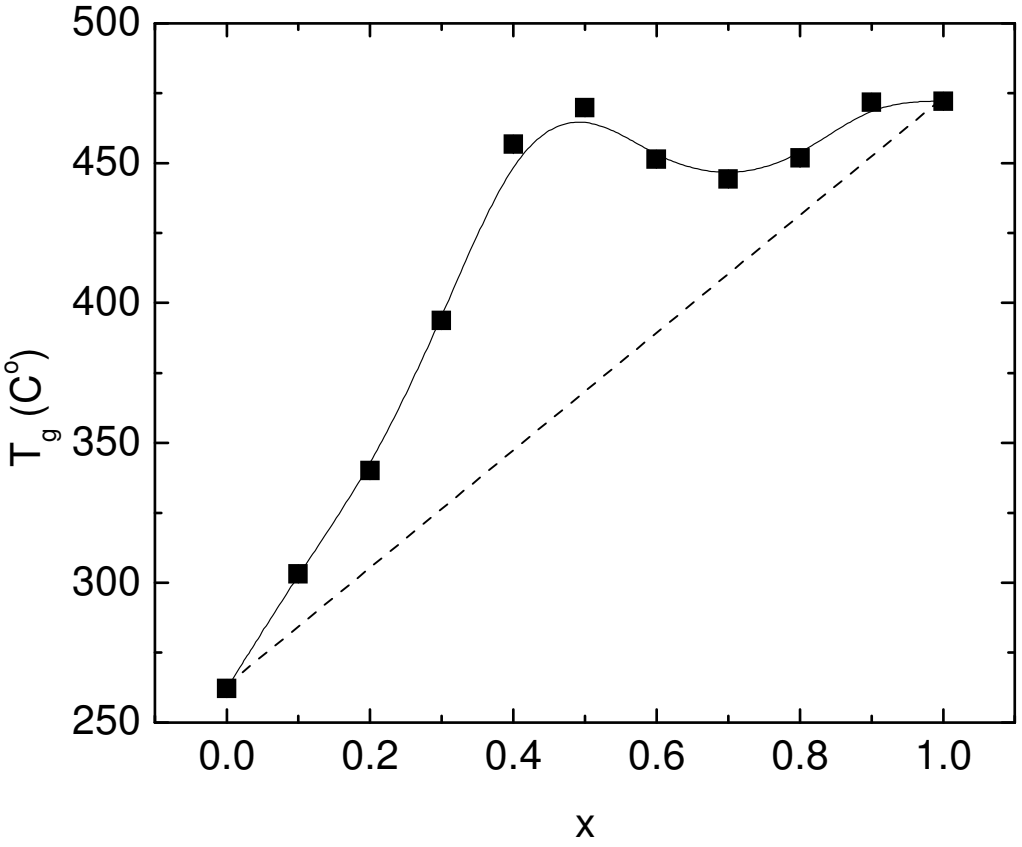

Figure 3-6

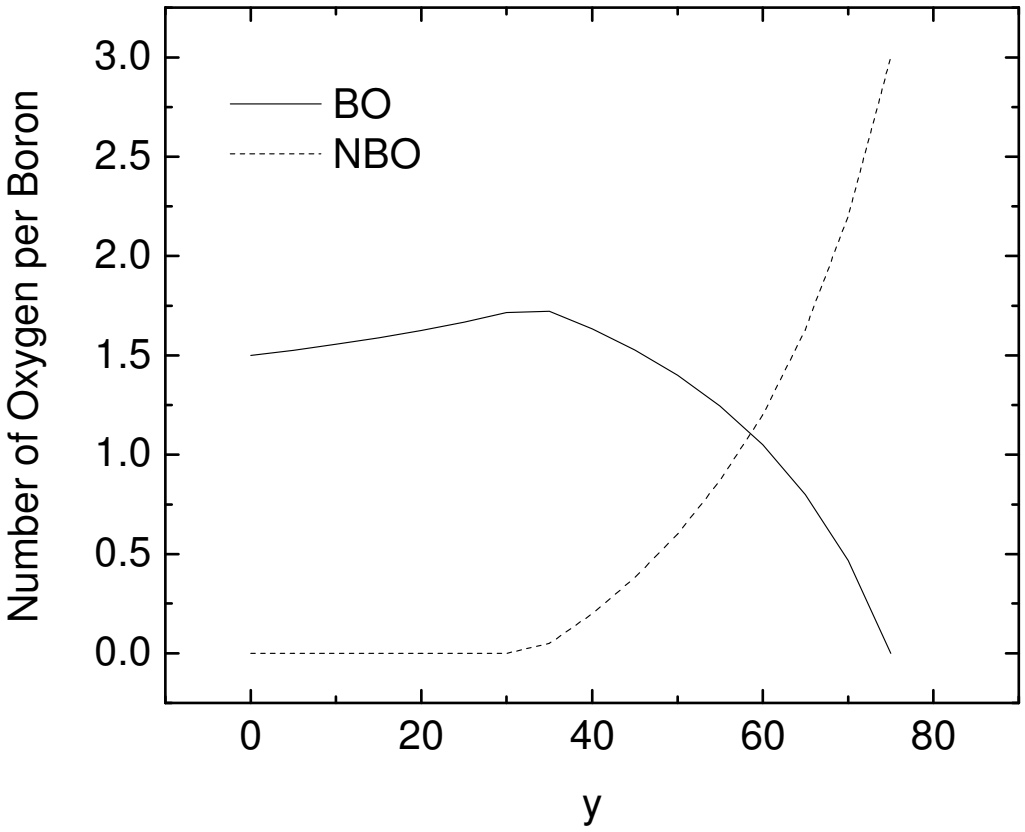
Number of Oxygen per Boron
3.0
2.5
2.0
1.5
1.0
0.5
0.0
BO
NBO
0
20
40
60
80
y

Figure 3-7

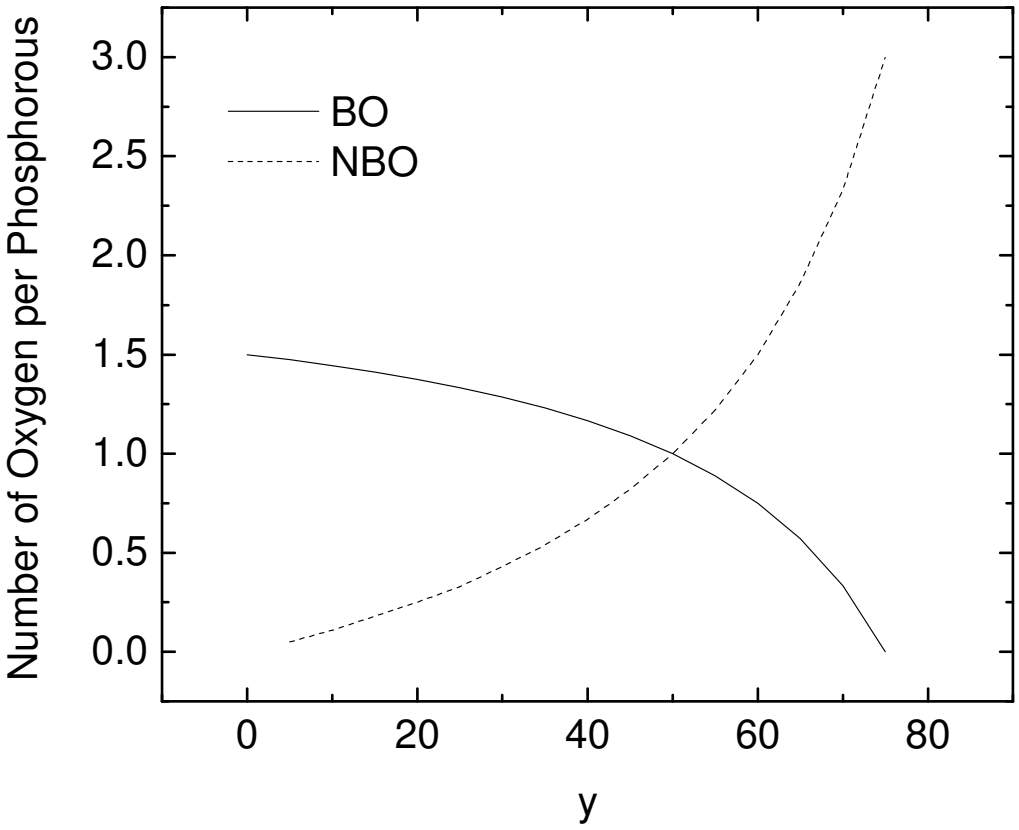
Number of Oxygen per Phosphorous
3.0
2.5
2.0
1.5
1.0
0.5
0.0
BO
NBO
0
20
40
60
80
y

Figure 3-8

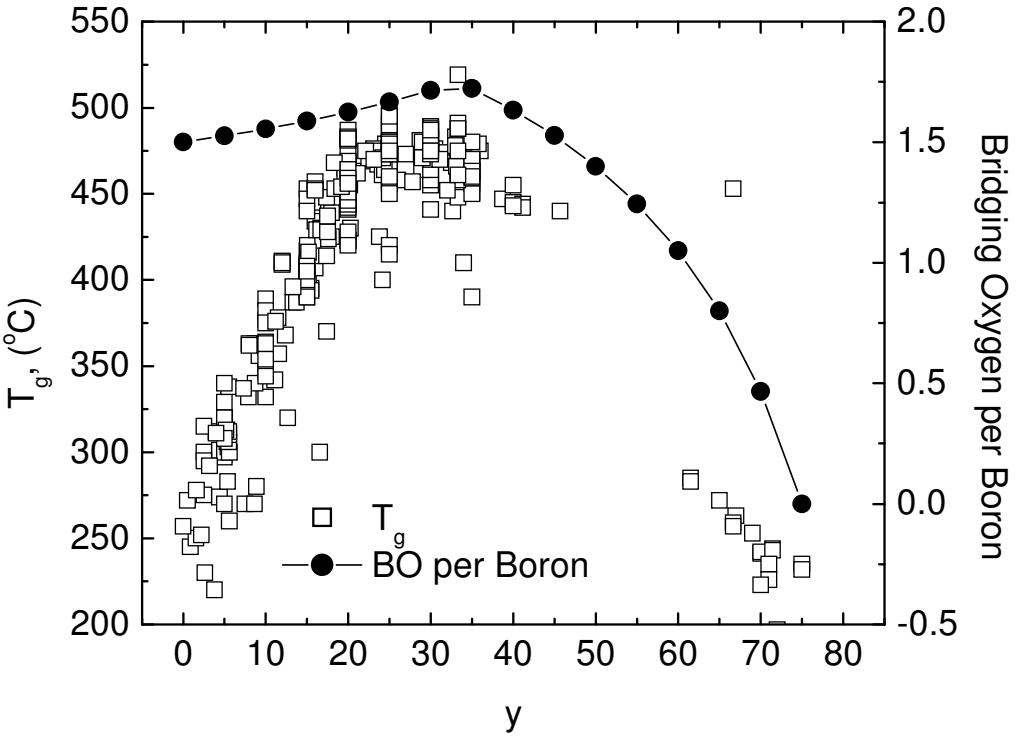
550
500
450
400
350
300
250
200
2.0
1.5
1.0
0.5
0.0
-0.5
0
10
20
30
40
50
60
70
80
y
T_g, (°C)
Bridging Oxygen per Boron
T_g
BO per Boron

Figure 3-9

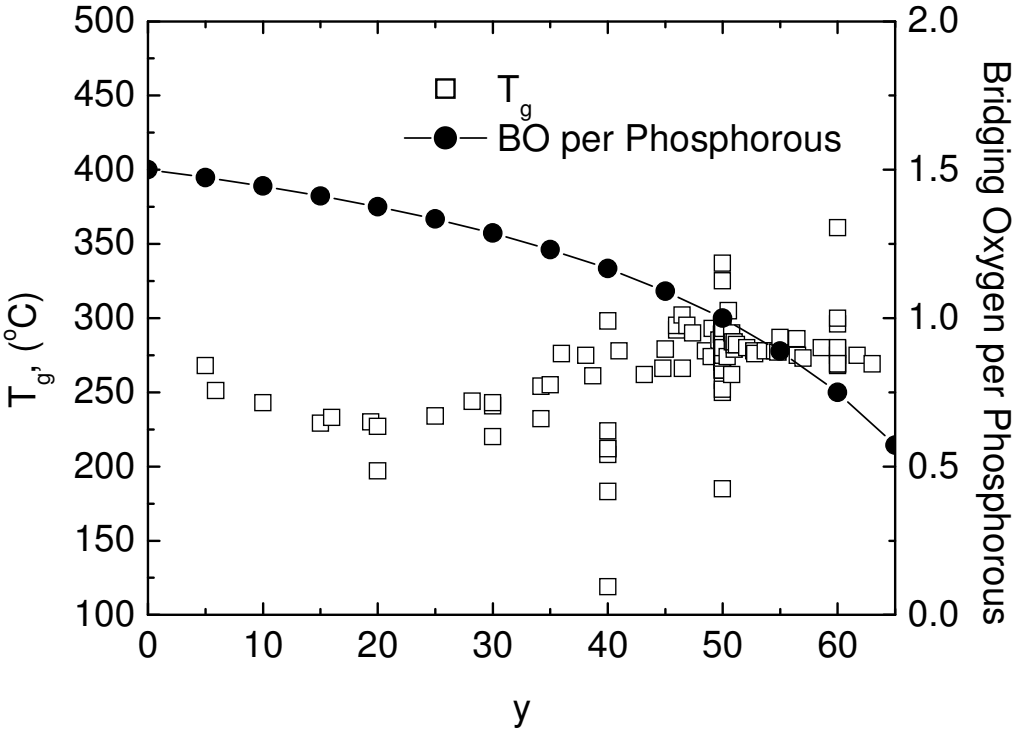
500
450
400
350
300
250
200
150
100
T_g, (°C)
0
10
20
30
40
50
60
y
2.0
1.5
1.0
0.5
0.0
Bridging Oxygen per Phosphorous
T_g
BO per Phosphorous

Figure 3-10

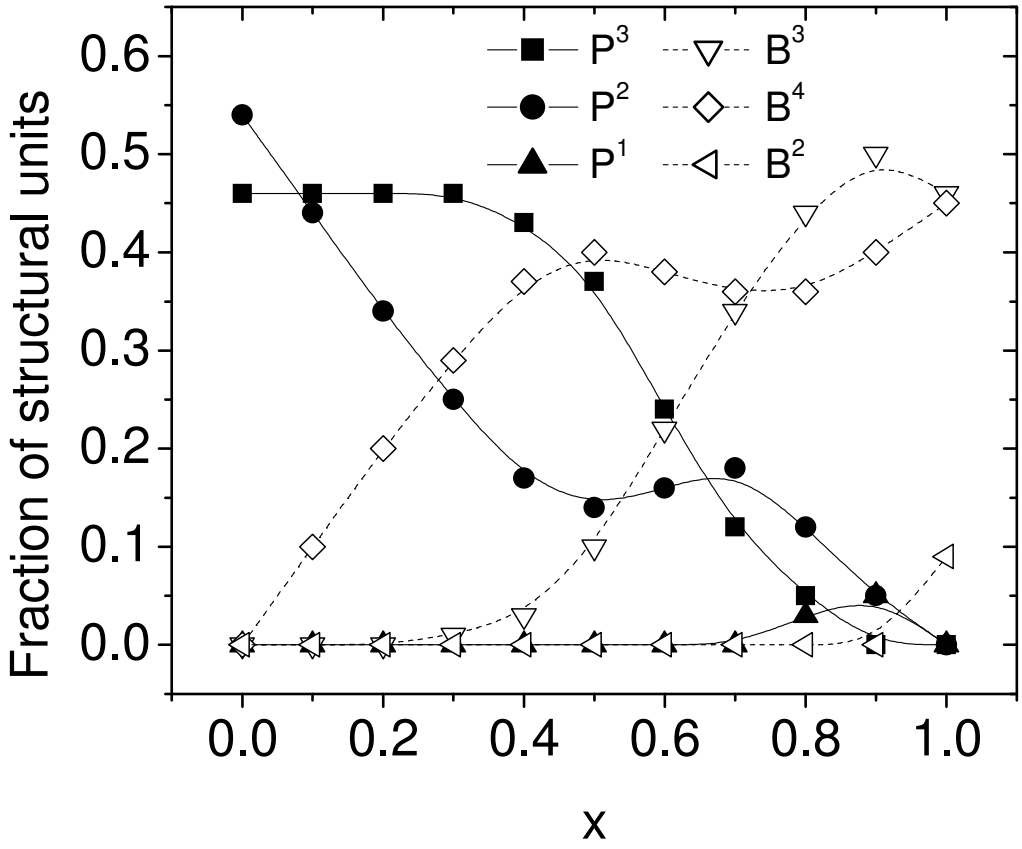
Fraction of structural units
x
0.0
0.1
0.2
0.3
0.4
0.5
0.6
0.0
0.2
0.4
0.6
0.8
1.0
P3
P2
P1
B3
B4
B2

Figure 3-11

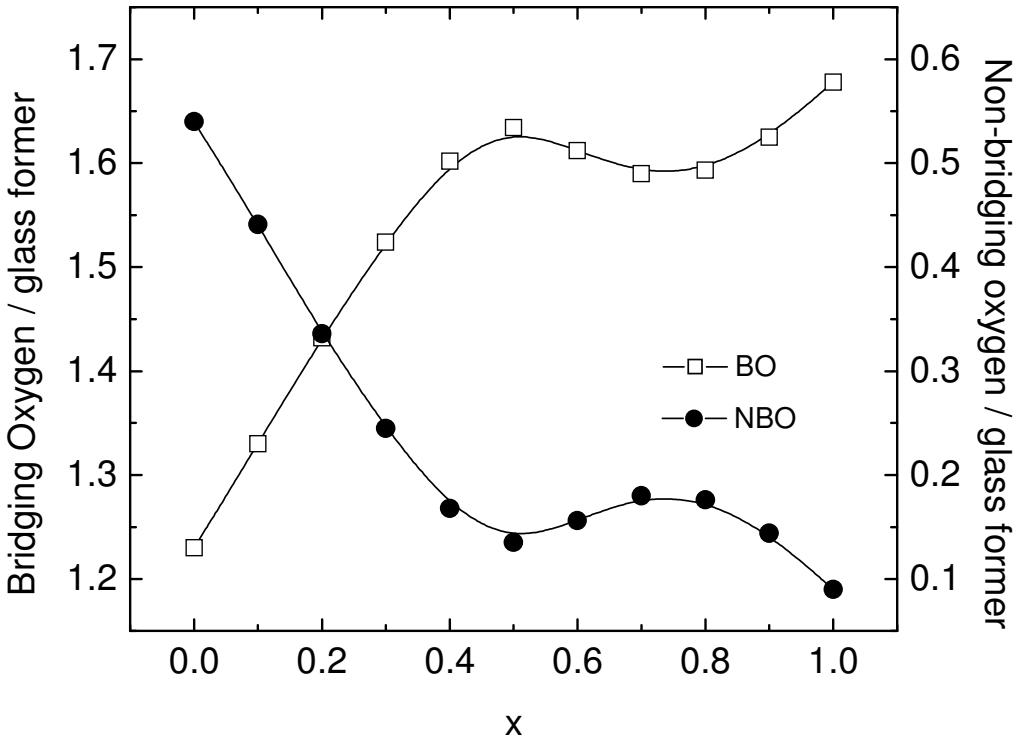
Bridging Oxygen / glass former
Non-bridging oxygen / glass former
x
BO
NBO
1.7
1.6
1.5
1.4
1.3
1.2
0.6
0.5
0.4
0.3
0.2
0.1
0.0
0.2
0.4
0.6
0.8
1.0

Figure 3-12

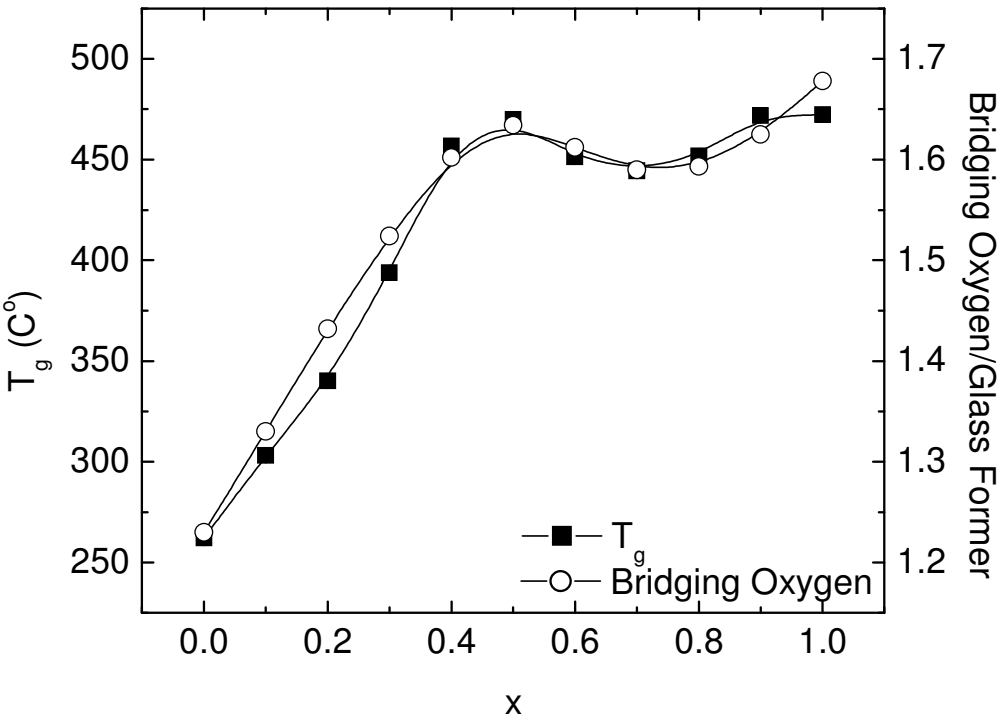
500
450
400
350
300
250
1.7
1.6
1.5
1.4
1.3
1.2
T_g (C^o)
Bridging Oxygen/Glass Former
T_g
Bridging Oxygen
0.0
0.2
0.4
0.6
0.8
1.0
x

Figure 3-13

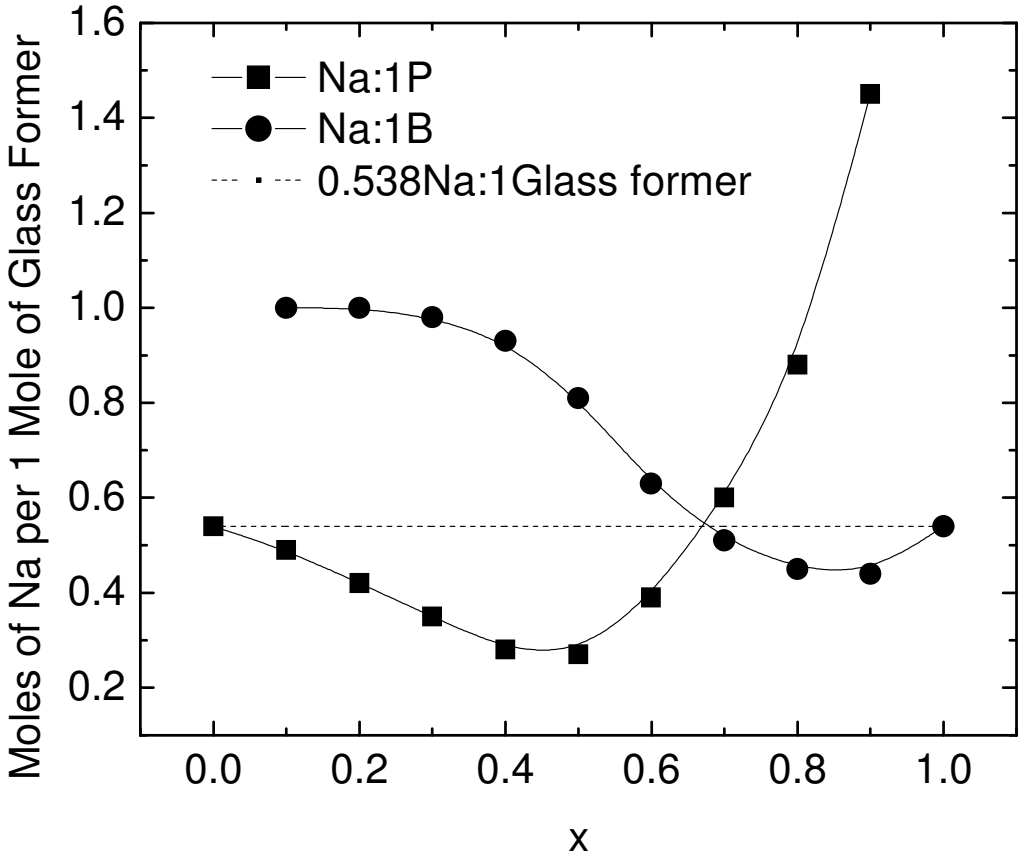
Moles of Na per 1 Mole of Glass Former
x
Na:1P
Na:1B
0.538Na:1Glass former
1.6
1.4
1.2
1.0
0.8
0.6
0.4
0.2
0.0
0.2
0.4
0.6
0.8
1.0

Figure 3-14

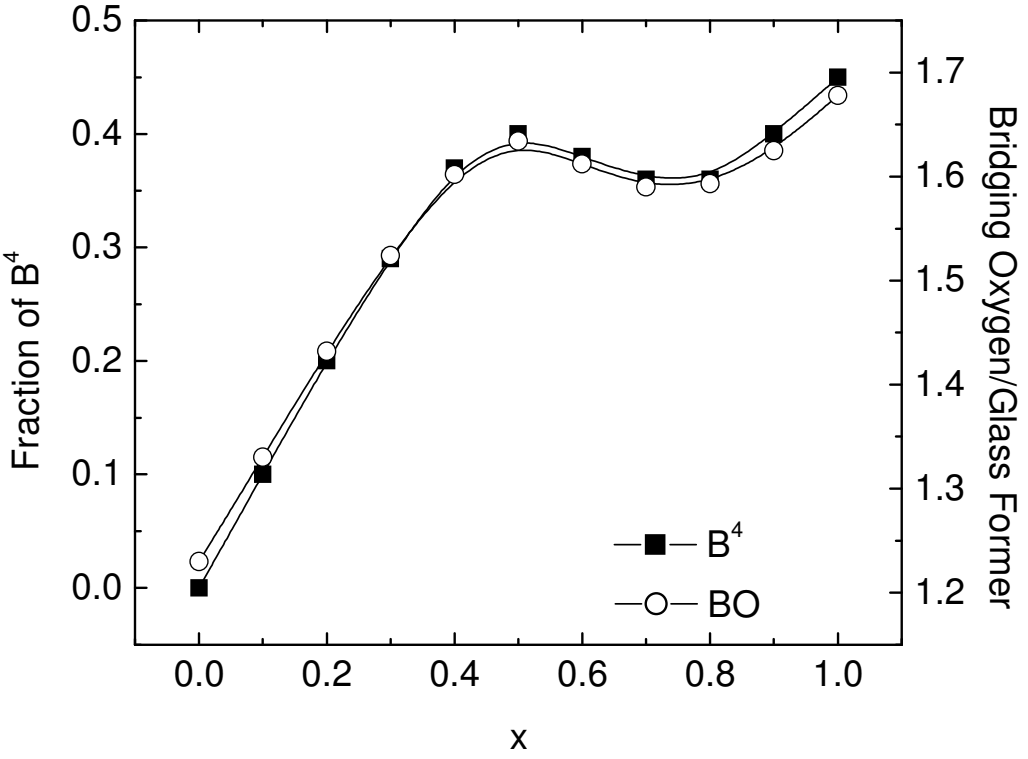
Fraction of B4
Bridging Oxygen/Glass Former
x
B4
BO
0.0
0.1
0.2
0.3
0.4
0.5
1.2
1.3
1.4
1.5
1.6
1.7
0.0
0.2
0.4
0.6
0.8
1.0

Figure 3-15

Table 3-1

x	Na:P	Na:B
0	0.54:1	0.00:1
0.1	0.49:1	1.00:1
0.2	0.42:1	1.00:1
0.3	0.35:1	0.98:1
0.4	0.28:1	0.93:1
0.5	0.27:1	0.81:1
0.6	0.39:1	0.63:1
0.7	0.60:1	0.51:1
0.8	0.88:1	0.45:1
0.9	1.45:1	0.44:1
1	0.00:1	0.54:1

Table 3-2

x	P^3	ΔP^3	B^3	ΔB^3	P^2	ΔP^2	B^4	ΔB^4	P^1	ΔP^1	B^2	ΔB^2
0	0.46	0.00	0.00	0.00	0.54	0.10	0.00	-0.10	0.00	0.00	0.00	0.00
0.1	0.46	0.00	0.00	0.00	0.44	0.11	0.10	-0.10	0.00	0.00	0.00	0.00
0.2	0.46	0.01	0.00	-0.01	0.34	0.09	0.20	-0.09	0.00	0.00	0.00	0.00
0.3	0.46	0.02	0.01	-0.02	0.25	0.08	0.29	-0.08	0.00	0.00	0.00	0.00
0.4	0.43	0.07	0.03	-0.07	0.17	0.03	0.37	-0.03	0.00	0.00	0.00	0.00
0.5	0.37	0.12	0.10	-0.12	0.14	-0.02	0.40	0.02	0.00	0.00	0.00	0.00
0.6	0.24	0.12	0.22	-0.12	0.16	-0.02	0.38	0.02	0.00	0.00	0.00	0.00
0.7	0.12	0.07	0.34	-0.10	0.18	0.06	0.36	0.00	0.00	-0.03	0.00	0.00
0.8	0.05	0.05	0.44	-0.07	0.12	0.07	0.36	-0.03	0.03	-0.02	0.00	0.00
0.9	0.00	0.00	0.50	0.04	0.05	0.05	0.40	-0.05	0.05	0.05	0.00	-0.09
1	0.00		0.46		0.00		0.45		0.00		0.09	

Chapter 4. Structural Studies of Mixed Glass Former 0.35 Na_2O + 0.65 [xB_2O_3 + (1-x)P_2O_5] Glasses by Raman and ^{11}B and ^{31}P Magic Angle Spinning Nuclear Magnetic Resonance Spectroscopy

A paper to be submitted to the Journal of Non-Crystalline Solids

Randilynn Christensen[1], Jennifer Byer[2], Garrett Olson[2], Steve W. Martin[3]

4.1 Abstract

The mixed glass former effect (MGFE) is defined as a non-linear and non-additive change in the ionic conductivity with changing glass former composition at constant modifier composition. In this study, sodium borophosphate glasses, 0.35 Na_2O + 0.65 [xB_2O_3 + (1-x)P_2O_5], $0 \leq x \leq 1$ glasses, which have been shown to exhibit a positive MGFE, have been prepared and examined through Raman and ^{11}B and ^{31}P Magic Angle Spinning Nuclear Magnetic Resonance Spectroscopy. Through examination of the short range order structures found in the glasses, those in the first coordination sphere around the glass forming cations boron (B) and phosphorous (P), it was determined that the minority glass former, P for $0.7 \leq x \leq 0.9$ and B for $0.1 \leq x \leq 0.7$, that is they are "over modified" and contain more Na_2O charge compensations

relative to the binary sodium borate and sodium phosphate glasses, respectively. The changes in the intermediate range order structures, those in the second coordination sphere around the glass forming cations B and P, were observed in the changes in chemical shifts over the composition range x. The changes observed in the chemical shifts with x are too large to be caused solely by changing Na:Glass Former (GF) ratios and indicates that cross network bonding between phosphorous to boron through bridging oxygen (P-O-B) must be a major contributor to the intermediate range order structure of these glasses. While not fully developed, a first order thermodynamic analysis based upon the Gibbs Free Energies of formation of the various phases in this system has been applied and can be used to account for preferential formation of tetrahedral boron groups in these glasses and this structural change is a predominate cause of the changing modifier to glass former ratio with composition x in these ternary mixed glass former glasses.

4.2 Introduction

4.2.1 Background

Energy storage is a growing concern in an ever increasingly battery driven society. Batteries power everything from cell phones to computers to medical devices to automobiles. The development of safer, smaller, and more energy dense batteries is in demand. Ion conducting glasses are an important type of solid electrolyte that may be used to answer this need. A currently unexplained change in the ionic conductivity in

glasses known as the mixed glass former effect (MGFE) has been seen in many mixed glass former (MGF) glasses [1-8] such as $Li_2S + GeS_2 + GeO_2$ glasses [9] and $Li_2S + SiS_2 + GeS_2$ glasses [3]. This change in the ionic conductivity is non-linear and non-additive and can be observed as either a decrease or an increase in the ionic conductivity with changing glass former fraction at constant modifier composition between the two binary glass forming systems. A positive MGFE with a maximum deviation from linearity at x = 0.4 in the ionic conductivity has been observed in the 0.35Na2O+0.65[xB2O3+(1-x)P2O5] glasses under study in this work and is shown in Figure 4-1 [10]. While this phenomena has not been fully explained [2, 3, 7, 11], increases in the ionic conductivity of up to two orders of magnitude have been observed in other MGF glasses reported in the literature [1, 2]. Understanding the cause of the MGFE is crucial to the effort of engineering glasses with higher ionic conductivities and other improved physical properties.

It is our hypothesis that structural changes at the short range order (SRO) levels and intermediate range order (IRO), caused by the mixing of the two glass former networks, are the underlying cause of the MGFE. These changes at the SRO level must necessarily effect changes at the intermediate range order (IRO) level was well. In order to confirm these hypotheses, the link between the physical properties, structure, and composition of MGF glasses is being explored.

To better understand the effect of composition on the physical properties and structure, all components of the glasses in the present study were carefully chosen.

Oxygen was selected as the anion with Na, P, and B as the cations. Boron and phosphorous were chosen because of their nuclear magnetic resonance spectroscopy (NMR) accessible isotopes, ^{11}B and ^{31}P. Oxygen was chosen as the anion because of the strong glass forming ability of B_2O_3 and P_2O_5. Sodium was chosen as the glass modifier and ionic charge carrier because its radioactive isotope is useful for tracer diffusion measurements and ^{23}Na is useful in NMR studies. In addition, B_2O_3 [12-14] and P_2O_5 [15] glasses, their binary glassy counter parts, $Na_2O + B_2O_3$ [14, 16] and $Na_2O + P_2O_5$ [17-20], and some ternary alkali borophosphate glasses [8, 21-24] have been well studied in the literature. The structures of the binary glasses have been examined and then used to verify the x = 0 and x = 1 experimental data and provide starting points for the analysis of the structures of the ternary sodium borophosphate glass forming system.

4.2.2 Glass Structure Notations

The short range glass structures will be referred to as J^n_{mK} where J is the glassformer connected to n number of bridging oxygens (BOs), m number of the BOs bonding to glass former K and n-m BOs go to glass former J. For example, P^n_{mB} indicates a phosphorous atom with n number of BOs that bond to m number of boron atoms and (n-m) number phosphorous atoms. If no mK is denoted then it is unknown what glass former is being bridged to by oxygen. The short range structures present in the binary glasses and their compositional ranges are shown in Figure 4-2 and Figure 4-3.

4.2.3 Glass Modifer:Glass Former Ratio Notation

When discussing the number of sodium ions ionicially bound to a glass former structural unit, the ratio Na:B or Na:P will be used. Na represents the mole fraction of Na ionically bonded to the glass former they are in ratio with, B or P. B and P represents the total mole fraction of boron or phosphorous, respectively. If this ratio remained contant across the full composition range of glasses, x, then at each composition the ratio would be constant and equal to 2*0.35:2*0.65=0.35:0.65 for both B and . At each composition x, the actual amount of Na, B, and P would be 2*0.35, 2*x*0.65, and 2*(1-x)*0.65. However, we find that the sharing of Na is not equal across the compositions of glasses. For example, a Na:B ratio of 0.65:1.17, which reduces to 0.35:0.585, in a $0.35Na_2O$ + $0.65[x\ B_2O_3 + (1-x)P_2O_5]$ glass at x = 0.9, means that 0.65 moles or 100% of the Na in the glass is ionicially bonded to boron structural units and that there are 1.17 moles of boron. I this case, the ratio of Na:P must be 0:0.065, where there are zero moles of Na ionically bonded to the 0.13 moles of phosphorous present in the glass. Even when the unequal sharing of the Na occurs, the ratio of modifier to total glass former of Na:[B+P] is always equal to 0.35:0.65.

4.3 Experimental Methods

4.3.1 Sample Preparation

The starting materials were sodium carbonate (Na_2CO_3, 99.5% Fisher Scientific), ammonium di-hydrogen phosphate dibasic ($(NH_4)_2H_2PO_4$, 98.8% Fisher Scientific), and

boric acid (H_3BO_3, 99.5% Fisher Scientific). After weighing and mixing the appropriate amounts, the starting materials were calcined in platinum crucibles between 900°C and 1100°C for 0.5 hour to 1 hour in an electric furnace in a fume hood. After the melt was bubble free, the crucible was removed from the furnace and allowed to cool to room temperature. Once cool, the sample was weighed to determine the weight lost from NH_3, H_2O, and CO_2. The slightly hygroscopic samples were then transferred to a high quality nitrogen atmosphere glove box (< 5ppm O_2 and H_2O) and remelted in an electric furnace at 1000°C-1100°C for 10 minutes. To create bulk samples, the melt was quenched in preheated brass molds at temperatures 40°C below the glass transition temperature, (T_g). Bulk samples were round discs approximately 20 mm in diameter and 2 mm thick. The bulk samples were annealed 40°C below the T_g for 0.5 hour, then cooled to room temperature at a rate of 2°C/minute. Due to their hygroscopic character, all samples were stored in the N_2 atmosphere glove box. All of the glasses were checked for crystallization with x-ray diffraction (XRD) and found to be x-ray amorphous. Samples were checked for weight loss and found to be within ±1.5 wt. % of their target weight. Sodium, oxygen, and phosphorous concentrations were checked by energy dispersive spectroscopy (EDS) and found to be within ± 4 at.% of the target compositions. Infrared spectroscopy was used to ensure that all of the glasses did not contain residual NH_3, CO_2, and H_2O.

4.3.2 Raman Spectroscopy

Raman spectra were collected using a Renishaw InVia Raman Spectrometer Microscope. An Argon laser at 488 nm with 20 mW of power was used for excitation.

4.3.3 Magic Angle Spinning – Nuclear Magnetic Resonance (MAS-NMR)

Single pulse ^{31}P and ^{11}B MAS NMR spectra were obtained using a Bruker AV-600 Spectrometer, using a 4 mm zirconia probe spinning at 12 and 10 kHz respectively. ^{31}P MAS-NMR spectra were measured at 242.95 MHz, with a 90^{o} pulse of 2µs, a delay of 300s, and 16 scans. ^{11}B MAS-NMR spectra were recorded at 192.55 MHz, using a 25^{o} tipping angle of 1µs, a delay of 3s, and 40 scans. The tipping angle of the boron spectra was determined by finding the pulse length where the resulting area under the curve of trigonal to tetrahedral peaks were equal in borax, ($Na_2B_4O_7$-$10H_2O$, Fisher Scientific, 99.5%). Chemical shifts were reported relative to 85% phosphoric acid, (H_3PO_4) and BF_2-Et_2O solution for ^{31}P and ^{11}B respectively. An example of the ^{31}P and ^{11}B MAS-NMR spectra are shown in Figure 4-4 and Figure 4-5.

4.4 Results and Discussion

4.4.1 Raman Spectroscopy

The Raman spectra of $0.35Na_2O + 0.65[xB_2O_3 + (1\text{-}x)P_2O_5]$ glasses are shown in Figure 4-6 and are comparable to spectra found in the literature for similar glasses [18, 25-29]. Due to the stronger Raman scattering cross-section of the phosphate SRO

structural units than the borate structural units, the Raman spectra of sodium borophosphate glasses show Raman bands that are more intense for the modes arising from the phosphate groups than the modes from the borate structural groups. However, as is the common practice in Raman spectroscopy, we have scaled each spectra to the same intensity for the strongest peak. The results of such scaling produces Raman repctra that are more easily interpreted, but masks the sensitivity issue.

4.4.1.1 Raman Spectra in x = 0 Glass

The Raman spectra of the binary $0.35Na_2O + 0.65P_2O_5$ glass shows three main peaks at 665 cm^{-1}, 1164 cm^{-1}, and 1315 cm^{-1}. The broad peak at 665 cm^{-1} arises from the symmetric stretching of the BO in the P-O-P linkage [18]. The peak at 1164 cm^{-1} is assigned to the symmetric stretch of the two non-bridging oxygen (NBO) present in a P_P^2 unit, the $(PO_2)_{sym}$ mode, and the 1315 cm^{-1} peak is assigned to the P=O symmetric stretching mode found only in P_P^3 units, the $(P{=}O)_{sym}$ mode [18, 27].

4.4.1.2 Raman Spectra in $0.1 \leq x \leq 0.2$ *Glasses*

When boron is added to the binary sodium phosphate glass at x = 0.1, the spectra show that several changes must be occurring in the glass structure. In addition to the $(PO_2)_{sym}$ stretch at 1164 cm^{-1}, the P^2 unit stretch also produces an asymmetric stretching mode at 1280 cm^{-1} [27]. The peaks at 1190 cm^{-1} and 1330 cm^{-1} are "strained" variants of the symmetric and asymmetric P^2 stretches, respectively [27]. These variations each have

a specific structure that differs from the normal P^2 modes. In their studies of binary lithium phosphate glasses, Hudgens *et al.* [27] associated the strained modes with rings composed of $P^3$and P^2 units and crosslinking P^3 units between metaphosphate units, P^2, that form long chains. The ^{11}B NMR spectra to be discussed below will show that at x = 0.1 only B_P^4 units are present, suggesting that boron has more Na^+ modifying it than a binary sodium borate glass with a Na:B ratio of 1:1. This indicates a chemical reaction of $B^2 + B^3 + P^2 \rightarrow B^4 + P^3$. We suggest that one of two structural changes are taking place. The first is that sodium removal from the P^2 units, to modify the boron unit to form the observed B^4 units, causes the formation of strained P^3-O-P^2 bonds. A second interpretation is that a B^4 unit is part of a phosphate chain or ring, forming P^2-O-B^4-O-P^2 bonds.

In these predominately phosphorous rich glasses, the peak at 665 cm^{-1} develops shoulders at 630 cm^{-1}, 690 cm^{-1}, and 775 cm^{-1}. In binary sodium borate glasses peaks in this region originate from vibrations of the metaborate superstructural unit. However, a metaborate superstructural unit is composed of three trigonal boron units and we will show that only B^4 units are observed in the ^{11}B MAS-NMR until x = 0.3, where only a barely detectable 2% of the boron are in trigonal coordination. Hudgens *et al*. suggested that a peak at 775 cm^{-1} correspond to the asymmetric stretch of the BO linking two phosphorous in the $(POP)_{asym}$ stretch in $P^2_{mP^2}$, $P^2_{mP^3}$, $P^3_{mP^3}$ [27, 30]. Therefore, we attribute the 630 cm^{-1}, 690 cm^{-1}shoulder peaks to the POB stretches in $P^2_{mB^4}$ and $P^3_{mB^4}$ and the shoulder at 775 cm^{-1} to the asymmetric stretches of POP.

4.4.1.3 Raman Spectra in $0.3 \leq x \leq 0.5$ *Glasses*

The decreasing frequencies of the positions of P^3 and P^2 peaks in the Raman spectra with increasing boron contents may also indicate a change in IRO structure. For example, the P^3 peak at 1318 cm^{-1} shifts approximately -115 cm^{-1} to lower frequencies from with changing glass composition, x = 0 to x = 0.8 and the P^2 peak at 1162 cm^{-1} shifts -63 cm^{-1} to lower frequencies with changing glass composition, x = 0 to x = 0.9 in the Raman spectra. To determine the origin for this frequency shift, we must first determine if there is such a frequency shift in these peaks that occur in the binary glasses that contain P^3 or P^2 units, the $0.35 \leq y \leq 0.66$ range. The work of Nelson *et al.*[31] shows that the wavenumber shift of P^3 and P^2 peaks with changing sodium content, in binary sodium phosphate glass, is ~40 cm^{-1} and ~23 cm^{-1}, respectively, between 33 and 66% Na_2O. In the binary glass, the authors attributed these shifts are attributed to changing numbers of P^3-O- P^2 links and P^2-O-P^1 links caused by the changing sodium content. As Na_2O is added to the binary glasses the numbers of P^2 and P^1 groups must increase and hence the intensity of P^3-O-P^2 and P^2-O-P^1 peaks must also increase. Since the experimental wavenumber shifts of the peak in the ternary glasses are much larger than those in the binary sodium phosphate glass, -115cm^{-1} versus -40cm^{-1} and -63cm^{-1} versus -23cm^{-1}, it is reasonable to assume that there must be another reason for the shifts in the peak position in the ternary glass. One obvious possibility is to attribute shifts in peak position to increasing numbers of P-O-B links on the P^3 and P^2 units. We further explore

this structural hypothesis below when we examine the ^{31}P and ^{11}B MAS-NMR of these glasses.

For the x = 0.3 glass, the mode arising from the P_P^2 peak at 1164 cm^{-1} is joined by a shoulder at 1124 cm^{-1} indicating a possible change in the next nearest neighbor bonding to this unit and a likely suggestion is the formation of the P_{1B}^2 unit. At an even lower frequency, the peak at 1059 cm^{-1} is assigned to the P=O symmetric stretch of the P_{2B}^2 unit. As the boron content increases, the peak at 1124 cm^{-1} and 1315 cm^{-1} shifts to lower wavenumbers, indicating increasing replacement of P_{2P}^2 by P_{1B}^2 and P_{3P}^3 by P_{1B}^3, respectively.

A new peak at 720 cm^{-1} appears at the x = 0.3 glass. We assigned the mode to the ring breathing vibrations of six-membered rings containing trigonal boron and two B^4 units. This assignment is supported by the presence of both a trigonal and tetrahedral boron peak in the ^{11}B NMR, see below. The weak peak at 505 cm^{-1} is attributed to di-borate groups or rings with one or two B^4 [25, 30]. These are the first indication of trigonal boron units in the structure [26, 30, 32].

4.4.1.4 Raman Spectra in $0.6 \leq x \leq 0.9$ *Glasses*

For the glass with x = 0.6, the peak at 720 cm^{-1} is joined by a peak at 770 cm^{-1} and we assign these to the ring breathing vibrations of six-membered rings containing multiple trigonal boron units and one B^4 unit. For the glass at x = 0.8 a new shoulder appears at 990cm^{-1}. At the same composition, the ^{31}P spectra shown below suggests the

presence of P^1 units. Although the Raman wavenumber shift in binary $0.66Na_2O + 0.33P_2O_5$ glass is commonly, $1025cm^{-1}$, due to the predominance of boron at this ternary composition, it is likely that the P^1 unit has its only bridging oxygen bonding to boron, which would cause a shift to lower wavenumber [18]. Therefore, we can assign this new peak at $990cm^{-1}$ to the P_{1B}^1 unit.

The P^1, P^2, and P^3 peaks are present in the glasses up until x = 0.9. However, the changing intensity of the peaks suggest that at x = 0.8, P^3 units are transformed to P^1 units. Although both the P^1 and P^2 peaks overlap with peaks from the boron diborate groups, the weak intensity of the diborate peaks at x = 1, suggests that the diborate contribution to the ternary glasses peak intensity is small.

4.4.1.5 Raman Spectra in x = 1 Glass

The binary sodium borate glass at x = 1, shows a strong peak at 760 cm^{-1} that arises from the merging of two peaks, one at 720 cm^{-1} and another at 770 cm^{-1}, which are seen in glasses with lower x values. Therefore, the peak at 760 cm^{-1} is assigned to the breathing vibrations of ring units containing one or two B^4 units. The weaker bands at 980 cm^{-1} and 1102 cm^{-1} arise from vibrations of loose and interconnected diborate groups, respectively [30]. The broad peak at 1490 cm^{-1} is assigned to the bivrational modes of the B_B^2 units. The presence of the B^3 unit can be inferred from the presence of more polymerized, less modified, superstructural units such as the diborate and triborate units, and the limited amount of sodium, Na_2O=0.35, which requires the presence of

unmodified SRO structural units. We will quantify the composition dependence of all of these units below by using a combination of Raman, ^{31}P, and ^{11}B MAS-NMR spectroscopies.

4.4.2 3.2 ^{31}P MAS-NMR

The central peak and first two satellite transitions of the ^{31}P MAS-NMR spectra were fitted with the minimum number of Gaussian curves needed to achieve a good fit with a residual error of less than 3%. An example of the fitting is shown in Figure 4-9. The SRO structural units present at each composition x, were identified by using the SRO structural units present in the binary glasses, $yNa_2O + (1-y)P_2O_5$, their chemical shift ranges as established in the literature, [33] and by the examination and assignments made in the Raman spectra presented above, Figure 4-10.

4.4.2.1 ^{31}P MAS-NMR of x = 0 Glass

Raman [34] and NMR spectroscopy studies [17, 19] and Van Wazer's fully ionic model have [35] shown that a binary $0.35Na_2O + 0.65P_2O_5$ glass is composed of 54% P_P^3 and 46% P_P^2 SRO structural units. As such, the resonances at ˉ26 ppm and ˉ39 ppm in the x = 0 spectra, Figure 4-7, are assigned to the resonances of the P^2 and P^3 SRO structural units, respectively, where the deconvolution and area analysis gives the exact same percentages 54% P_P^3 and 46% P_P^2.

4.4.2.2 ^{31}P MAS-NMR $0.1 \leq x \leq 0.8$ Glasses

As boron substituted for phosphorous in the network, the chemical shift of the P^3 and P^2 peaks increases in frequency with x, indicating that the phosphorous nucleus is becoming less shielded. In the binary sodium phosphate glasses, a shift to higher ppm values is associated with the depolymerization of the phosphorous network, P^3, P^2, and P^1 units being converted to P^2, P^1, and P^0 units, respectively. The changing SRO results in changes in the IRO. For example, with increasing Na content, $P^3_{P3} \rightarrow P^3_{P2}$, $P^2_{P3} \rightarrow P^2_{P2}$, and $P^2_{P2} \rightarrow P^1_{P2}$ [17]. Therefore, in order to examine if the chemical shift in the ^{31}P MAS-NMR spectra is a result of depolymerization of the phosphorous network or other changes in IRO, such as the substitution of B in the second coordination sphere we compared the magnitude of the change in the chemical shifts of the 31P MAS-NMR resonaces in the ternary glasses to the changes in chemical shift in the binary glasses as shown in Figure 4-10. As described above, the ^{31}P MAS-NMR peaks shift to higher frequencies with the addition of boron. In the $0.35Na_2O + 0.65[xB_2O_3 + (1\text{-}x)P_2O_5]$ glasses, the P^3 peak is first observed in the x = 0 glass at ⁻39 ppm and is last observed at x = 0.8 at approximately ⁻16 ppm, see Figure 4-7, a change of +23ppm. P^3 groups are present in binary sodium phosphate glasses over the compositional range of $0 \leq y \leq 0.5$ and changes in the chemical shift from ⁻55 to ⁻36 ppm have been observed with changing y, Figure 4-10 [17], a change of +19ppm. The chemical shift of the P^3 group in the ternary glasses with changing x is therefore larger than the change in chemical shift seen in the binary glasses, $yNa_2O + (1\text{-}y)P_2O_5$, over changing y. This indicates that there must

be changes in the IRO beyond the increasing fractions of P^3 units bonded to P^2 units, as seen in the binary glasses.

Similar changes occur in the P^2 structural unit which shifts from ¯26 to ¯5 ppm at x = 0 to x = 0.9, which is larger than the P^2 shift of ¯32 to ¯15 ppm observed in binary $yNa_2O + (1\text{-}y)P_2O_5$ glasses with changing y, although not as large as the chemical shift change seen for the P^3 units. This presumably arises from the fact that the P^3 unit can and probably does form three bridge bonds to boron units at highest x, whereas the P^2 unit can only form two bridge bonds to boron units.

4.4.2.3 ^{31}P MAS-NMR of $0.8 \leq x \leq 0.9$ Glasses

At x = 0.8, a new peak emerges, which has the chemical shift to be equivalent to that of a P^1 unit [19]. However, the literature cited above does not support the existence of P^1 units in binary $yNa_2O + (1\text{-}y)P_2O_5$ glass until $y \geq 0.5$ [19]. This indicates that the ratio of Na bonded to phosphorous, Na:P, is no longer 0.35:65 as in the binary glass, but suggests an Na:P ratio higher than 1:1, as would be required to produce the P^1 structural group in the binary glass.

The chemical shifts of P^1 structural units, ~3 ppm are not outside the possible chemical shift ranges determined by the binary glasses, ¯8 to 8 ppm. Similar to the decreasing effect of the IRO on the P^2 unit, the effect of IRO may not be strong enough to affect the chemical shift of the P^1 units as they can form only one bridge bond to boron. P_B^3 and P_B^2 units are still present in the $0.8 \leq x \leq 0.9$ range.

4.4.3 ^{11}B MAS-NMR

The areas under the curve of the central and first two satellite transitions of the ^{11}B spectra were determined to establish the relative fractions of the boron in trigonal and tetrahedral units. The spectra arising from the tetrahedral unit was then fit with the minimum number of Gaussian curves needed to achieve a good fit with a residual error of less than 3%. The SRO structural units present at each composition x, were identified by using the SRO structural units present in the binary glasses $yNa_2O + (1\text{-}y)B_2O_3$ and their chemical shift ranges as established in the literature [33, 36], Figure 4-10.

4.4.3.1 ^{11}B MAS-NMR of x = 1 Glass

As seen in many other studies of binary alkali borate glasses, two primary peaks were observed in the ^{11}B MAS-NMR spectra of binary sodium borate glass at x = 1 shown in Figure 4-8. A quadrupole broadened peak, centered approximately at 12 ppm arises from the presence of trigonal boron units. A centrally symmetric peak at -1 ppm is assigned to the B^4 units where the asymmetry parameter, η, is nearly zero and the quadrapolar effect is removed. With the addition of phosphorous to the network, these primary peaks shift in the negative ppm direction.

4.4.3.2 ^{11}B MAS-NMR of $0.9 \leq x \leq 0.1$ Glasses

At x = 0.6, a new tetrahedral peak appears at ⁻4 ppm indicating the presence of B_P^4 SRO units. The trigonal peak is no longer present for glasses with $x \leq 0.3$ indicating that all boron are in tetrahedral coordination. By x = 0.2, the original tetrahedral peak at ⁻1 ppm has been completely replaced by the second peak at ⁻5 ppm indicating that all B4 units must have at least one bridging oxygen to phosphorous.

The B^4 peak in ^{11}B MAS-NMR shifts to higher frequencies with increasing boron content. Unlike phosphorous, the size of the B^4 chemical shift of -0.6 to -5.5 ppm is within the chemical shift limit of 50 to ⁻31 ppm for binary sodium borate glasses [36]. It has been shown that the chemical shift of the B^4 group in binary alkali borate glasses is to higher frequencies with increasing alkali oxide concentration [36]. Therefore, we would expect the highest chemical shift to correspond to the most heavily modified borate composition. In this way, the x = 1 composition should be the most heavily modified, but it is at the x =0.1 and 0.2 compositions that appear to be the most heavily modified. Therefore, the structural modification by sodium cannot be the primary influence on the chemical shift of the B^4 structural group.

Van Wullen *et al.* observed a similar trend in chemical shift in the B^4 peaks of ^{11}B MAS-NMR in sodium borosilicate glasses [37, 38] and argued that sodium borosilcates were composed of homogeneously intermixed and interlinked SiO_4, BO_3, and BO_4 polyhedra. They found that silicon linked to B^4 groups via bridging oxygens increased the shielding of the B^4 unit, thereby reducing the B^4 chemical shift by

approximately 0.5 ppm per bridging bond. They also found that boron trigonal units linked to B^4 groups via bridging oxygen decreased shielding, increasing the chemical shift by approximately 0.5 ppm per bridging bond. Likewise, the chemical shift was also found to be more negative if B^4 groups were linked to $SiO_{4/2}$ or $BO_{4/2}$ tetrahedra rather than boron trigonal polyhedral. The finding of Van Wullen *et al.* suggests that the negative change in the chemical shift of the B^4 peaks in the present ^{11}B spectra may be caused by increased linkages of P_2O_5 to BO_4 tetrahedra with decreasing x, increasing amounts of P in the glasses.

Another interesting aspect of the ^{11}B spectra is the presence of two B^4 peaks, which suggests that there are changes in the IRO. Kroker *et al.* observed a single peak for tetrahedral borons in binary sodium or lithium borate glasses [39, 40]. However, binary potassium, rubidium, and cesium borate glasses do show evidence of at least two distinct tetrahedral peaks. After further investigation by MQ-MAS, Aguiar and Kroeker determined that the most likely cause of the two different kinds of B^4 units were the existence of two B^4 sites arising from triborate rings and non-ring (isolated) B^4 units [41]. The reason for a single B^4 peak in sodium borate glasses was suggested to be a smaller chemical shift difference between these different types of B^4 units, rather than a lack of ring or non-ring tetrahedral units in the glass. Similar work by Elbers *et al.* was conducted on silver borophosphate glasses in which multiple B^4 signals were observed in the ^{11}B MAS-NMR spectra [15]. Further $^{11}B\{^{31}P\}$and $^{31}P\{^{11}B\}$ REDOR experiments on silver borophosphate glasses showed that the additional signals in the MAS-NMR came from tetrahedral boron units linked to three or less phosphorous atoms. Therefore, the

presence of multiple B^4 peaks can be attributed to changes in IRO, most likely B^4-O-P linkages.

4.5 Discussion

4.5.1 The Presence of BPO_4

Many other investigations of borophosphate glasses have considered the possibility of BPO_4 structural units present in the glasses, having the same structure as in crystalline BPO_4. A BPO_4 unit consists of a $(B^4)^-$ unit that is not charge compensated by a Na^+, but by a tetrahedral phosphorous unit with four bridging oxygen with a positive charge, $(P^4)^+$. Several authors proposed the existence of BPO4 units in sodium borophosphates [23, 42], lithium borophosphate [43], zinc borophosphate [44], while others such as Elbers *et al.* [15] examined silver borophoshate, Ducel *et al*. examined at sodium borophohsphate [45] and did not find evidence for the formation of BPO_4. Rinke *et al*. [46] showed that the Raman spectra of BPO_4 crystal has a strong peak at ~490cm^{-1}, weaker peaks at 1120cm^{-1} and 240cm^{-1}, and minor peaks at 465cm^{-1} and 1080cm^{-1}. In our Raman spectra presented and analyzed above, we do not see evidence of BPO_4 as we do not see evidence of a peak at 240cm^{-1}. While the 490cm^{-1} peaks could be associated with BPO_4 this seems unlikely as the intensity in this region increases with increasing boron content and remains significant even in the x = 1 composition where there is no phosphorous avalible for this unit. The 1120cm^{-1} peak could also be associated with the presence of BPO_4 and this peak is present from $0.3 \leq x \leq 0.9$, but as it is a secondary peak

of weak intensity and the primary peak at 490cm^{-1} and the other secondary peaks are both not present, the presence of BPO_4 in these glasses seems unlikely.

Villa et al [47] showed that crystalline BPO_4 has a peak in ^{11}P MAS-NMR at $^{-}$30 ppm, when referenced to 85% H_3PO_4. Our ^{31}P MAS-NMR shows a broad peak that covers a range of ppm, including $^{-}$30 ppm from $0 \leq x \leq 0.6$. However, the fitting of the broad peak with a minimum of curves necessary to achieve a good fit, do not require a peak for the BPO_4. When Brow *et al.* [44] and Zyer-Dusterer *et al.* [23] investigated borophosphate glasses with ^{11}B MAS-NMR they did not find a specific chemical shift associated with BPO_4 units, but found that a B^4 units bridging to one and two P units have a chemical shift of $^{-}$3.8 and $^{-}$4.1 ppm respectively.

4.5.2 The Presence of Phase Separation

Evidence of phase separation, that would suggest two separate binary networks, was not observed in the corresponding conductivity data, glass transition temperature, or by visual inspection of the samples. This suggests homogeneous glasses, although a detailed SEM/TEM study of the glasses has not been conducted. Furthermore, the systematic wavenumber shifts of the Raman peaks and chemical shift of the ^{31}P and ^{11}B MAS-NMR peaks which have been assigned to the progressive changes in B-O-P bonding, strongly suggest that P and B strongly interact and form a continuously and homogeneously intermixed network. This would be incompatible to separate and distinct phase separated B-O-B and P-O-P networks.

4.5.3 SRO Atomic Fraction Model

In order to begin the SRO structural analysis an atomic fraction model was created using the structural data from the Raman and NMR spectra. The fitted areas of the NMR spectra were then scaled by x and by (1-x) for boron and phosphorous, respectively, to determine their fractions in the ternary glasses. By applying charge neutrality to all compositions, the numbers of Na^+ must equal the numbers of P^2, $2*P^1$, B^4, and B^2 groups and confining phosphorous and boron to the SRO structural units observed in the Raman spectra at each composition, x, the type and fractions of all SRO structural units were adjusted until each sample was charge neutral, Figure 4-11 and Table 4-1.

The atomic fraction model, Figure 4-11, shows there are six different SRO structural units present in the $0.35Na_2O + 0.65[xB_2O_3 + (1-x)P_2O_5]$ glasses. At $x = 0$, P^3 and P^2 groups make up 46 and 54% of the SRO structural groups, respectively, in exact agreement with literature and the Van Wallen model as discussed previously. With the addition of boron, the fraction of P^3 groups remains steady until $x > 0.3$, while the number of P^2 groups rapidly decrease as the Na^+ preferentially bonds to the boron to form B^4 units. Although boron is the minority glass former in the $0.1 \leq x \leq 0.3$ region, the preferential bonding of sodium to boron causes the boron to be overly modified, Na:B > 0.35:0.65, when compared to the $0.35Na_2O + 0.65B_2O_3$ binary glass, Na:B = 0.35:0.65. In the $0.1 \leq x \leq 0.3$ region, the conversion of P^2 units to P^3 units and the simultaneous

conversion of the B^3 units to B^4 can be summarized in the following chemical reaction, $P^2 + B^3 \rightarrow P^3 + B^4$.

In the $0.4 \leq x \leq 0.7$ range, boron continues to be overly modified. The number of P^2 units goes through a maxima at $x = 0.7$, while the number of P^3 units decreases. The number of B^4 units reaches a maxima at $x = 0.5$ and the number of B^3 units increases. In the $0.7 \leq x \leq 0.9$ compositional region, phosphorous is the minority glass former and it is also overly modified compared to the binary $0.35Na_2O + 0.65P_2O_5$ glasses. This over modification can be seen by the preferential bonding of sodium to phosphorous to form of P^1 structural units and the decrease in concentration of B^2 units to zero with the addition of P. Hence, a balanced chemical reaction that is consistent with this behavior is, therefore: $P^3 + 2B^2 \rightarrow P^1 + 2B^3$. Note that there is the requirement that two B^2 groups react with one P^3 group to produce one P^1 group due to the double negative charge carried by the P^1 group. This behavior presumably explains the rapid decrease of the fractions of the B^2 and the rapid increase of the fractions of the B^3 groups in this region, yet the slower changes in the fractions of the P^3 and P^2 groups with the addition of B at the other compositional limit. It remains an open question why the B^4 and P^2 groups are evidently uninvolved in this compositional region. However, we provide the start of answer by examining the Gibb's Free-Energy of Formations of the various compounds corresponding to these SRO groups.

4.5.4 Solution Thermodynamics of the Ternary Mixed Glass Former System

The results presented above lead to the questions, "Why doesn't the ratio of modifier:glass former remain constant?" To begin to answer to this question, we look to the Gibbs free energies of formation of the various compounds that correspond to the various SRO structures in this system and how we can apply our structural model of these glasses to investigate the relative thermodynamic stability of these various structural groups in these glasses. Because these ternary Na B P O compositions appear to form stable, completely reacted homogeneous liquid solutions at the melting temperatures we have used, ~1,000^{o}C, and appear not to demix or phase separate upon cooling, this suggests that these liquids have achieved a minimum in Gibbs free energy though the various chemical reactions that produce the SRO structures that we observe spectroscopically. A constant modifier:glass former ratio would result in a linear exchange of SRO structures that would be suggestive of two non-interacting structural networks. That we find a non-linear behavior in the SRO structure of these glasses suggests that the changing modifier:glass former ratio may result in a lower still Gibbs Free Energy that is produced through the chemical reaction to produce a linear wqual sharing structure of these glasses. This suggests a strong chemical interaction of the borate and phosphate networks. We can attempt to verify this hypothesis using available data for the Gibbs free energy of formation for each of the SRO groups corresponding to the local identifiable SRO structural units shown in Figure 4-2 and Figure 4-3 and calculate the change in Gibbs free energy as a function of the composition of the liquid (glassy) state SRO structures using both of these models. However, it is recognized that

interaction between the borate and phosphate SRO structural units, mixed bonding, would produce the kinds of mixed IRO structures we have descried above and these mixed bonds would have a contribution to the Gibb's Free Energies of these glasses. However, the thermodynamic values of these mixed structure are either unknown or poorly known and hence outside of our ability to use them. None-the-less, it is the formation of the various SRO groups that we are most interested in and it is the thermodynamic properties of the corresponding crystalline compound that we know the most about, so we being the thermodynamic analysis of these structural units.

In these calculations, a few approximations will still have to be made given the lack of complete thermodynamic data that is available for the large numbers of structures and compositions that are reported in this study. We first recognize that the structures are formed at elevated temperatures, ~1000^{o}C, and as such we must consider the Gibbs free energy in Equation 4-1. As we purposefully quench these liquids in a matter of a few hundred milliseconds to just a few seconds it is reasonable to assume that the structures in equilibrium at elevated temperature are those quenched into the room temperature structure. Hence, we need the change in Gibb's Free Energies at elevated temperatures. Now because of the condensed (solid and liquid) character of these reactions the entropy change, $\Delta S_{rxn}(T)$, will be small. Therefore, $\Delta G_{rxn}(T)$, will have a weak temperature dependence and can be approximated as Equation 4-2.

$$\left(\frac{\delta \Delta G_{rxn}(T)}{\delta T}\right)_P = -\Delta S_{rxn}(T) \qquad \textit{Equation 4-1}$$

$\overline{\Delta G_{rxn}}(T) \sim \overline{\Delta G_{rxn}}(298K)$ *Equation 4-2*

where G is the Gibbs free energy, T the temperature, H is the enthalpy, and S is the entropy.

In order to calculate the Gibbs free energy changes that accompany the formation of the equilibrium compositions for the various structural groups in the series of $0.35Na_2O+0.65[xB_2O_3+(1-x)P_2O_5]$ glasses we used Equation 4-3.

$$\overline{\Delta G_{rxn}}(T) = \overline{\Delta G_f}(products, T) - \overline{\Delta G_f}(reactants, T) \quad \text{Equation 4-3}$$

$$\Delta\overline{G_f}(reactants, 298K) = \sum F_i \, \overline{\Delta G_f}(i)$$

$$\Delta\overline{G_f}(reactants, 298K) = F_{Na_2O}\overline{\Delta G_f(Na_2O)} + F_{B_2O_3}\overline{\Delta G_f(B_2O_3)} + F_{P_2O_5}\overline{\Delta G_f(P_2O_5)}$$

where

$$F_{Na_2O} = \frac{0.35}{1.3}$$

$$F_{B_2O_3} = \frac{0.65 * x}{1.3}$$

and

$$F_{P_2O_5} = \frac{0.65 * (1 - x)}{1.3}$$

Similarly,

$$\overline{\Delta G_f}(Products, 298K) = \sum F_i \, \overline{\Delta G_f}(i)$$

$$\overline{\Delta G_f}(Products, 298K)$$

$$= F_{B^3}\overline{\Delta G_f}(B^3) + F_{B^4}\overline{\Delta G_f}(B^4) + F_{B^2}\overline{\Delta G_f}(B^2) + F_{P^3}(P^3)$$

$$+ F_{P^2}\overline{\Delta G_f}(P^2) + F_{P^1}\Delta\overline{G_f}(P^1)$$

$$\overline{\Delta G_f}(Products, 298K)$$

$$= F_{B^3}\overline{\Delta G_f}(BO_{3/2}) + F_{B^4}\overline{\Delta G_f}(NaBO_2)_{Tetrahedral}$$

$$+ F_{B^2}\overline{\Delta G_f}(NaBO_2)_{Trigonal} + F_{P^3}\overline{G_f}(PO_{5/2})$$

$$+ F_{P^2}\overline{G_f}(NaPO_3) + F_{P^1}\overline{G_f}(Na_2PO_{7/2})$$

where $\overline{G_f}(i)$ is the molar Gibbs energy of formation of the i^{th} structural unit and F_i is the fraction of the i^{th} structural unit. The Gibbs free energy of formation of structural units, i, in the crystalline state at 298°C taken from various sources are listed in Table 4-2. Using these values the Gibbs free energy of reaction were calculated using the compositional dependence of the fractions of the SRO structural units of the proportional sharing (linear) model and the Raman and NMR structural model.

As can be seen in Figure 4-12, the Gibbs free energy calculated from the constant modifier model and from the Raman and NMR experimental data are both negative and give a thermodynamic basis for why these liquids form stable homogeneously fully reacted and intermixed solutions. The formation of the intermixed SRO of the ternary glasses makes them more thermodynamically stable than glasses that have a SRO based on a constant modifier:glass former ratio for compositions $0.1 \leq x \leq 0.7$ and suggests why the Na^+ ions are unequally shared between the two glass formers in this range. The main cause of the unequal sharing of the Na^+ in this compositional range appears to be

associated with the fact that the B^4 unit has the largest and most negative of all the Gibbs free energies of formation of the SRO structural units observed in these glasses. This is at least a partial thermodynamic answer to why the formation of the B^4 group can proceed upon the addition of B_2O_3 to the $x > 0$ compositions. The boron removes the Na^+ from the P^2 units to form more energetically favorable B^4 groups. Even though there are less moles of boron than phosphorous in the $0.1 \leq x \leq 0.4$ range, the fact that the $\overline{\Delta G_f}(B^4)$ is nearly 3.5 times more negative than$\overline{\Delta G_f}(P^2)$ results in an overall decrease in free energy.

At this point, it is unknown why the calculated Gibbs free energy of the variable modifier model becomes more positive than that of the constant modifier model in the ternary glass compositions at $0.8 \leq x \leq 0.9$, making them less thermodynamically favorable. Reasons for this thermodynamic favorability of the constant modifier model could be due to the inaccuracies of the calculation method. The most obvious of the inaccuracies of the method used is the use of the Gibbs free energies of pure crystalline phases that do not account properly for the effects of neighboring atoms (IRO) in a glass. Other inaccuracies could arise from the treatment of glasses as ideal solutions and the assumption of lack of temperature dependence, among other issues. The effects of IRO in glasses includes the distribution of bond angles and/or bond lengths of the known B-O-B and P-O-P bonds. In addition, the B-O-P bonding we believe to be present in this system must be accounted for as well. We are exploring these inaccuracies in order to improve this modeling.

4.6 Conclusions

The SRO and IRO structure of $0.35Na_2O + 0.65[xB_2O_3 + (1-x)P_2O_5]$ glass were examined through Raman and ^{31}P and ^{11}B MAS-NMR spectroscopy. Changes in the SRO structures were observed that indicate that the minority glass former has more sodium per glass former than the majority glass former. In the Raman spectra, the IRO of the glasses was also found to change with changing x, although the exact relationship is not known. The changing peak positions of phosphorous peaks in the Raman data indicates changes in the next nearest neighbors that cannot be accounted for by changing ratios of P^3 to P^2 links or P^2 to P^1 links caused by changing Na:P ratio. The peak position changes is caused by P-O-B bonding. The MAS-NMR spectra showed anomalous chemical shifts in the ternary glasses that could not be accounted for by changing Na:glass former ratio, also suggesting changing IRO. The large change in ^{31}P chemical shift of P^3 and P^2 units with increasing x, and the decrease in ^{11}B chemical shift of B^4 units with decreasing x, indicate that phosphorous is linked to boron through a bridging oxygen. A thermodynamic treatment was developed that gives some indication of the underlying thermochemical reason for the variable modifier:glass former ratio and strongly suggest that it is the large thermodynamic stability of the B^4 group that drives the unequal sharing of the added modifier in these glasses.

4.7 Acknowledgements

This research was supported by the National Science Foundation under grant number DMR-0710564 and this research support is gratefully acknowledged. The authors would also like to acknowledge the help of NMR spectroscopist Shu Xu, for which we are very grateful.

4.8 References

[1] A. Agarwal, V.P. Seth, P.S. Gahlot, S. Khasa, M. Arora, S.K. Gupta, J. Alloys Compd., 377 (2004) 225-231.
[2] A. Pradel, N. Kuwata, M. Ribes, J. Phys. Condens. Matter, 15 (2003) S1561-S1571.
[3] A. Pradel, C. Rau, D. Bittencourt, P. Armand, E. Philippot, M. Ribes, Chem. Mater., 10 (1998) 2162-2166.
[4] P.S.S. Prasad, A.N.D. Rani, S. Radhakrishna, Solid State Commun., 77 (1991) 967-971.
[5] P.S.S. Prasad, A.N.D. Rani, S. Radhakrishna, Mater. Chem. Phys., 25 (1990) 487-499.
[6] R.V. Salodkar, V.K. Deshpande, K. Singh, J. Power Sources, 25 (1989) 257-263.
[7] M. Jamal, G. Venugopal, M. Shareefuddin, M. Narasimha Chary, Mater. Lett., 39 (1999) 28-32.
[8] D. Zielniok, C. Cramer, H. Eckert, Chem. Mater., 19 (2007) 3162-3170.
[9] Y. Kim, J. Saienga, W. Martin Steve, J Phys Chem B, 110 (2006) 16318-16325.
[10] R. Christensen, J. Byer, G. Olson, S.W. Martin, To Be Published, (2011).
[11] R.S. Gedam, V.K. Deshpande, Solid State Ionics, 177 (2006) 2589-2592.
[12] P.C. Taylor, E.J. Friebele, J. Non-Cryst. Solids, 16 (1974) 375-386.
[13] S. Prabaker, K.J. Rao, C.N.R. Rao, Proc. R. Soc. Lond., 429 (1990) 1-15.
[14] G.E. Jellison, P.J. Bray, J. Non-Cryst. Solids, 29 (1978) 187-206.
[15] S. Elbers, W. Strojek, L. Koudelka, H. Eckert, Solid State Nuclear Magnetic Resonance, 27 (2005) 65-76.
[16] P.J. Bray, A.E. Geissberger, F. Bucholtz, I.A. Harris, J. Non-Cryst. Solids, 52 (1982) 45-66.
[17] R.K. Brow, J. Non-Cryst. Solids, 263 (2000) 1-28.
[18] S.W. Martin, European Journal of Solid State and Inorganic Chemistry, 28 (1991) 163-205.
[19] R.K. Brow, R.J. Kirkpatrick, G.L. Turner, J. Non-Cryst. Solids, 116 (1990) 39-45.
[20] R.K. Sato, R.J. Kirkpatrick, R.K. Brow, J. Non-Cryst. Solids, 143 (1992) 257-264.
[21] M. Villa, M. Scagliotti, G. Chiodelli, J. Non-Cryst. Solids, 94 (1987) 101-121.
[22] L. Koudelka, P. Mosner, M. Zeyer, C. Jager, J. Non-Cryst. Solids, 351 (2005) 1039-1045.
[23] M. Zeyer-Dusterer, L. Montagne, G. Palavit, C. Jager, Solid State Nuclear Magnetic Resonance, 27 (2005) 50-64.
[24] D. Qiu, P. Guerry, I. Ahmed, D.M. Pickup, D. Carta, J.C. Knowles, M.E. Smith, R.J. Newport, Mater. Chem. Phys., 111 (2008) 455-462.
[25] B.N. Meera, J. Ramakrishna, J. Non-Cryst. Solids, 159 (1993) 1-21.
[26] E.I. Kamitsos, G.D. Chryssikos, Journal of Molecular Structure, 247 (1991) 1-16.
[27] J.J. Hudgens, R.K. Brow, D.R. Tallant, S.W. Martin, J. Non-Cryst. Solids, 223 (1998) 21-31.
[28] J.F. Ducel, J.J. Videau, M. Couzi, Phys. Chem. Glasses, 34 (1993) 212-218.
[29] Z. Zhang, N. Soga, Phys. Chem. Glasses, 32 (1991) 142-148.
[30] E.I. Kamitsos, M.A. Karakassides, Phys. Chem. Glasses, 30 (1989) 19-26.
[31] C. Nelson, D.R. Tallant, Phys. Chem. Glasses, 26 (1985) 119-122.

[32] W.L. Konijnendijk, J.M. Stevels, J. Non-Cryst. Solids, 18 (1975) 307-331.
[33] R.K. Brow, C.A. Click, T.M. Alam, J. Non-Cryst. Solids, 274 (2000) 9-16.
[34] R. Christensen, J. Byer, G. Olson, W. Martin Steve, To Be Published, (2012).
[35] J.R. Van Wazer, Phosphorus and its compounds, Interscience Publishers, New York,, 1958.
[36] V.K. Michaelis, P.M. Aguiar, S. Kroeker, J. Non-Cryst. Solids, 353 (2007) 2582-2590.
[37] W.L. van, W. Muller-Warmuth, Solid State Nucl Magn Reson, 2 (1993) 279-284.
[38] L. van Wüllen, W. Müller-Warmuth, D. Papageorgiou, H.J. Pentinghaus, J. Non-Cryst. Solids, 171 (1994) 53-67.
[39] S. Kroeker, P.M. Aguiar, A. Cerquiera, J. Okoro, W. Clarida, J. Doerr, M. Olesiuk, G. Ongie, M. Affatigato, S.A. Feller, Physics and Chemistry of Glasses-European Journal of Glass Science and Technology Part B, 47 (2006) 393-396.
[40] S. Kroeker, S.A. Feller, M. Affatigato, C.P. O'Brien, W.J. Clarida, M. Kodama, Phys. Chem. Glasses, 44 (2003) 54-58.
[41] P.M. Agular, S. Kroeker, Solid State Nuclear Magnetic Resonance, 27 (2005) 10-15.
[42] P.S. Anantha, K. Hariharan, Mater. Chem. Phys., 89 (2005) 428-437.
[43] S. Lee, J. Kim, D. Shin, Solid State Ionics, 178 (2007) 375-379.
[44] R.K. Brow, J. Non-Cryst. Solids, 194 (1996) 267-273.
[45] J.F. Ducel, J.J. Videau, K.S. Suh, J. Senegas, Phys. Chem. Glasses, 35 (1994) 10-16.
[46] M. Villa, M. Scagliotti, G. Chiodelli, J. Non-Cryst. Solids, 94 (1987) 101-121.
[47] CRC Handbook of Chemistry and Physics, Boca Raton CRC Press, Cleveland, 2011.
[48] D.R. Gaskell, Introduction to the Thermodynamics of Materials, Taylor and Francis, Washington D.C., 1995.
[49] C.T. Huang, R.Y. Lin, Metall. Trans. B, 20B (1989) 197-204.

4.9 Figures

4.10 Tables

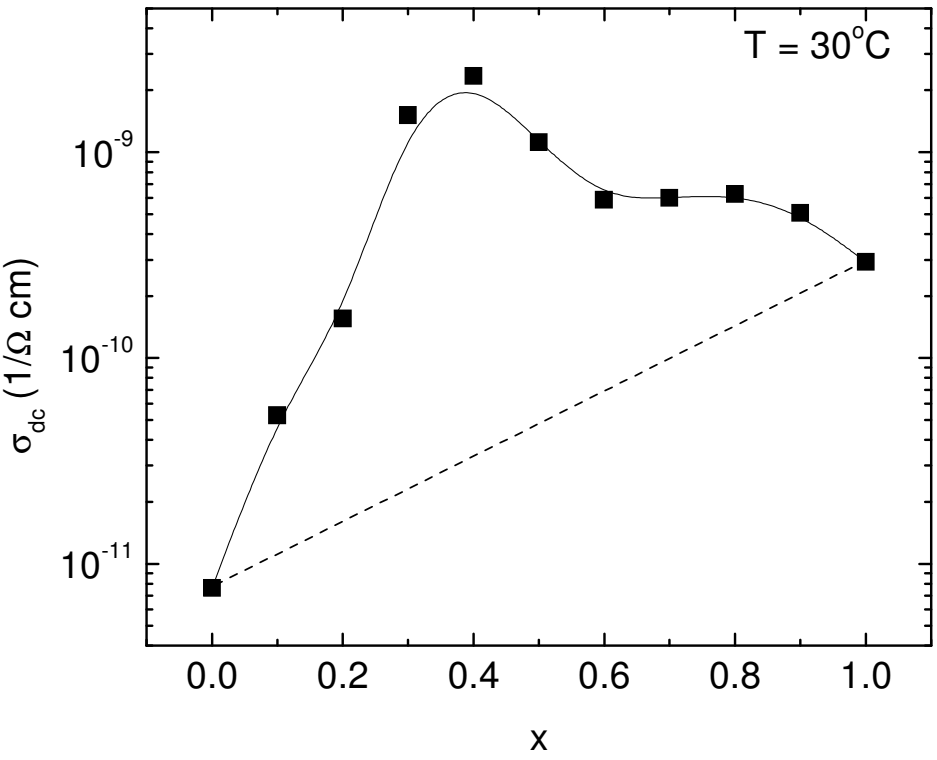

Figure 4-1

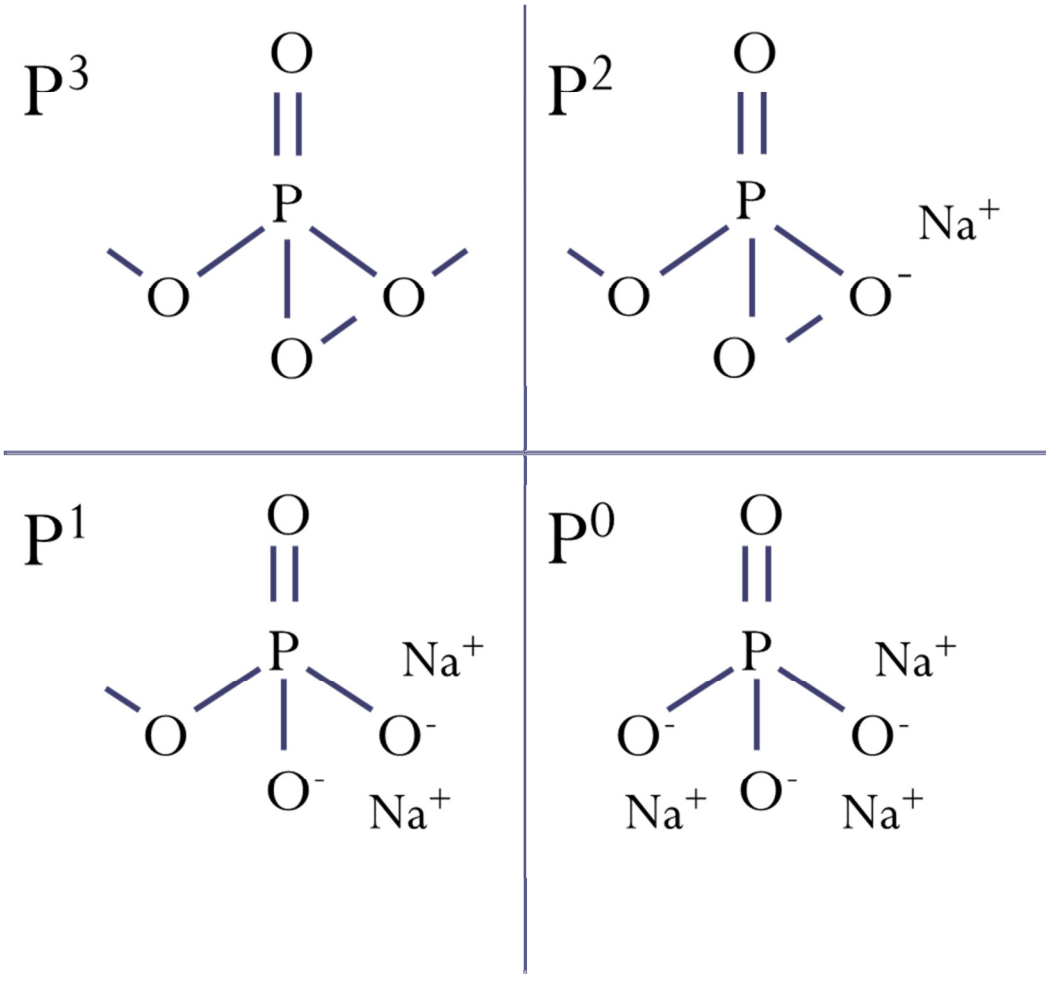

Figure 4-2

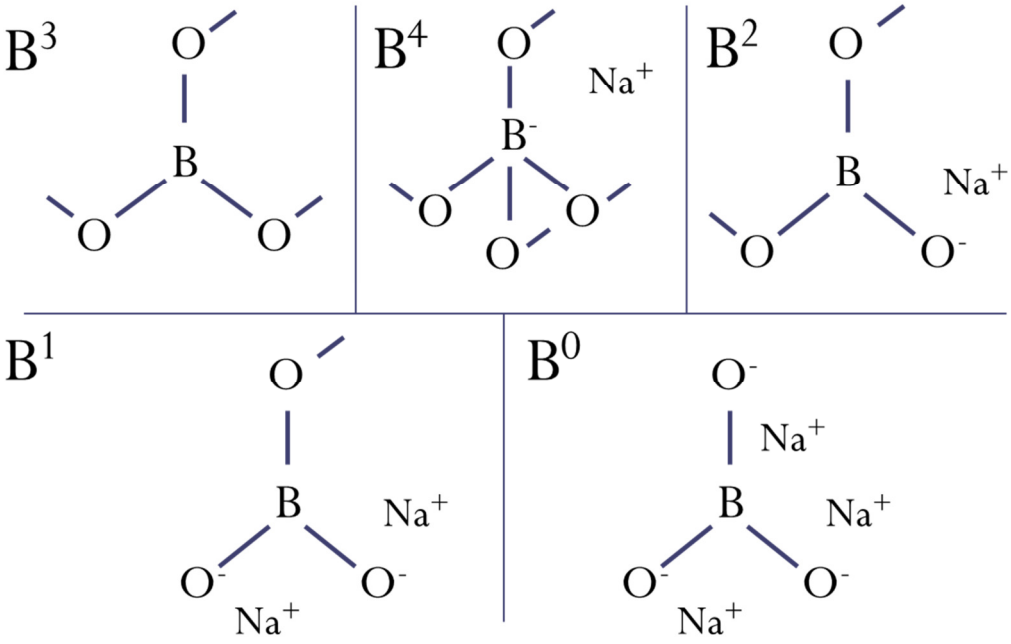

Figure 4-3

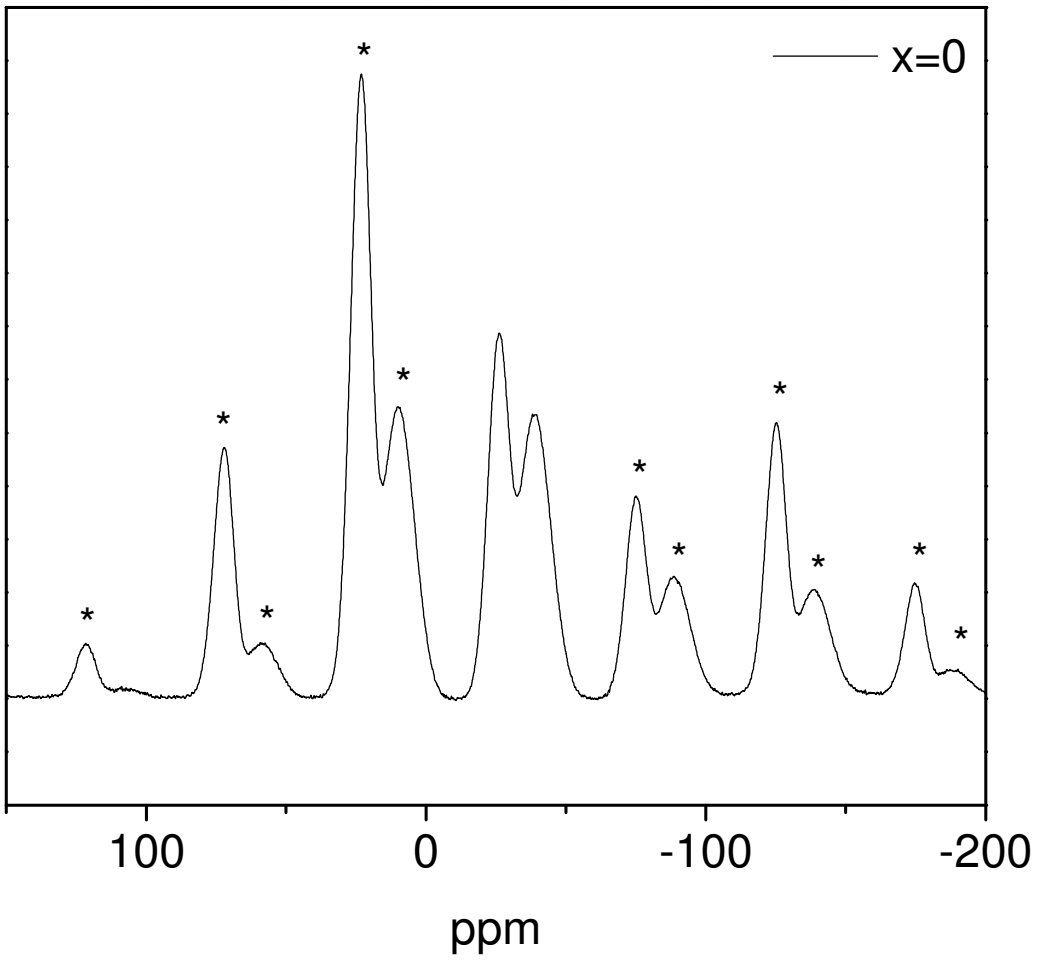

Figure 4-4

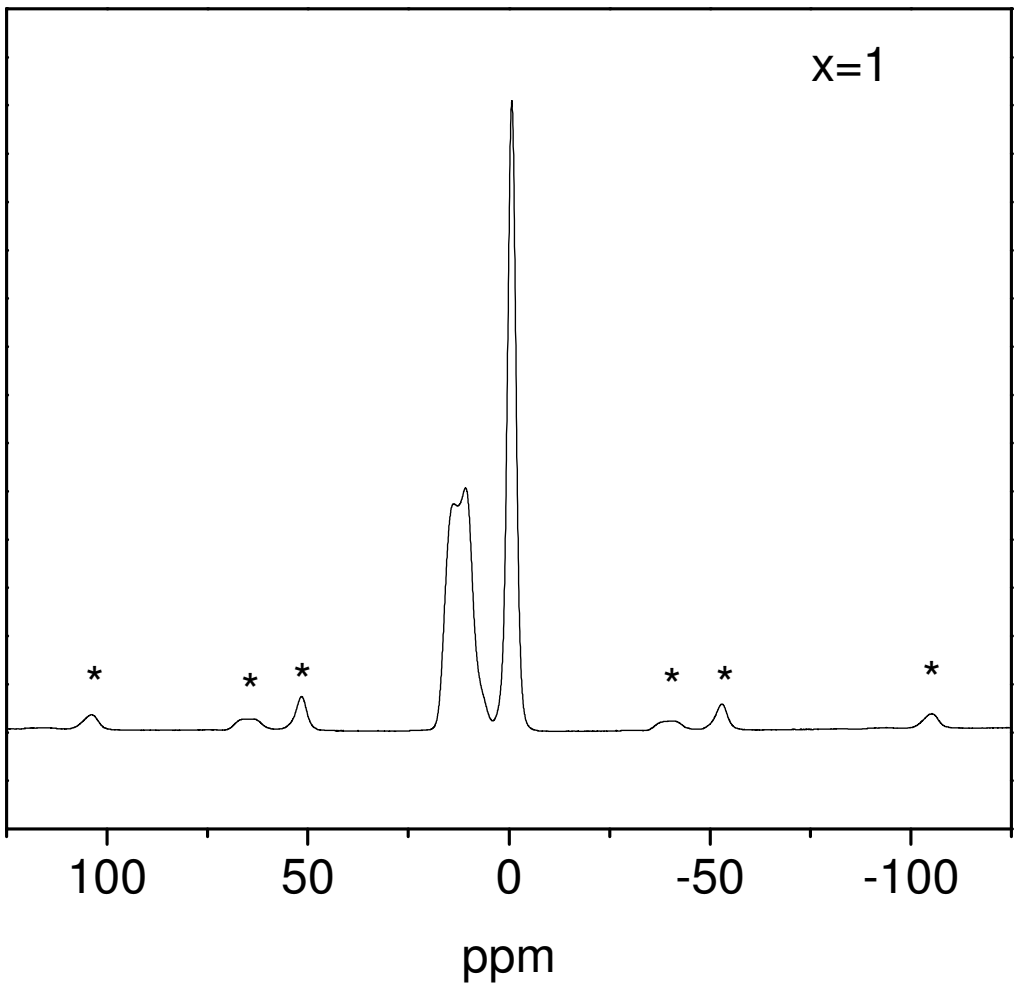

Figure 4-5

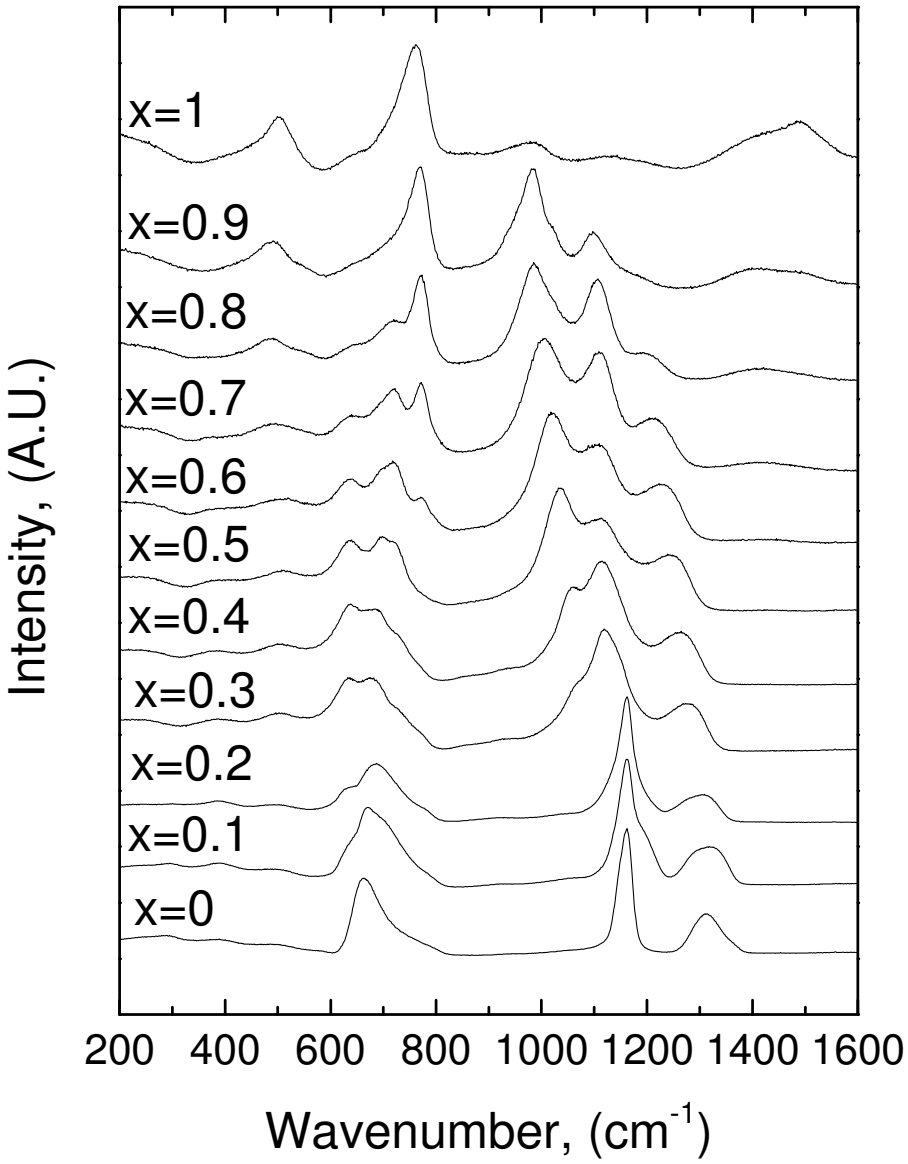
x=1
x=0.9
x=0.8
x=0.7
x=0.6
x=0.5
x=0.4
x=0.3
x=0.2
x=0.1
x=0
Intensity, (A.U.)
200 400 600 800 1000 1200 1400 1600
Wavenumber, (cm-1)

Figure 4-6

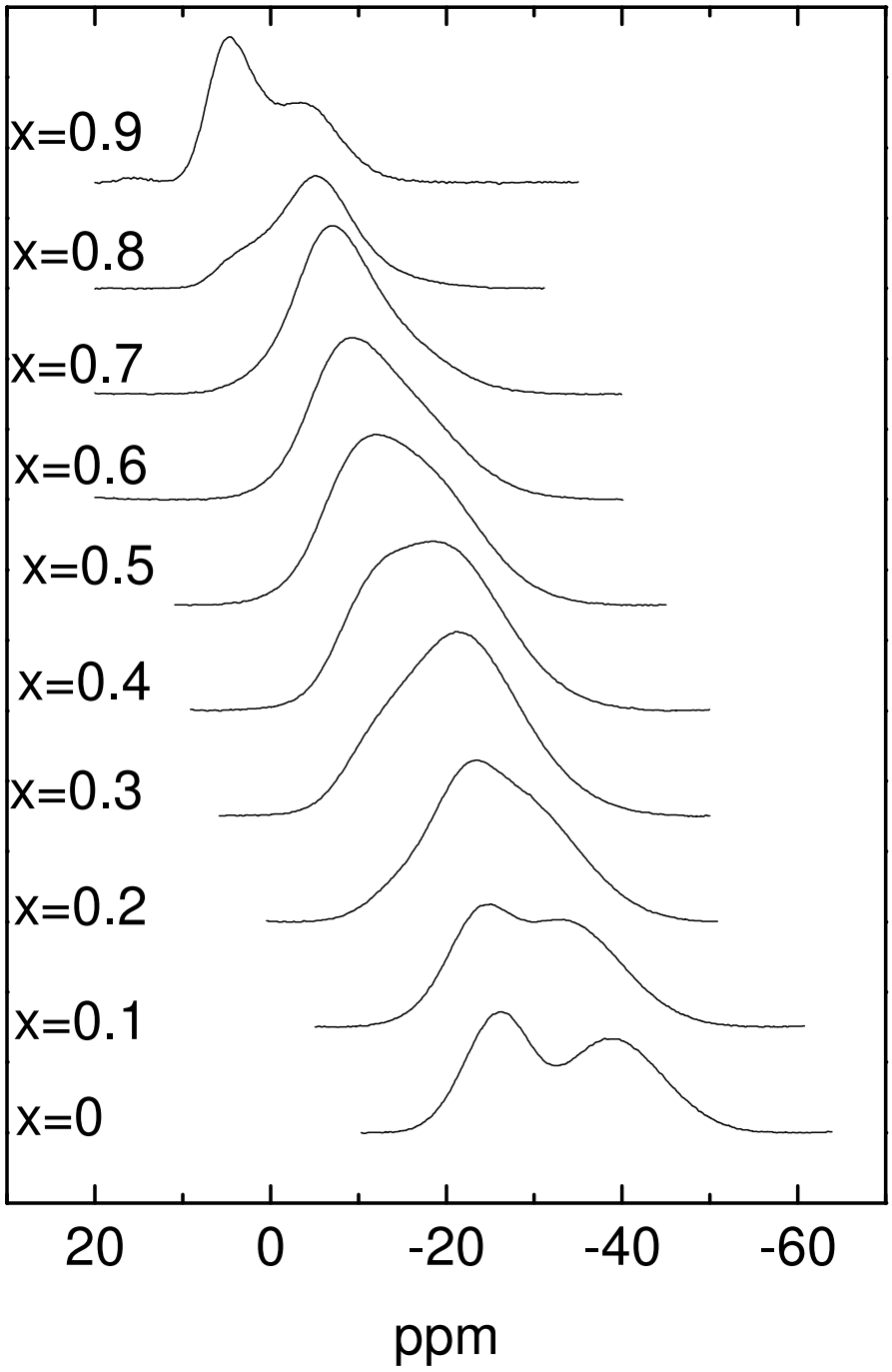

Figure 4-7

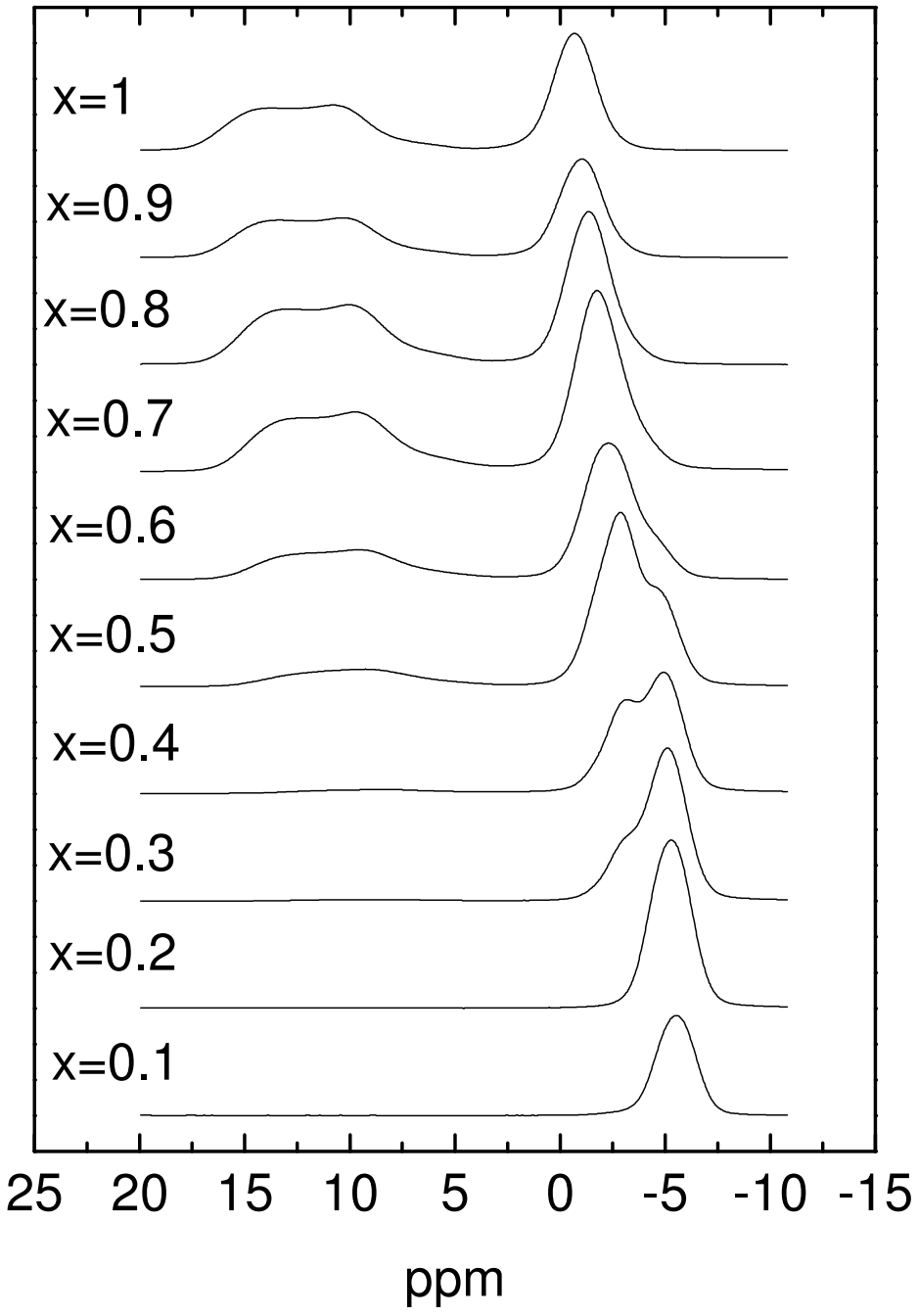

Figure 4-8

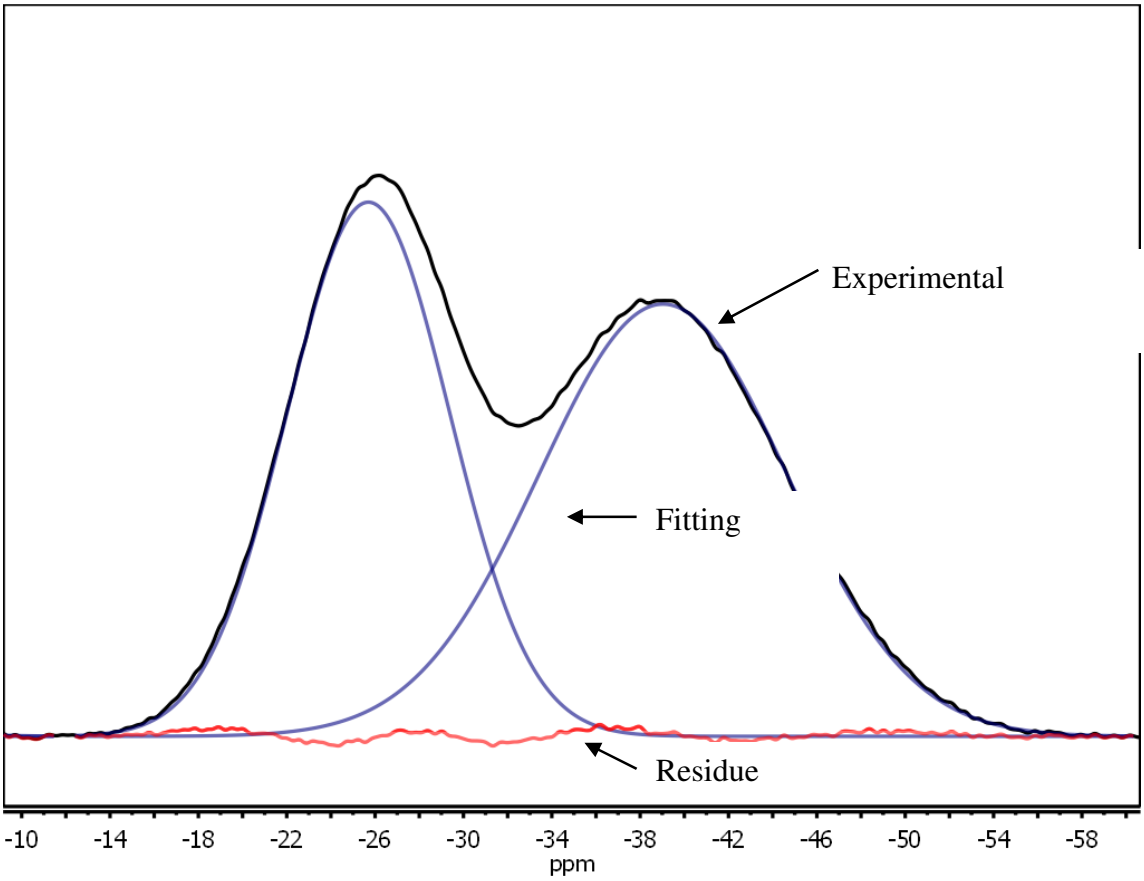
Experimental
Fitting
Residue
-10
-14
-18
-22
-26
-30
-34
-38
-42
-46
-50
-54
-58
ppm

Figure 4-9

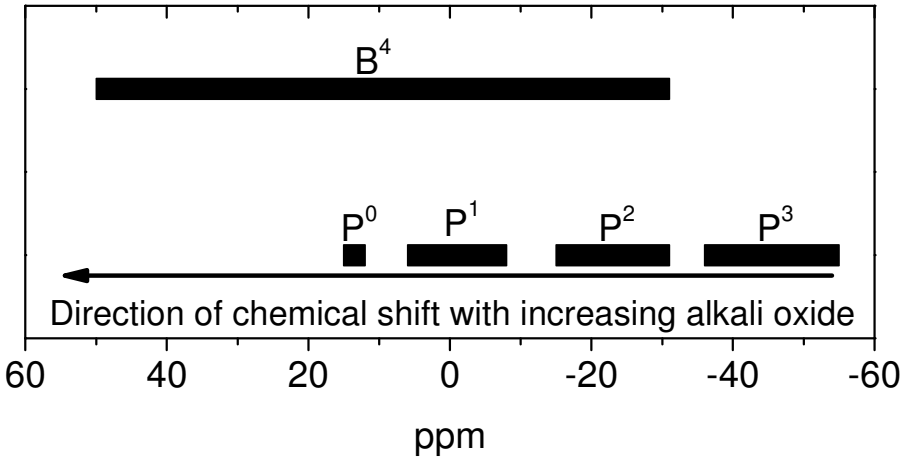
B4
P0
P1
P2
P3
Direction of chemical shift with increasing alkali oxide
60
40
20
0
-20
-40
-60
ppm

Figure 4-10

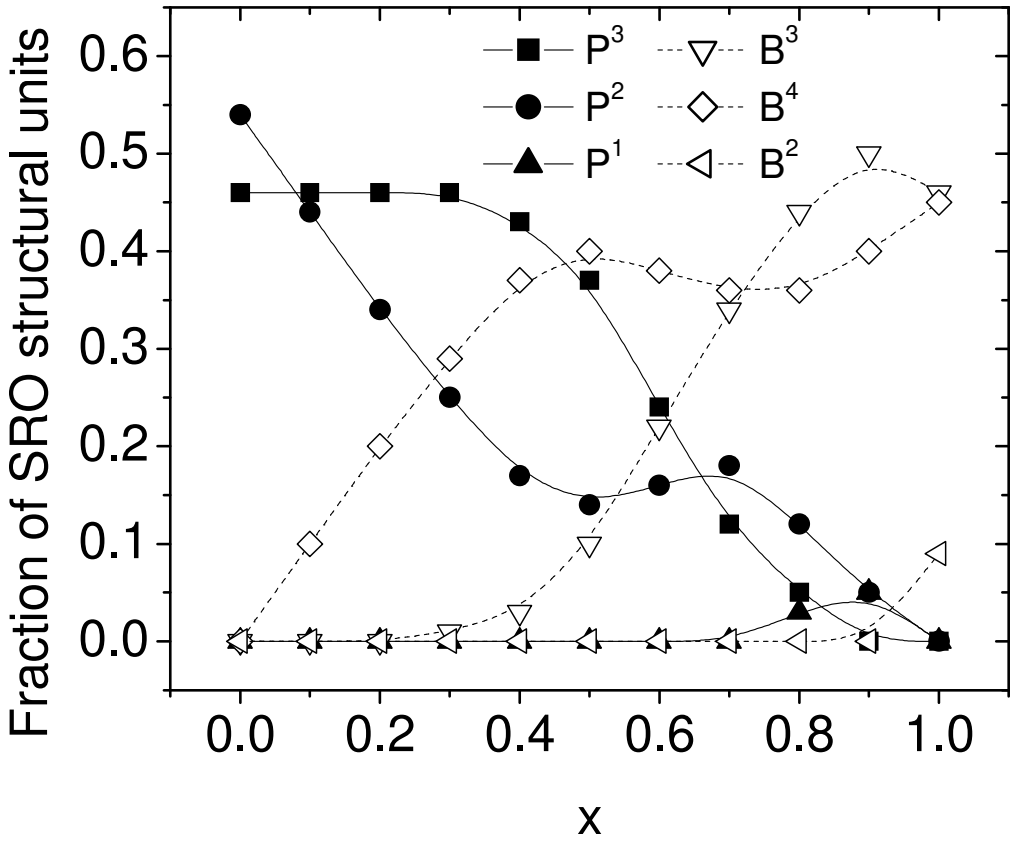
Fraction of SRO structural units
0.0
0.1
0.2
0.3
0.4
0.5
0.6
0.0
0.2
0.4
0.6
0.8
1.0
x
P3
P2
P1
B3
B4
B2

Figure 4-11

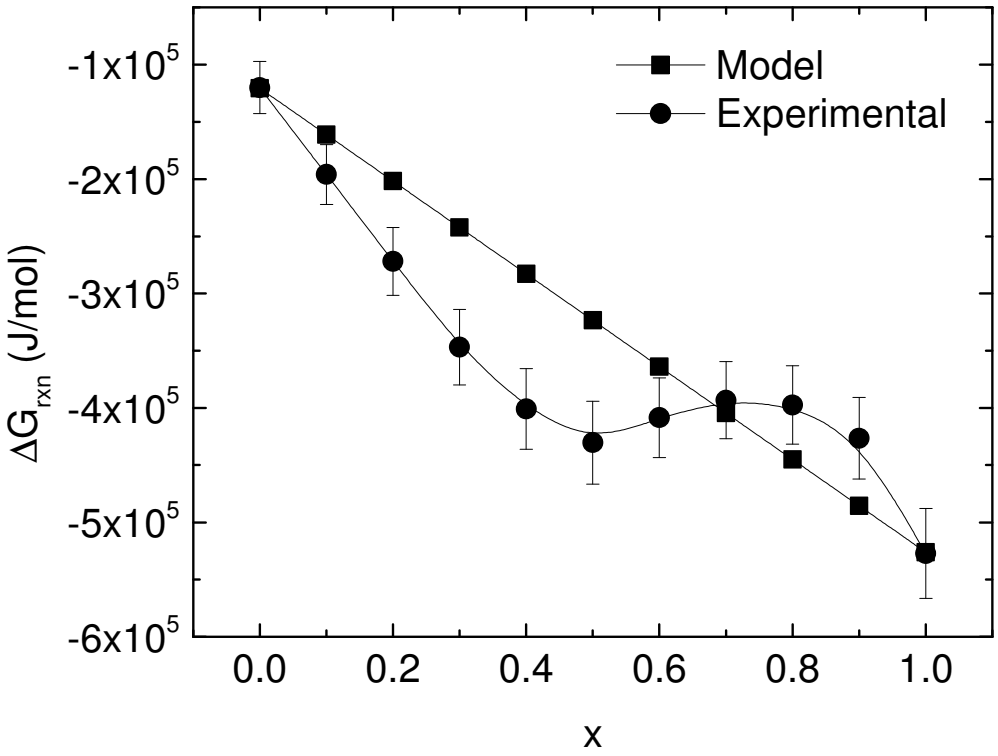
Model
Experimental
-1x10^5
-2x10^5
-3x10^5
-4x10^5
-5x10^5
-6x10^5
ΔG_rxn (J/mol)
0.0
0.2
0.4
0.6
0.8
1.0
x

Figure 4-12

Table 4-1

x	P^3	P^2	P^1	B^3	B^4	B^2
0	0.46	0.54	0.00	0.00	0.00	0.00
0.1	0.46	0.44	0.00	0.00	0.10	0.00
0.2	0.46	0.34	0.00	0.00	0.20	0.00
0.3	0.46	0.25	0.00	0.01	0.29	0.00
0.4	0.43	0.17	0.00	0.03	0.37	0.00
0.5	0.37	0.14	0.00	0.10	0.40	0.00
0.6	0.24	0.16	0.00	0.22	0.38	0.00
0.7	0.12	0.18	0.00	0.34	0.36	0.00
0.8	0.05	0.12	0.03	0.44	0.36	0.00
0.9	0.00	0.05	0.05	0.50	0.40	0.00
1	0.00	0.00	0.00	0.46	0.45	0.09

Table 4-2

i	$\Delta G_f(i)_{crystal}$	
	J/mol	Reference
$BO_{3/2}$	-597150	[48]
$NaBO_2$ Tetrahedral	-950850	[48]
$NaBO_2$ Trigonal	-920700	[48]
$PO_{5/2}$	-673640	[49]
$NaPO_3$	-268320	[49]
$Na_2PO_{7/2}$	-440273	[50]
Na_2O	-376569	[48]
B_2O_3	-1194300	[48]
P_2O_5	-1347280	[49]

Chapter 5. Ionic Conductivity of Mixed Glass Former 0.35 Na_2O + 0.65 [xB_2O_3 + (1-x)P_2O_5] Glasses

A paper to be submitted to the Journal of Non-Crystalline Solids

Randilynn Christensen[1], Jennifer Byer[2], Garrett Olson[2], Steve W. Martin[3]

5.1 Abstract

The mixed glass former effect (MGFE) is defined as a non-linear and non-additive change in the ionic conductivity with changing glass former fraction at constant modifier composition between two binary glass forming compositions. In this study, mixed glass former (MGF) sodium borophosphate glasses, 0.35 Na_2O + 0.65 [xB_2O_3 + (1-x)P_2O_5], $0 \leq x \leq 1$, have been prepared and their physical properties such as ionic conductivity have been studied. The ionic conductivity exhibits a strong, positive MGFE and a corresponding negative non-linear, non-additive change in activation energy with changing glass former content. The Anderson Stuart (A-S) model was applied to explain the increase in ionic conductivity and the decrease in activation energy. The trend of the A-S model was found to be in excellent agreement with our experimental data. From the A-S model, we found that the changing columbic forces with composition are much stronger than the changing volume (mechanical-strain) forces. The dependence of the columbic energy term on the relative dielectric permittivity suggests that the polarization

of the bridging oxygen connecting B^4 units to P units, resulting from the larger phosphorous electronegativity, is the underlying cause of the MGFE.

5.2 Introduction

5.2.1 Background

Energy storage is a growing concern in an ever increasingly battery driven society. Batteries power everything from cell phones to computers to medical devices to automobiles. The development of safer, smaller, and more energy dense batteries is in demand. Ion conducting glasses are an important type of solid electrolyte that may be used to answer this need. A currently unexplained change in the ionic conductivity in glasses known as the mixed glass former effect (MGFE) has been seen in many mixed glass former (MGF) glasses [1-8] such as $Li_2S + GeS_2 + GeO_2$ glasses [9] and $Li_2S + SiS_2 + GeS_2$ glasses [3]. This change in the ionic conductivity is non-linear and non-additive and can be observed as either a decrease or an increase in the ionic conductivity with changing glass former fraction at constant modifier composition between the two binary glass forming systems. A positive MGFE with a maximum deviation from linearity at x = 0.4 in the ionic conductivity has been observed in this system and is shown in Figure 5-5 [10]. While this phenomena has not been fully explained [2, 3, 7, 11], increases in the ionic conductivity of up to two orders of magnitude have been observed in other MGF glasses reported in the literature [1, 2]. Understanding the cause of the MGFE is crucial

to the effort of engineering glasses with higher ionic conductivities and other improved physical properties.

It is our hypothesis that structural changes at the short range order (SRO) level, caused by the mixing of the two glass former networks, is the underlying cause of the MGFE. This mixing of the two glass formers at the SRO level must necessarily effect changes at the intermediate range order (IRO) level was well. In order to confirm these hypotheses, the link between the physical properties, structure, and composition of MGF glasses is being explored.

To better understand the effect of composition on the physical properties and structure, all components of the glasses in the present study were carefully chosen. Oxygen was selected as the anion with Na, P, and B as the cations. Boron and phosphorous were chosen because of their nuclear magnetic resonance spectroscopy (NMR) accessible isotopes, ^{11}B and ^{31}P. Oxygen was chosen as the anion because of the strong glass forming ability of B_2O_3 and P_2O_5. Sodium was chosen as the glass modifier and ionic charge carrier because its radioactive isotope is useful for tracer diffusion measurements and ^{23}Na is useful in NMR studies. In addition, B_2O_3 [12-14] and P_2O_5 [15] glasses, their binary glassy counter parts, $Na_2O + B_2O_3$ [14, 16] and $Na_2O + P_2O_5$ [17-20], and some ternary alkali borophosphate glasses [8, 21-24] have been well studied in the literature. The structures of the binary glasses have been examined and then used to verify the x = 0 and x = 1 experimental data and provide starting points for the analysis of the structures of the ternary sodium borophosphate glass forming system.

5.2.2 Glass Structure Notations

The short range glass structures will be referred to as J^{n}_{mK} where J is the glassformer connected to n number of bridging oxygens (BOs), m number of the BOs bonding to glass former K and n-m BOs go to glass former J. For example, P^{n}_{mB} indicates a phosphorous atom with n number of BOs that bond to m number of boron atoms and (n-m) number phosphorous atoms. If no mK is denoted then it is unknown what glass former is being bridged to by oxygen. The short range structures present in the binary glasses and their compositional ranges are shown in Figure 5-1 and Figure 5-2.

5.3 Experimental Methods

5.3.1 Sample Preparation

The starting materials were sodium carbonate (Na_2CO_3, 99.5% Fisher Scientific), ammonium di-hydrogen phosphate dibasic ($(NH_4)_2H_2PO_4$, 98.8% Fisher Scientific), and boric acid (H_3BO_3, 99.5% Fisher Scientific). After weighing and mixing the appropriate amounts, the starting materials were calcined in platinum crucibles between 900^{o}C and 1100^{o}C for 0.5 hour to 1 hour in an electric furnace in a fume hood. After the melt was bubble free, the crucible was removed from the furnace and allowed to cool to room temperature. Once cool, the sample was weighed to determine the weight lost from NH_3, H_2O, and CO_2. The slightly hygroscopic samples were then transferred to a high quality nitrogen atmosphere glove box (< 5ppm O_2 and H_2O) and remelted in an electric furnace

at 1000°C-1100°C for 10 minutes. To create bulk samples, the melt was quenched in preheated brass molds at temperatures 40°C below the glass transition temperature, (T_g). Bulk samples were round discs approximately 20 mm in diameter and 2 mm thick. The bulk samples were annealed 40°C below the T_g for 0.5 hour, then cooled to room temperature at a rate of 2°C/minute. Due to their hygroscopic character, all samples were stored in the N_2 atmosphere glove box. All of the glasses were checked for crystallization with x-ray diffraction (XRD) and found to be x-ray amorphous. Samples were checked for weight loss and found to be within ±1.5 wt. % of their target weight. Sodium, oxygen, and phosphorous concentrations were checked by energy dispersive spectroscopy (EDS) and found to be within ± 4 at.% of the target compositions. Infrared spectroscopy was used to ensure that all of the glasses did not contain residual NH_3, CO_2, and H_2O.

5.3.2 Ionic Conductivity

Bulk samples 20mm in diameter and approximately 2 mm thick were polished to optical transparency and sputtered with gold electrodes. Samples were measured from 0.01Hz to 10MHz at 0 to 300°C using a Novocontrol Dielectric Spectrometer.

5.4 Results

An example of the a.c. conductivity measurements over the temperature and frequency ranges that were performed on all samples can be seen in a complex

impendence plot, Figure 5-3. The semicircle at high frequency arises from the bulk response of the glass to the applied electric field. The polarization "tail" at low frequency arises from the space charge polarization effects of Na^+ ion accumulation at the electrodes. The bulk resistances were obtained from the intersection of the bulk response semicircle with the Z' real part of the complex impedance axis at low frequencies. The bulk resistance was then used to calculate the d.c. conductivity by using the cell constant (sample thickness/electrode area) of the prepared glasses samples.

The temperature dependence of the ionic conductivities are shown in Figure 5-4. For all samples, the conductivity increases in a linear fashion over a ln(σ) v. 1/T plot, following an Arrhenius type behavior at temperatures below T_g

$$\sigma_{dc} = \frac{A}{T} exp(-\frac{\Delta E_a}{RT}) \qquad \textit{Equation 5-1}$$

where σ_{dc} is the direct current ionic conductivity. T is the temperature in Kelvins, E_a is the activiation energy of the Na+ ion, R is the gas constant, A is the pre-exponential factor, and σ_o is the ionic conductivity at 0K. We then used the Arrhenius equation, as modified by Equation 5-1 [51], to calculated the activation energy of ionic conduction, ΔE_a. The activation energy and the room temperature conductivities can be seen in Figure 5-5. The ionic conductivity of sodium phosphate glass at x = 0 is $7.63x\ 10^{-12}$/ohm cm. With the addition of boron, the Na^+ ion conductivity increases to a maximum of $2.34x10^{-9}$/ohm cm at x = 0.4. Further additions of boron cause the conductivity to decreases to $5.86E^{-10}$/ohm*cm at x = 0.6. The conductivity remains nearly constant through x = 0.8, then continues to decrease to $2.93x10^{-10}$/ohm cm in the sodium borate

glass. As expected from Eq. 5.1 above, the activation energy has an opposing trend to the ionic conductivity. The maximum activation energy is 84.36 kJ/mol at x = 0. A decrease to 61.86 kJ/mol at x = 0.4 is followed by an increase to 64.24 kJ/mol at x = 0.6. The activation energy remains nearly constant until it increases to 65.91 kJ/mol at x = 1.

5.5 Discussion

5.5.1 The Anderson Stuart Model

The cationic conductivity is given as $\sigma = ne\mu$, where σ is the ionic conductivity, e is the electric charge, n is the number of mobile ions (Na^+) per unit volume, and μ is the mobility of the ions. Both n and μ are temperature dependent. As the number of ions remains constant, it suggests that the number of mobile ions at a given temperature are also constant. Therefore, at a constant temperature, the change in ionic conductivity with glass former composition may be more related to a change in the mobility of the ions.

How can we evaluate the changing mobility of the sodium ion? We know that $\sigma_{dc} = \frac{\sigma_0}{T}\exp(-\frac{\Delta E_a}{RT})$, therefore we can think of the mobility of the sodium ion in terms of the energy it needs to leave one charge compensating site and "hop" to another site, the activation energy, ΔE_a. Anderson and Stuart [52] proposed that the activation energy consisted of the energy required to move the ion from one charge compensating site to another, ΔE_b and the energy required to deform the network structure by generating a hole large enough for the ion to pass through, ΔE_s, known as the electrostatic binding

and strain energy respectively. The binding energy is described by the sum of the columbic forces acting on the ion as it moves away from its charge compensating site and the strain energy describes the mechanical forces acting on the ion as the structure dilates to allow the ion to move between sites.

$$\Delta E_s = 4\pi G r_D (r_{Na} - r_D)^2 \qquad \textit{Equation 5-2}$$

The strain energy can be written as Equation 5-2, where G is the shear modulus, r_D is the doorway radius, and r_{Na} is the radius of the Na^+ ion. The unknowns are G and r_D. We can estimate the shear modulus by taking the literature values of sodium borate and applying the trend seen in the glass transition temperature [34] results in an estimation of G seen in Figure 5-6. We can calculate the doorway radius using data from x-ray diffraction on our samples [53] and the literature. Feil et al. [54] reported that $r_{Na} = 0.97\text{Å}$ and $r_O = 1.28\text{Å}$. Our diffraction data and Reverse Monte Carlo modeling [55] reported that Na has a five-fold oxygen coordination and a distance between Na-BO and Na-NBO of 2.3Å. This suggests that oxygen is in a trigonal bi-pryamidal structure with Na^+ at the center, where the center of each oxygen is 2.3Å from the center of the Na^+ ion. This allows us to calculate a doorway radius, $r_D = 0.71\text{Å}$. Once G and r_D are known, the change in strain energy with composition can be calculated using Equation 5-2. The results of this calculation can be seen in Figure 5-8.

$$\Delta E_b = \frac{\beta Z_{Na} Z_O e^2}{\varepsilon_0 \varepsilon_{hf}} \left[\frac{1}{r_{Na} + r_O}\right] \qquad \textit{Equation 5-3}$$

The binding energy can be written as Equation 5-3,where e is the ion charge, ε_0 is the permittivity of free space, ε_{hf} is the high frequency dielectric constant, $r_{Na} = 0.97\text{Å}$ is the ionic radius of Na, $r_O = 1.28\text{Å}$ is the ionic radius of oxygen, $\beta = \frac{2.1 - r_{Na}}{3.5}$ is the finate displacement factor, and $Z_{Na} = 1$ and $Z_O = 2$ are the valence of sodium and oxygen respectively. The high frequency dielectric constant relates to the dielectric response in the immediate vicinity of the alkali. In oxide glasses the high frequency range is generally between 10^5 and 10^{12} Hz [56] at temperatures below the glass transition temperature.

The binding energy can be calculated using the permittivity as determined by our impedance spectroscopy experiments, Figure 5-7. The results of these binding energy calculations can be seen in Figure 5-8. By observing the trends in the binding and strain energy, it is clear that the binding energy is the dominant contributor to the total activation energy as it is much larger than the strain energy. The total activation energy can be seen in Figure 5-9. Although the total calculated activation energy is nearly an order of magnitude larger than the experimentally determined values, the overall trends are very comparable, as seen in Figure 5-9.

5.5.2 Cause of increased ionic conductivity

It is clear that the trend of the total activation energy depends on the binding energy and that the binding energy relies on the changes in dielectric permittivity with composition, but why does the dielectric permittivity change? We suggest that it is the

IRO associated with the B^4 unit that is causing increased dielectric permittivity, and therefore decreased activation energy. At $0.1 \leq x \leq 0.4$, there are more phosphorous atoms than boron atoms and NMR studies have shown a majority of the boron to be in tetrahedral coordination [34], 7% of boron are in trigonal configuration at x = 0.4. Therefore, the B^4 unit must bridge to more phosphorous units than boron units, especially at lower x where less boron is present. As P^{+5} is more electronegative than B^{+3}, P-O-B bonding would polarize the oxygen, decreasing the charge density of the B^4 unit. This decreased charge density means the Na^+ ion is less tightly bound, so it takes less energy for the Na^+ ion to hop to the next charge compensation site.

How does this explain the maxima in dielectric permittivity at x = 0.4 and 0.5 and x = 0.8 in addition to the maxima in ionic conductivity at x = 0.4? At x = 0.4 B^4 makes up 37% of the SRO structural units and at x = 0.5 B^4 makes up 40% of the SRO structural units according to NMR data[34]. However, at x = 0.4 and x = 0.5 P units make up 60% and 50% of the SRO units. The NMR data indicates that the number of $B_P^4 > B_B^4$ until x = 0.4, after which B_B^4 is the dominant boron tetrahedral unit. So the maximum in conductivity occurs where there is greatest number of B_P^4.

To understand the maximum at x = 0.8, we must consider the changes in SRO with x. As x increases, the number of B^4-O-P bridges decrease, but the number of $P_{B^4}^2$ and $P_{B^4}^1$ increase. If we say that P^2 and P^1 are more basic than P^3, than as they bridge to B, their Na-NBO bond increase in strength. However, the $B_{P^2}^4$ or $B_{P^1}^4$ bonds to Na^+

would be weaker than B_{P3}^{4}. Therefore, even though B^4 units now bridging to fewer phosphorous, the phosphorous units are more basic, allowing increased conductivity.

5.6 Conclusion

The strong positive MGFE observed in the ionic conductivity of 0.35 Na_2O + 0.65 [xB_2O_3 + (1-x)P_2O_5] glasses, relates to the negative change in activation energy with changing composition. The activation energy was explained thought the Anderson-Stuart Model, which suggested that the columbic binding energy was much greater than the strain energy. This resulted in the A-S model having a strong dependence on the dielectric permittivity. The changing dielectric permittivity was found to be the cause of the MGFE by the polarization of B^4-O-P bonds by the more electronegative phosphorous atom.

5.7 References

[1] A. Agarwal, V.P. Seth, P.S. Gahlot, S. Khasa, M. Arora, S.K. Gupta, J. Alloys Compd., 377 (2004) 225-231.
[2] A. Pradel, N. Kuwata, M. Ribes, J. Phys. Condens. Matter, 15 (2003) S1561-S1571.
[3] A. Pradel, C. Rau, D. Bittencourt, P. Armand, E. Philippot, M. Ribes, Chem. Mater., 10 (1998) 2162-2166.
[4] P.S.S. Prasad, A.N.D. Rani, S. Radhakrishna, Solid State Commun., 77 (1991) 967-971.
[5] P.S.S. Prasad, A.N.D. Rani, S. Radhakrishna, Mater. Chem. Phys., 25 (1990) 487-499.
[6] R.V. Salodkar, V.K. Deshpande, K. Singh, J. Power Sources, 25 (1989) 257-263.
[7] M. Jamal, G. Venugopal, M. Shareefuddin, M. Narasimha Chary, Mater. Lett., 39 (1999) 28-32.
[8] D. Zielniok, C. Cramer, H. Eckert, Chem. Mater., 19 (2007) 3162-3170.
[9] Y. Kim, J. Saienga, W. Martin Steve, J Phys Chem B, 110 (2006) 16318-16325.
[10] R. Christensen, J. Byer, G. Olson, S.W. Martin, To Be Published, (2011).
[11] R.S. Gedam, V.K. Deshpande, Solid State Ionics, 177 (2006) 2589-2592.
[12] P.C. Taylor, E.J. Friebele, J. Non-Cryst. Solids, 16 (1974) 375-386.
[13] S. Prabaker, K.J. Rao, C.N.R. Rao, Proc. R. Soc. Lond., 429 (1990) 1-15.
[14] G.E. Jellison, P.J. Bray, J. Non-Cryst. Solids, 29 (1978) 187-206.
[15] S. Elbers, W. Strojek, L. Koudelka, H. Eckert, Solid State Nuclear Magnetic Resonance, 27 (2005) 65-76.
[16] P.J. Bray, A.E. Geissberger, F. Bucholtz, I.A. Harris, J. Non-Cryst. Solids, 52 (1982) 45-66.
[17] R.K. Brow, J. Non-Cryst. Solids, 263 (2000) 1-28.
[18] S.W. Martin, European Journal of Solid State and Inorganic Chemistry, 28 (1991) 163-205.
[19] R.K. Brow, R.J. Kirkpatrick, G.L. Turner, J. Non-Cryst. Solids, 116 (1990) 39-45.
[20] R.K. Sato, R.J. Kirkpatrick, R.K. Brow, J. Non-Cryst. Solids, 143 (1992) 257-264.
[21] M. Villa, M. Scagliotti, G. Chiodelli, J. Non-Cryst. Solids, 94 (1987) 101-121.
[22] L. Koudelka, P. Mosner, M. Zeyer, C. Jager, J. Non-Cryst. Solids, 351 (2005) 1039-1045.
[23] M. Zeyer-Dusterer, L. Montagne, G. Palavit, C. Jager, Solid State Nuclear Magnetic Resonance, 27 (2005) 50-64.
[24] D. Qiu, P. Guerry, I. Ahmed, D.M. Pickup, D. Carta, J.C. Knowles, M.E. Smith, R.J. Newport, Mater. Chem. Phys., 111 (2008) 455-462.
[25] O.L. Anderson, D.A. Stuart, J. Am. Ceram. Soc., 37 (1954) 573-580.
[26] R. Christensen, J. Byer, G. Olson, W. Martin Steve, To Be Published, (2012).
[27] R.S. Le, S. Martin, R. Christensen, Y. Ren, V. Petkov, J. Phys.: Condens. Matter, 23 (2011) 035403/035401-035403/035410.
[28] D. Feil, S. Feller, J. Non-Cryst. Solids, 119 (1990) 103-111.

[29] M. Schuch, R. Christensen, C. Trott, P. Maass, S.W. Martin, J. Phys. Chem. C, 116 (2012) 1503-1511.
[30] G.N. Greaves, K.L. Ngai, Physical Review B, 52 (1995) 6358-6380.
[31] R. Christensen, J. Byer, G. Olson, W. Martin Steve, Journal of Non-Crystalline Solids, (2012).
[32] R. Christensen, J. Byer, G. Olson, W. Martin Steve, Journal of Non-Crystalline Solids, Submitted (2011).

5.8 Figures

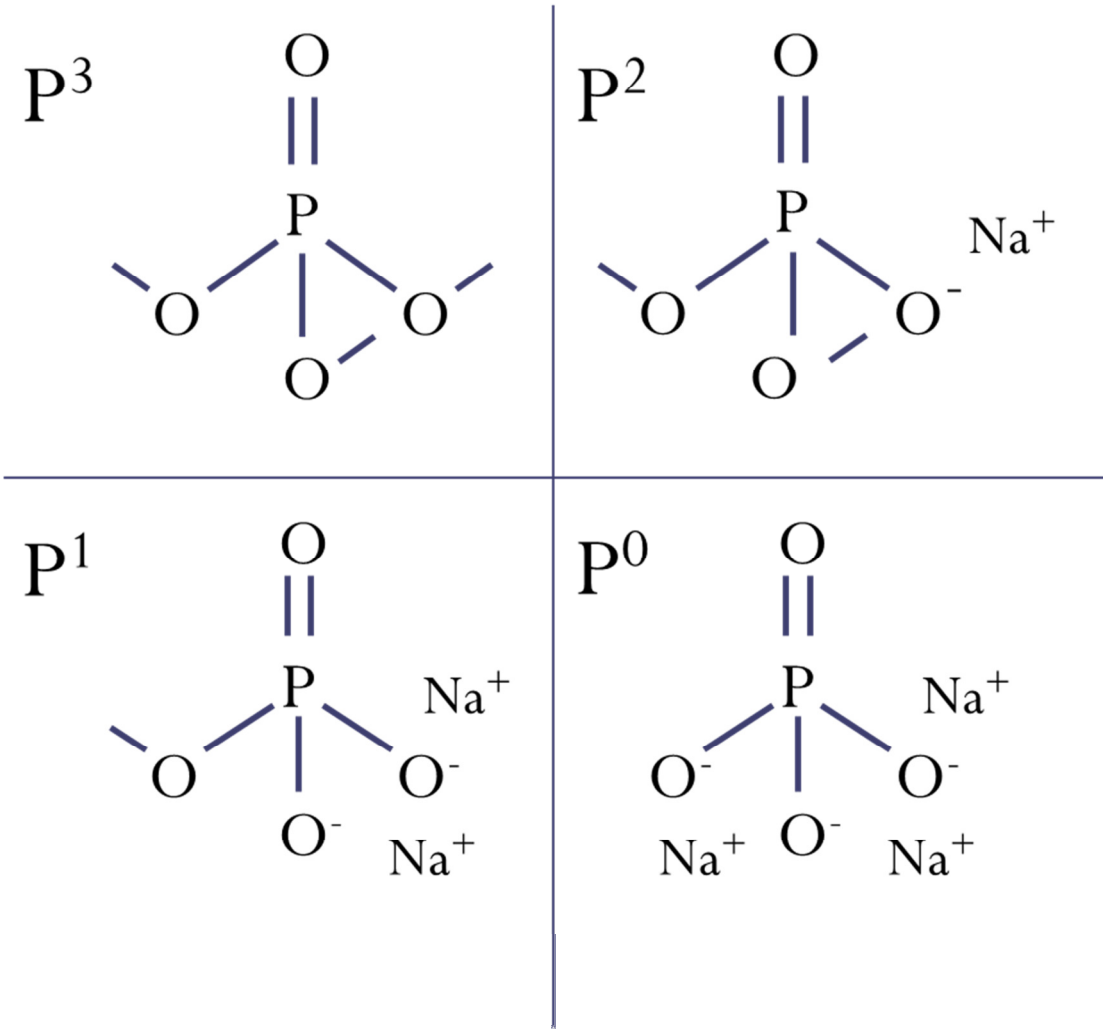

Figure 5-1

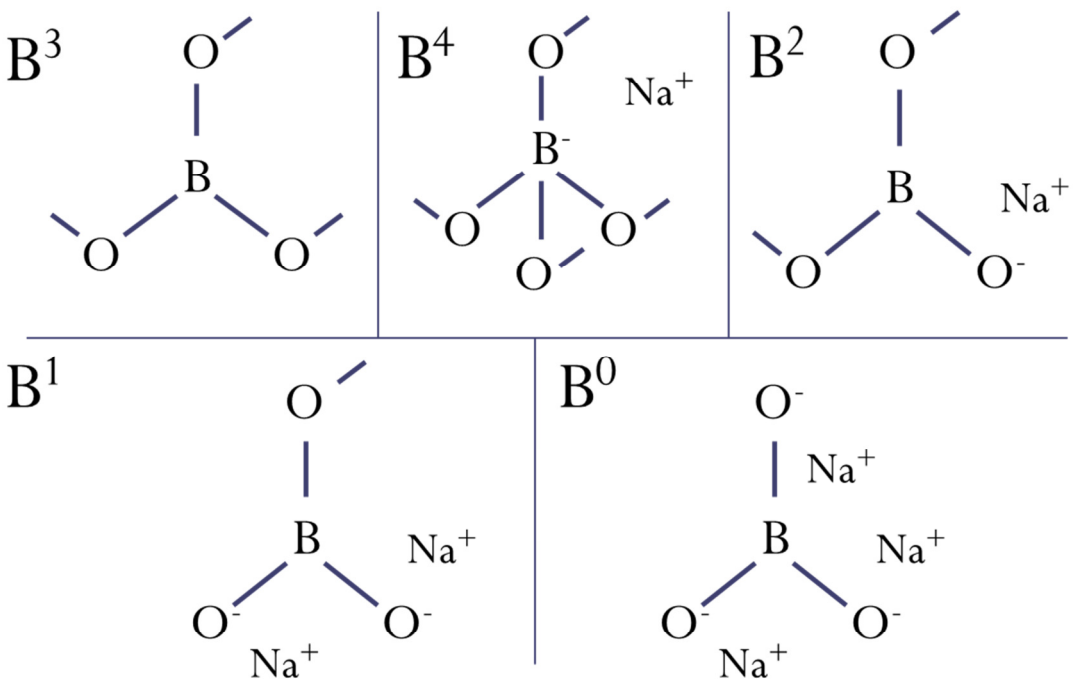

Figure 5-2

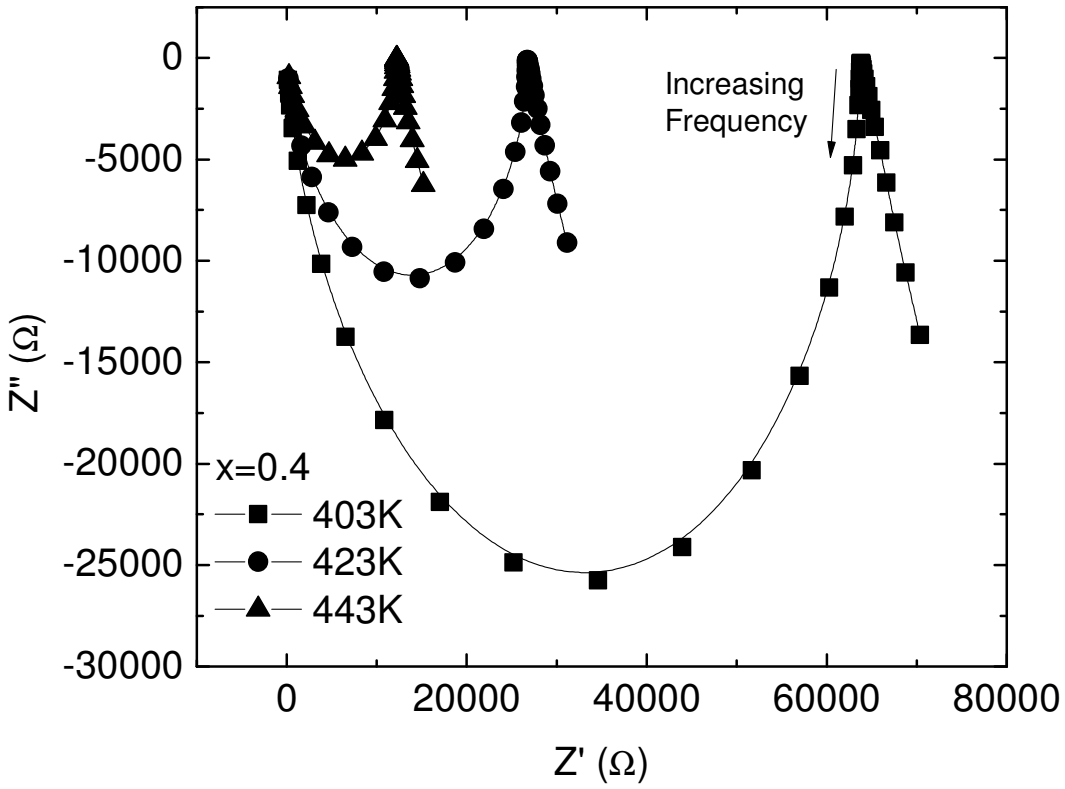
0
-5000
-10000
-15000
-20000
-25000
-30000
Z'' (Ω)
0
20000
40000
60000
80000
Z' (Ω)
Increasing
Frequency
x=0.4
403K
423K
443K

Figure 5-3

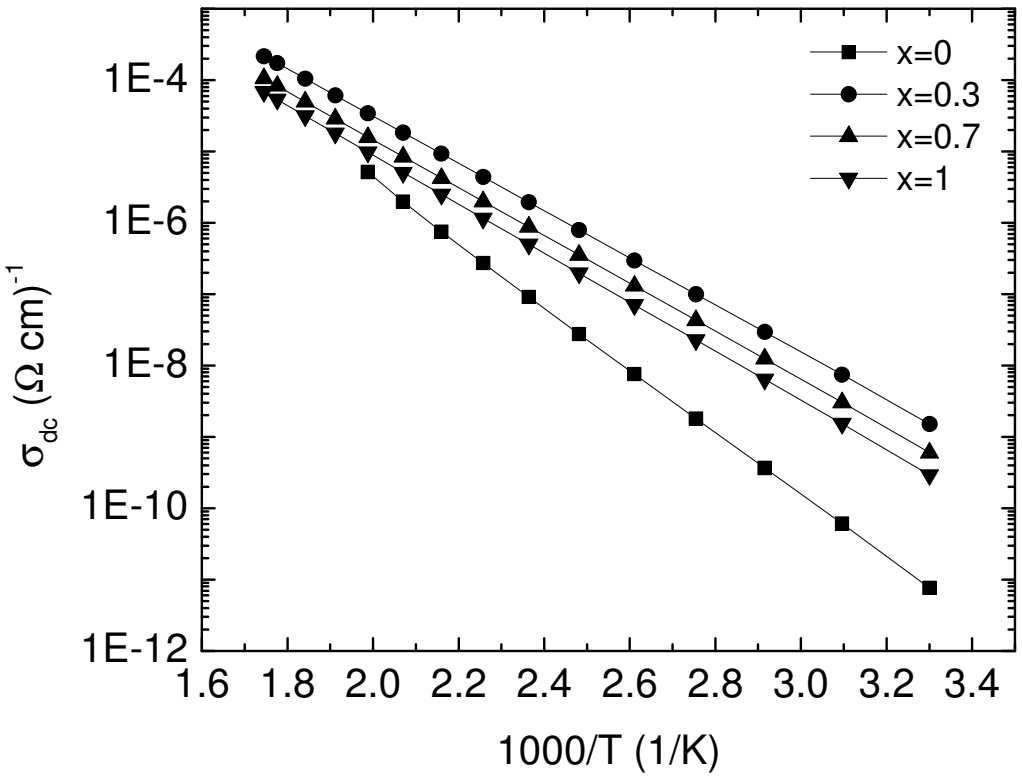
x=0
x=0.3
x=0.7
x=1
1E-4
1E-6
1E-8
1E-10
1E-12
σdc (Ω cm)-1
1.6
1.8
2.0
2.2
2.4
2.6
2.8
3.0
3.2
3.4
1000/T (1/K)

Figure 5-4

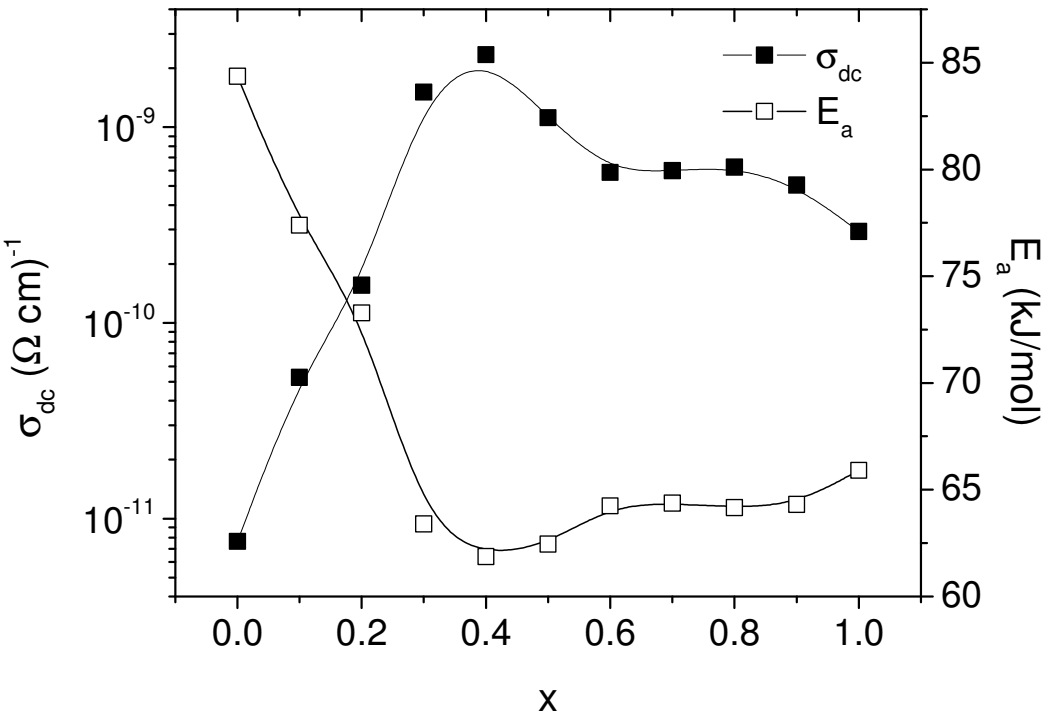
σdc
Ea
10-9
10-10
10-11
σdc (Ω cm)-1
85
80
75
70
65
60
Ea (kJ/mol)
0.0
0.2
0.4
0.6
0.8
1.0
x

Figure 5-5

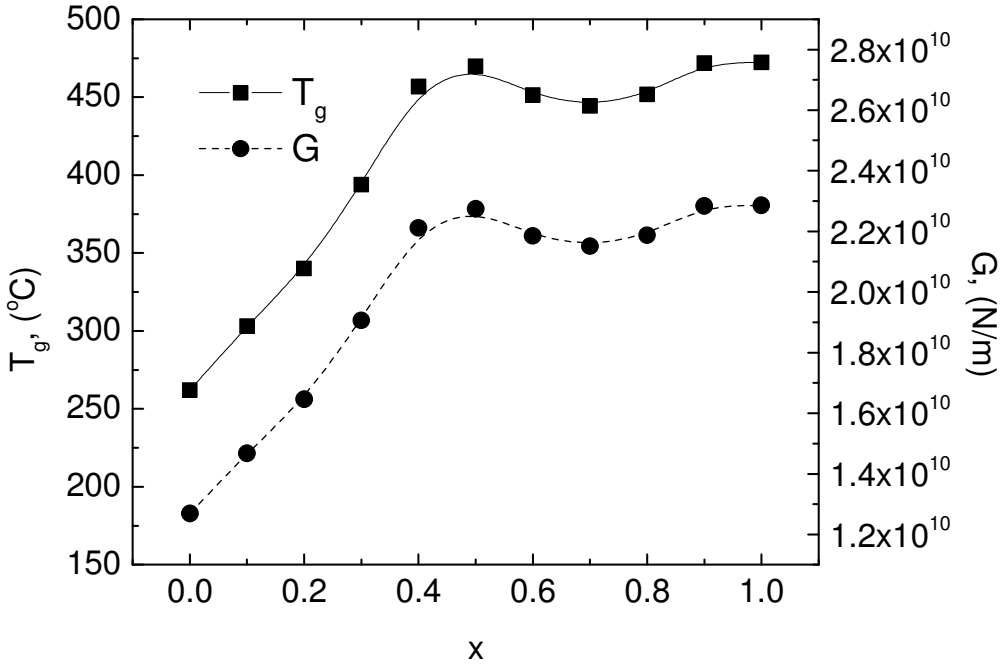
500
450
400
350
300
250
200
150
T_g, (°C)
T_g
G
0.0
0.2
0.4
0.6
0.8
1.0
x
$2.8x10^{10}$
$2.6x10^{10}$
$2.4x10^{10}$
$2.2x10^{10}$
$2.0x10^{10}$
$1.8x10^{10}$
$1.6x10^{10}$
$1.4x10^{10}$
$1.2x10^{10}$
G, (N/m)

Figure 5-6

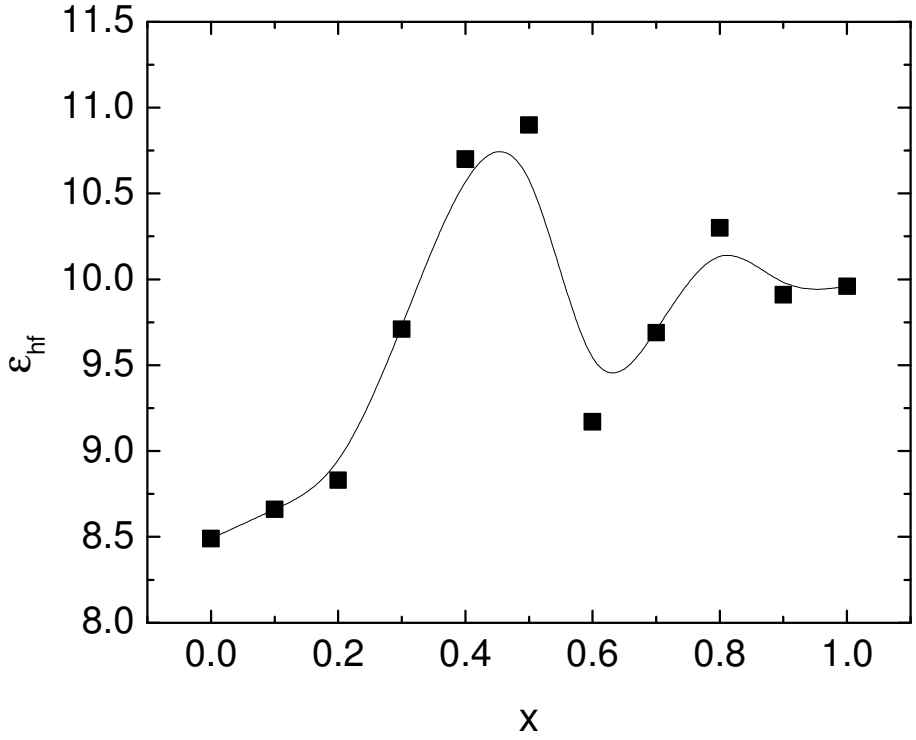

Figure 5-7

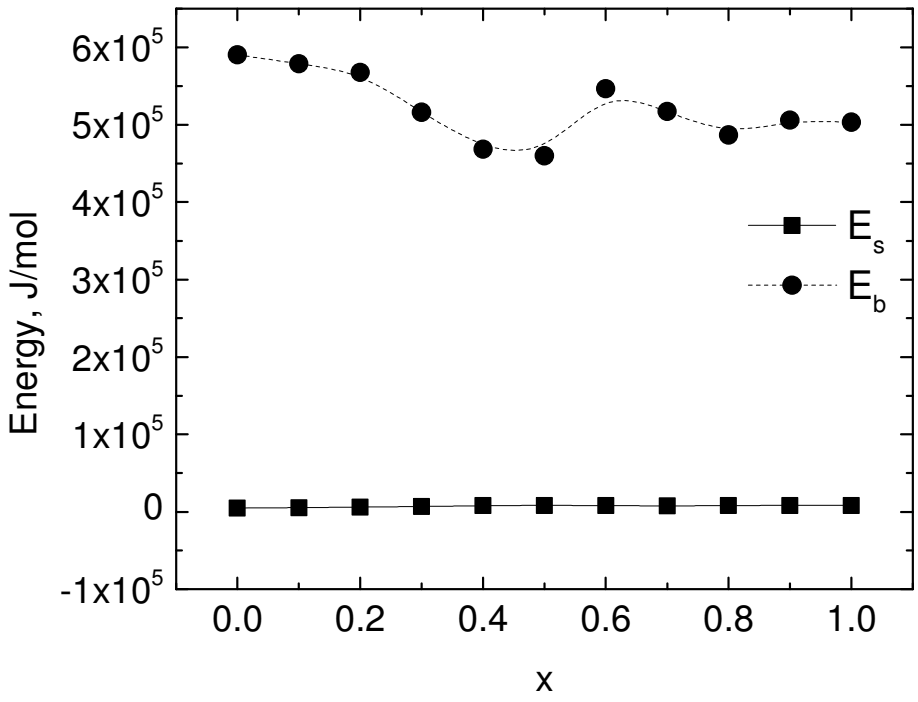
6x10^5
5x10^5
4x10^5
3x10^5
2x10^5
1x10^5
0
-1x10^5
Energy, J/mol
0.0
0.2
0.4
0.6
0.8
1.0
x
E_s
E_b

Figure 5-8

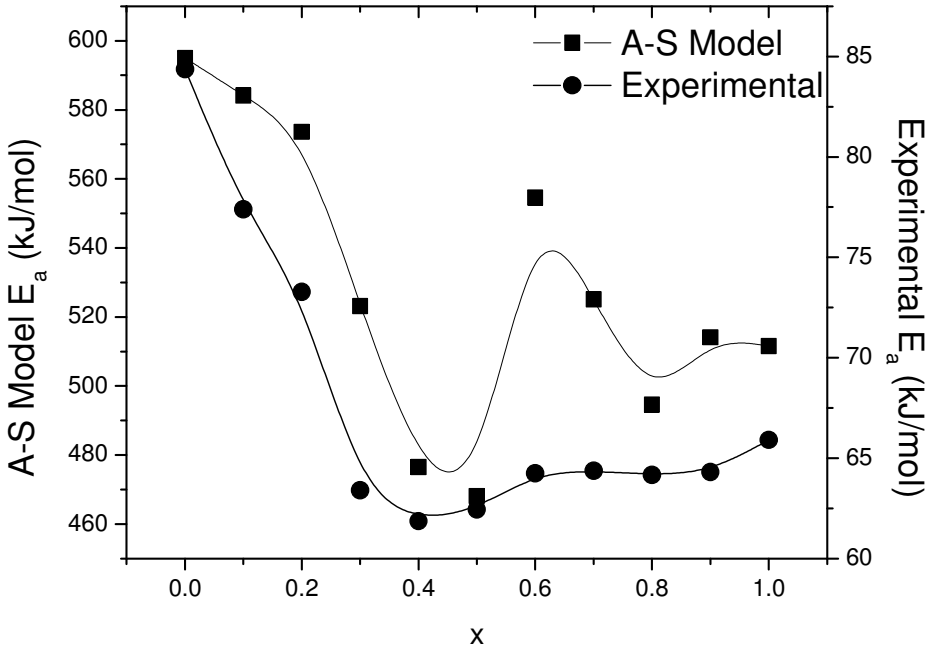
A-S Model
Experimental
A-S Model E_a (kJ/mol)
Experimental E_a (kJ/mol)
x
600
580
560
540
520
500
480
460
85
80
75
70
65
60
0.0
0.2
0.4
0.6
0.8
1.0

Figure 5-9

Chapter 6. Conclusion

6.1 General Conclusions

In an effort to understand the underlying cause of the mixed glass former effect, the physical properties, structure, and composition was studied in $0.35Na_2O + 0.65[xB_2O_3 + (1-x)P_2O_5]$ glasses. Positive non-additive and non-linear trends were seen in the ionic conductivity, density, and glass transition temperature with changing glass former composition, with maximum deviations from linear at x = 0.4. Likewise, negative non-additive and non-linear trends were observed in the molar and free volumes and the activation energy.

Through structural investigation it was determined that the modification of the phosphorus and boron SRO structural units by Na in the ternary glasses were not the same as in their binary counterparts. It was found in the ternary glasses that the minority glass former was overly modified compared to the binary glass. In addition, evidence of cross network bridging of boron to phosphorous through a bridging oxygen was observed. The MGFE was found to be strongly linked to the tetrahedral boron unit bonded to phosphorous SRO units through ionic conduction model by Anderson and Stuart. Bridging oxygen between phosphorous and boron were found to be polarized, causing decreasing bond strengths that resulted in increased ionic conductivity

6.2 Future work

To further support our research, two-dimensional NMR studies that can confirm the correlation of tetrahedral boron units to phosphorous, such as REDOR would be extremely valuable. Quantification of these bonds would also be very useful.

6.3 Acknowledgements

I would like to thank Steve W. Martin for persuading me to study glass. I think it turned out rather well! His guidance, support, and confidence in me have been invaluable.

Thanks to Christian Bishchoff for all his discussions about glass and the MGFE, coffee journeys, and for being an excellent collaborator on the MGFE project!

A big thank you to my undergraduate researches Jennifer Byer and Garrett Olson, without you guys, this thesis would probably be much shorter. I would also like to thank the Glass and Optical Materials Group at Iowa State, Wenlong Yao, InSeok Seo, Michael Haynes, Austin Shaw, Seth Berbano, Maxwell Marple, Kathy Schuler, Lisa Rueschoff, and Emma White for all their help and patience.

Thanks to Sara Cady and Shu Xu at the Iowa State Chemical Instrumentation Facility for all the NMR help!

A special thanks to my husband Doug Little for putting up with all my crazy for the last five years.

This research was supported by the National Science Foundation under grant number DMR-0710564 and this research support is gratefully acknowledged.